

OLGGA: The OptimaL Ground Grid Application

by

Songyan Li

A Thesis Presented in Partial Fulfillment
of the Requirements for the Degree
Master of Science

Approved April 2016 by the
Graduate Supervisory Committee:

Daniel J. Tylavsky, Chair
Raja Ayyanar
Vijay Vittal

ARIZONA STATE UNIVERSITY

May 2016

ABSTRACT

The grounding system in a substation is used to protect personnel and equipment. When there is fault current injected into the ground, a well-designed grounding system should disperse the fault current into the ground in order to limit the touch potential and the step potential to an acceptable level defined by the IEEE Std 80. On the other hand, from the point of view of economy, it is desirable to design a ground grid that minimizes the cost of labor and material. To design such an optimal ground grid that meets the safety metrics and has the minimum cost, an optimal ground grid application was developed in MATLAB, the Optimal Ground Grid Application (OL-GGA).

In the process of ground grid optimization, the touch potential and the step potential are introduced as nonlinear constraints in a two layer soil model whose parameters are set by the user. To obtain an accurate expression for these nonlinear constraints, the ground grid is discretized by using a ground-conductor (and ground-rod) segmentation method that breaks each conductor into reasonable-size segments. The leakage current on each segment and the ground potential rise (GPR) are calculated by solving a matrix equation involving the mutual resistance matrix. After the leakage current on each segment is obtained, the touch potential and the step potential can be calculated using the superposition principle.

A genetic algorithm is used in the optimization of the ground grid and a pattern search algorithm is used to accelerate the convergence. To verify the accuracy of the

application, the touch potential and the step potential calculated by the MATLAB application are compared with those calculated by the commercialized grounding system analysis software, WinIGS.

The user's manual of the optimal ground grid application is also presented in this work.

ACKNOWLEDGMENTS

I would like to express my sincere gratitude to Dr. Daniel Tylavsky, my advisor, for his expert guidance throughout my study and research. He gave me the opportunity to learn and conduct research on ground grid optimization and shaped my writing skills.

I would like to thank my committee members, Dr. Raja Ayyanar and Dr. Vijay Vittal, for their valuable time and suggestions.

I would like to thank Salt River Project for their financial support. Mr. Thomas LaRose is the Executive Engineer as well as the supervisor for this project. His valuable advice and feedback are essential for this work.

I am also grateful to Scott Mongrain, a doctoral student currently at ASU. He has spent much of his valuable time shaping my writing skills.

Finally, I would like to thank my parents and my friends for their constant support.

TABLE OF CONTENTS

	Page
LIST OF TABLES.....	vii
LIST OF FIGURES	viii
NOMENCLATURE	x
CHAPTER	
1 INTRODUCTION	1
1.1 Overview	1
1.2 Literature Review	2
1.3 The Objective	6
1.4 Thesis Organization.....	7
2 MATHEMATICAL MODELS	8
2.1 The Two Layer Soil Model	8
2.2 Ground Grid Model	9
2.2.1 Ground Grid Segmentation.....	9
2.2.2 The Green's function in a Two Layer Soil Model	13
2.3 The Mutual Resistance Matrix Line-Line Model.....	17
2.4 The Mutual Resistance Matrix Point-Point Model.....	35
2.5 Modeling the Non-Orthogonal Ground Grid.....	37
2.5.1 The Earth Potential Equation for the Trapezoidal Ground Grid.....	38
2.5.2 The Rectangle Rule.....	43

CHAPTER	Page
2.5.3 Simpson's Rule.....	44
2.5.4 Coordinate Transformation.....	45
2.5.5 The Centroid of a Polygon.....	47
2.6 The Current Distribution Factor and the Ground Potential Rise.....	48
2.7 Calculating the Earth Potential, the Touch Potential, and the Step Potential.....	49
3 PROGRAM VALIDATION.....	54
3.1 Self-Consistency, Symmetry and Coordinate Independence	54
3.2 The Validation of Self-Consistency	56
3.2.1 The Self-Consistency of the Rectangular Ground Grid.....	56
3.2.2 The Self-Consistency of the L-Shaped Ground Grid.....	57
3.2.3 The Self-Consistency of the Trapezoidal Ground Grid	59
3.3 The Accuracy Requirement.....	62
3.4 The Parameter Limitations and the Segmentation Method	63
3.5 The Validation with WinIGS	65
3.5.1 The Validation for Square Ground Grids and Rectangular Ground Grids.....	65
3.5.2 The Validation for L-Shaped Ground Grids	68
3.5.3 The Validation for Trapezoidal Ground Grids.....	72

CHAPTER	Page
3.5.4 Plots of Errors	75
4 GROUND GRID OPTIMIZATION.....	77
4.1 The Safety Requirement.....	77
4.2 The Objective Function and Constraints	78
4.2.1 The Parameters and the Ground Grid Design Rules	78
4.2.2 The Objective Function.....	79
4.3 Genetic Algorithm and Pattern Search	81
4.4 Case Studies	82
5 CONCLUSIONS	89
5.1 Conclusions	89
REFERENCES	92
APPENDIX.....	94
A THE USER’S MANUAL	94
B LIST OF SOURCE CODE FILES OF OLGGA AND IMPLEMENTATION	
DIAGRAM	114
C OLGGA INSTALLATION INSTRUCTION CONTAINED	
IN THE README.TXT FILE	124

LIST OF TABLES

Table	Page
3.1 Validation of Symmetry for the Rectangular Ground Grid.....	57
3.2 Validation of Symmetry for the L-Shaped Ground Grid	59
3.3 Validation of Symmetry for the Trapezoidal Ground Grid	61
3.4 The Touch Potential and the Step Potential of Case I.....	66
3.5 The Touch Potential and the Step Potential of Case II.....	67
3.6 The Touch Potential and the Step Potential of Case III	68
3.7 The Touch Potential and the Step Potential of Case IV	69
3.8 The Touch Potential and the Step Potential of Case V	70
3.9 The Touch Potential and the Step Potential of Case VI.....	71
3.10 The Touch Potential and the Step Potential of Case VII.....	73
3.11 The Touch Potential and the Step Potential of Case VIII	74
3.12 The Touch Potential and the Step Potential of Case IX	75
4.1 The Optimal Design for the Rectangular Ground Grid.....	84
4.2 The Optimal Design for the L-Shaped Ground Grid.....	86
4.3 The Optimal Design for the Trapezoidal Ground Grid	88

LIST OF FIGURES

Figure	Page
2.1 Two Layer Soil Model	8
2.2 A Conductor along the x-Axis	10
2.3 Two Layer Soil Model with 3 Regions	13
2.4 The Source Point in the Upper Layer Soil	14
2.5 The Source Point in the Lower Layer Soil	16
2.6 The Source Point and the Field Point	18
2.7 The Segment and the Field Point	18
2.8 Two Segments	19
2.9 Two Parallel Segments in the Lower Layer	23
2.10 Segment A in the Lower Layer and Segment B in the Upper Layer	24
2.11 Two Parallel Segments in the Upper Layer	25
2.12 Segment A in the Upper Layer and Segment B in the Lower Layer	26
2.13 Two Perpendicular Segments in the Lower Layer	30
2.14 Segment A in the Lower Layer and Segment B in the Upper Layer	31
2.15 Two Perpendicular Segments in the Upper Layer	32
2.16 Segment A in the Upper Layer and Segment B in the Lower Layer	33
2.17 A Polygon	47
3.1 The L-Shaped Ground Grid in Case C	58
3.2 The L-Shaped Ground Grid in Case D.	59

Figure	Page
3.3 The Trapezoidal Ground Grid in Case E	60
3.4 The Trapezoidal Ground Grid in Case F.....	60
3.5 The Square Ground Grid.....	66
3.6 The Rectangular Ground Grid in Case II.....	67
3.7 The Rectangular Ground Grid in Case III.....	68
3.8 The L-Shaped Ground Grid in Case IV	69
3.9 The L-Shaped Ground Grid in Case V	70
3.10 The L-Shaped Ground Grid in Case VI	71
3.11 The Trapezoidal Ground Grid in Case VII	72
3.12 The Trapezoidal Ground Grid in Case VIII.....	73
3.13 The Trapezoidal Ground Grid in Case IX.....	74
3.14 The Difference in Percent for the Touch Potential	76
3.15 The Difference in Percent for the Step Potential	76
4.1 The Geometry of the Optimal Design.....	84
4.2 2D Plot and 3D Plot of the Touch Potential	85
4.3 The Perimeter of the L-Shaped Ground Grid	85
4.4 The Geometry of the Optimal Design.....	86
4.5 3D Plot of the Touch Potential.....	87
4.6 The Geometry of the Optimal Design.....	87
4.7 The 3D Plot of the Touch Potential for the Trapezoidal Ground Grid	88

NOMENCLATURE

α	Angle between the segment and the x-axis
β	Angle Between the segment and the x-axis
ϕ	Ground potential rise
ϕ_i	Average voltage
$\varphi(k)$	The integrand φ in the Green's function
$\Omega(k)$	The integrand Ω in the Green's function
ρ	Resistivity of the upper layer soil
ρ_1	Resistivity of the upper layer soil shown in the two layer soil model
ρ_2	Resistivity of the lower layer soil
σ_1	Conductivity of the lower layer soil
σ_2	Conductivity of the upper layer soil
σ_3	Conductivity of the air
$\theta(k)$	The integrand θ in the Green's function
A	The area of the polygon
a	Radius of the segment
C_{cond}	The cost of the horizontal ground grid conductor copper
$C_{connect}$	The cost of labor to make exothermic connection cable to cable or cable to rod

C_{drive}	The cost of labor to drive rods
C_{exo}	The cost of exothermic connector material and mold
c_i	Constant used in the indefinite integral
$Cost$	Total cost of labor and material to build a ground grid
C_{trench}	The cost of labor to trench, install cable, and back-fill
C_x	The x coordinate of the centroid
C_y	The y coordinate of the centroid
D	Thickness of the upper layer soil
DX	Intermediate function DX defined for convenience
$DX2$	Intermediate function $DX2$ defined for convenience
DY	Intermediate function DY defined for convenience
dI/du	Leakage current density
E_{earth}	Earth potential
E_i	Intermediate parameter defined for convenience
E_{step}	The calculated step potential
$E_{step_allowable}$	Maximum allowable step potential

E_{step_OLGGA}	The step potential calculated by OLGGA
E_{step_WinIGS}	The step potential calculated by WinIGS
E_{touch}	The calculated touch potential
$E_{touch_allowable}$	Maximum allowable touch potential
E_{touch_OLGGA}	The touch potential calculated by OLGGA
E_{touch_WinIGS}	The touch potential calculated by WinIGS
F	Intermediate function F defined for convenience
f	Function $f(x)$
G	Intermediate function G defined for convenience
G_{term}	Individual term in the Green's function
h	Bury depth of the ground mat
HLA	Half length of segment A
HLB	Half length of segment B
I_f	Fault current
IG_{term}	Individual term in the series expansion of the earth potential
I_j	Leakage current on the j^{th} segment
I_A	Leakage current on segment A
I_{total}	Total leakage current
$J_0(x)$	Bessel function of the first kind

K_{12}	Reflection coefficient between region 1 and region 2
K_{23}	Reflection coefficient between region 3 and region 2
L	Length of the segment
L_A	The length of segment A
L_B	The length of segment B
$Lh1$	Half length of segment 1
$Lh2$	Half length of segment 2
L_{h_total}	Total length of horizontal conductors
L_{mesh_max}	The coarsest allowable mesh dimension
L_{mesh_min}	The smallest allowable mesh dimension
L_{v_total}	Total length of rods
N	Total number of segments
N_{joints}	Total number of joints of conductors
N_{rod}	Total number of rods
N_{rod_max}	Maximum number of rods
NX	Intermediate function NX defined for convenience
$NX2$	Intermediate function $NX2$ defined for convenience

NY	Intermediate function NY defined for convenience
$PARL$	Individual term in the series expansion of the mutual resistance between two parallel segments
$PERP$	Individual term in the series expansion of the mutual resistance between two perpendicular segments
$P_{\sin i}$	Intermediate function $P_{\sin i}$ defined for convenience
P_{Xi}	Intermediate function P_{Xi} defined for convenience
P_{Yi}	Intermediate function P_{Yi} defined for convenience
r	Coordinate in the cylindrical coordinate system
R_{BA}	Mutual resistance between segment B and segment A
R_g	Ground resistance to the remote earth
R_{ij}	Mutual resistance between segment i and segment j
RM_{nterm}	Individual term in the series expansion of the mutual resistance between two segments that are not orthogonal or parallel to each other

$S_{ij}G$	Intermediate function defined to simplify the expression of the earth potential
t	Intermediate parameter
t_f	Fault duration
U	Intermediate function defined for convenience
u	Intermediate parameter u
v	Intermediate parameter v
V_1	The Green's function in the lower layer
V_2	The Green's function in the upper layer
V_3	The Green's function in the air
VX_{22}	The earth potential caused by the conductor along the x-axis in region 2
VX_{21}	The earth potential caused by the conductor along the x-axis in region 1
VZ_{22}	The earth potential caused by the conductor along the z-axis in region 2
VZ_{21}	The earth potential caused by the conductor along the z-axis in region 1
(X_A, Y_A, Z_{Ai})	Coordinate of the i^{th} image of segment A
(X_B, Y_B, Z_B)	Coordinate of segment B

(x_A, y_A, z_A)	Coordinate of segment A in the Green's function
(x_B, y_B, z_B)	Coordinate of segment B in the Green's function
(x_i, y_i, z_i)	Coordinate in Cartesian coordinate system
(x_{ni}, y_{ni}, z_{ni})	Coordinate in the new coordinate system
(x_{oi}, y_{oi}, z_{oi})	Coordinate in the old coordinate system
X	Intermediate function of the x coordinate
X_j	Intermediate variable of X
X_{sinj}	Intermediate variable X_{sinj} defined for convenience
Y	Intermediate function of the y coordinate
Y_j	Intermediate variable of Y
$YZSQR$	An intermediate variable
Z	Intermediate function of the z coordinate
$Z_{Ai}^{(j)}$	Intermediate variable defined for convenience

1 INTRODUCTION

1.1 Overview

The purpose of installing a ground grid in a substation or a power plant is to protect humans and equipment when there are fault currents injected into the ground. The fault current injected into the ground generates a voltage gradient at the earth's surface, so, on the surface of the ground, the voltage at one point would be different from the voltage at another point due to the resistive-voltage drop caused by the current flow. The voltage difference between a point that is in the substation or the power plant and the remote earth would also be generated by the fault current. This voltage difference is called the touch potential. The touch potential and the step potential that violates the design requirement would harm a person or equipment in the substation or the power plant.

According to IEEE Guide for Safety in AC Substation Ground [1], the touch potential and the step potential limits are given by equations. These limits depend on the soil parameters and the fault current magnitude and the duration of the fault. A well designed ground grid can disperse the fault current into the earth so that the voltage distribution on the surface of the earth will be more uniform, reducing the touch potential, the step potential, the ground resistance to the remote earth, and thus satisfy the safety requirement specified by [1].

The safety requirement is not the only thing that needs to be considered when designing a ground grid. Cost must also be considered. The objective is to minimize material and labor cost by using the fewest number of conductors and ground rods to build a ground grid that satisfies the safety requirement. Therefore we need to optimize the design of the ground grid.

An application that can be used to optimize ground grids has been developed by three students, including the author. The application can support four shapes of ground grids (square, rectangular, L-shaped, and trapezoid). The method that is used to calculate the touch potential, the step potential and the ground resistance to the remote earth in this project is a numerical method based on a computer program written in MATLAB code. The optimization algorithms that are used in this project are the Genetic Algorithm and Pattern Search. They are chosen because the optimization problem is nonlinear and the design variables are integers. Also we cannot guarantee that the optimization problem is convex.

1.2 Literature Review

In industry, the use of a two layer soil model is generally considered to be a good approximation of non-homogeneous soil [2]. The method used to make measurements from which a two layer soil model can be constructed is called the Wenner Method or Four-Pin method and is described in Sunde's book [2]. Wu [20] implemented this method to make an application that can build a two layer soil model from field data.

The method of building a two layer soil and its validation will not be discussed in this work.

Equations exist that allow one to calculate the touch potential and step potential for a ground grid built upon a two layer soil model. There are basically two ways of calculating the touch potential and the step potential. One way is using empirical, closed form equations [1]. The other way is to use a numerical method based on a computer simulation [3] [4] [5]. The first way [1] was the best that could be done for many years but, today, is considered by some to not be accurate enough to meet the safety requirements reliability standards. After computer programming became popular, the numerical approach has been widely used in ground grid analysis and for this purpose, ground grid design software, such as WINIGS, was created [14]. It should be noted that one drawback to WINIGS is that it does not have the capability of performing ground grid optimization. The numerical approach was used in this work to calculate the safety metrics, including the touch potential, the step potential, and the ground resistance.

To perform the calculations of the safety metrics using the numerical method, the first step that needs to be performed is conductor segmentation. The idea of segmentation was proposed by F. Dawalibi [6]. The leakage current forms a current density field in the soil. The potential at each point in the soil depends on the distribution of the current density field. The current density field satisfies a linear equation of the current density field in the literature [12]. This suggests the superposition principle

can be used to calculate the current distribution generated by all leakage current on the whole ground grid by summing over the current distributions generated by the leakage current on each segment.

In many textbooks, the Green's function is defined to be the field excited by a point source under certain boundary conditions. Because the earth resistivity is constant (within each layer) and not a function of current, Green's functions can be used along with the superposition principle.

A. P. Meliopoulos proposed explicit a Green's function expression for solution of the current field differential equation in a two layer soil model, which is expressed as an infinite series [12]. Two methods to calculate the voltage induced by the current leaking from each segment are given in the SOMIP [13]. The first method assumes the dimensions of the conductor segment under study can be neglected so that the segment can be treated as a point source. The second method is to integrate the Green's function multiplied by the leakage current density along the line segment to get the voltage induced by the leakage current of that segment.

A complex image method was invented by Y. L. Chow [7] to reduce the series of the Green's function into the summation of a finite number of terms. Many researchers have used this method [8][9][10][11].

In the ground grid optimization application described in this work, the equations proposed by A.P. Meliopoulos [12] were used to calculate the safety metrics for

square grids, rectangular grid, and L-shaped grids. Equations for calculating the mutual resistance between any two conductor segments that are parallel or orthogonal with any one of the axes was also provided in [12].

Triangular ground grid analysis was done in [15]. However, the author used stair-step-shaped conductors to approximate the hypotenuse of the trapezoidal ground grid, which was viewed to possibly be problematic.

Once the equation for calculating the safety metrics are derived, the optimization algorithms need to be selected. The optimization of a ground grid is a nonlinear mixed integer problem, with some nonlinear constraints, which are the safety metrics, i.e., the touch potential, the step potential and the ground resistance to the remote earth. Additionally, we cannot guarantee that the problem is convex. Traditional deterministic optimization algorithms cannot be used. Instead, the Genetic Algorithm (GA), a heuristic algorithm developed by J. Holland [16], was used in the application. Genetic Algorithms are probably the most popular evolutionary algorithms in terms of the diversity of their applications [17]. Ground grid optimization was studied using the GA in [18] and [19]. Pattern search has been used with GA to get the solution of the optimization in [20] and [21].

Research on the optimization of ground grids with non-uniform grid meshes was performed by [19]; however, the meshes in this work were restricted to having uniform size.

1.3 The Objective

The objective of this project is to develop a software application that can optimize the design of the ground grids with different shaped footprints, including square, rectangular, L-shaped, and trapezoid. The optimized ground grid must satisfy the safety requirements, which include the following items:

1. The touch potential must be lower than the maximum allowable value calculated from the equation in IEEE Std 80-2000 [1]

$$E_{touch_allowable} = (1000 + 1.5\rho) \frac{0.116}{\sqrt{t_f}} \quad (1.1)$$

where ρ is the upper soil earth resistivity and t_f is the time duration of the fault.

2. The step potential must be lower than the maximum allowable value calculated from the equation in IEEE Std 80-2000 [1]

$$E_{step_allowable} = (1000 + 6\rho) \frac{0.116}{\sqrt{t_f}} \quad (1.2)$$

where ρ is the upper soil earth resistivity and t_f is the time duration of the fault.

3. The ground resistance to the remote earth must be lower than 0.5 Ω .

Other design requirements, such as the minimum allowable mesh dimension, the maximum mesh dimension, the minimum number of ground rods, the minimum separation distance between adjacent ground rods, are provided by Salt River Project (SRP).

Since the equations used for calculating the earth potential induced by a conductor segment with an arbitrary orientation in a horizontal plane could not be found by the

author, the author has to derive the required equations from the Green's functions provided in [12] in order to deal with the trapezoidal ground grids. Two numerical integration methods to calculate the mutual resistance between any two conductor segments in any direction in a horizontal plane are used to calculate the mutual resistance matrix for the trapezoidal ground grids.

1.4 Thesis Organization

There are six chapters in the thesis including the introduction chapter and the conclusion chapter. The mathematical model used to calculate the safety metrics, the results of program validation, a short introduction on the optimization algorithms, and a user's manual of the Optimal Ground Grid Application are presented.

Chapter 2 presents the mathematical method used to calculate the touch potential, the step potential, and the ground resistance to the remote earth. These quantities are used as constraints in the optimization statement.

Chapter 3 presents the idea of self-consistency, and the validation of our application by comparing the results of our application with the results of WINIGS, a commercialized ground grid design software.

Chapter 4 presents a short introduction of the Genetic Algorithm and Pattern Search, and the description of the optimization of ground grids, including the objective function and constraints. Chapter 5 is the conclusion.

The appendix is the user's manual of Optimal Ground Grid Application.

2 MATHEMATICAL MODELS

This section presents the method by which the touch potential, the step potential and the ground resistance to the remote earth are calculated. An introduction to the two-layer soil model is given in the first section and the process of calculating the safety metrics is discussed in the following sections.

2.1 The Two Layer Soil Model

The two layer soil model is shown in Fig 2.1.

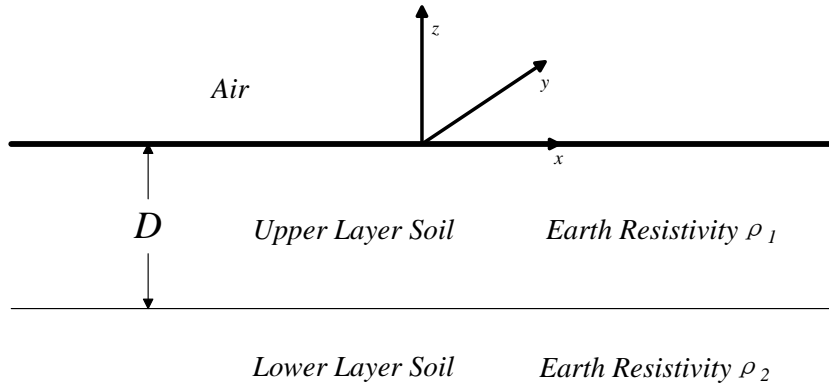


Fig 2.1 Two Layer Soil Model

The parameters ρ_1 , ρ_2 , and D are the parameters that best fit the apparent earth resistance. The least-square regression method that was used to obtain these parameters is presented in [20].

2.2 Ground Grid Model

According to IEEE standard, a ground grid is defined to be “a system of horizontal ground electrodes that consists of a number of interconnected, bare conductors buried in the earth, providing a common ground for electrical devices or metallic structures” [1]. In this work, the ground grid contains horizontal conductors and vertical ground rods. The horizontal conductors are bare conductors and form a ground mat, which is also defined in the IEEE standard [1]. The ground rods are bare conductors that must at least be placed on each corner of the ground grid, according the SRP ground grid design requirement for placing ground rods, BI03.05 [23]. The ground rods are evenly spaced along the outer grid perimeter, not less than one rod length apart [23]. The top of the ground rod is connected with the ground mat, so the depth of the top tip of the ground rod is the same as the depth of the ground mat. The internal resistance of the ground grid is neglected.

2.2.1 Ground Grid Segmentation

As a simple example, suppose we wish to calculate the earth potential induced by the current leaking from a conductor along the x-axis buried in the uniform soil with its center at the origin, as shown in Fig 2.2.

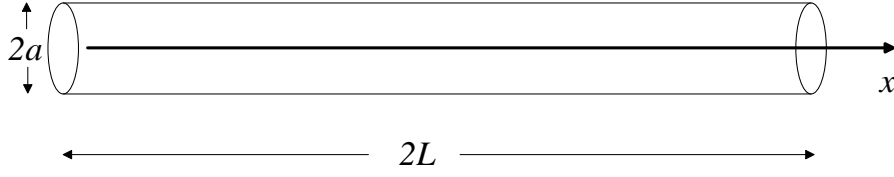


Fig 2.2 A Conductor along the x-Axis

To calculate such a potential, we need to know the leakage current density on this conductor, and that is obtained by solving the following equation from [2],

$$0 = \frac{d}{dx} \int_{-L/2}^{L/2} [(x-u)^2 + a^2]^{-1/2} \frac{dI}{du} du \quad (2.1)$$

where L is the length of the conductor, a is the conductor radius, and dI/du is the leakage current density.

The restriction on the total leakage current I_{total} on this conductor is

$$I_{total} = \int_{-L/2}^{L/2} \frac{dI}{du} du \quad (2.2)$$

One will soon find that no closed form solution for the leakage current density can be found for this equation. But such a problem can be solved numerically.

To obtain accuracy, we divide the conductor into N segments, each with a uniform length that is sufficiently short compared to the total length of the conductor. Suppose that the mutual resistance between the i^{th} conductor segment and the j^{th} conductor segment is R_{ij} , and the self-resistance of the i^{th} conductor segment is R_{ii} . The R_{ij} is calculated as the average potential on the i^{th} conductor segment induced by the leakage current on the j^{th} conductor segment and R_{ii} is calculated as the average potential induced by the leakage current on the surface of the i^{th} conductor segment itself. According to

the definition in Sunde's book [2], the mutual resistance is the same regardless of which conductor segment is the primary, and it only applies to linear circuits, in which the mutual resistance does not depend on the current. This means that we can exchange the two indices of R_{ij} without changing its value.

By the definition above, we can express the average voltage of the i^{th} conductor segment in terms of its self-resistance, the mutual resistance between the i^{th} conductor segment and other conductors, and the leakage current on each conductor,

$$\phi_i = \sum_{j=1}^N R_{ij} I_j \quad (2.3)$$

where ϕ_i is the average voltage of the i^{th} conductor, and I_j is the leakage current on the j^{th} conductor and N is the number of conductor segments in the model.

Because the resistivity of the conductor is neglected, the average potential of each conductor segment must be the same. Writing the above equation in a matrix form one obtains,

$$\begin{bmatrix} R_{11} & R_{12} & \cdots & R_{1N} \\ R_{21} & R_{22} & \cdots & R_{2N} \\ \vdots & \vdots & \ddots & \vdots \\ R_{N1} & R_{N2} & \cdots & R_{NN} \end{bmatrix} \begin{bmatrix} I_1 \\ I_2 \\ \vdots \\ I_N \end{bmatrix} = \begin{bmatrix} \phi \\ \phi \\ \vdots \\ \phi \end{bmatrix} \quad (2.4)$$

where the element in the column vector on the right-hand side of the equation is the potential of the conductor. The N by N matrix on the left hand side is called the mutual resistance matrix. The method by which its entries are calculated in a two-layer soil model is presented in the following sections.

One may notice immediately that the matrix equation (2.4) has $N+1$ unknown variables, but only N independent equations are written. The reason is that we did not take the restriction on the total current into consideration. Another equation is needed which constrains the total current injected into the earth to be equal to the fault current,

$$\sum_{j=1}^N I_j = I_{total} \quad (2.5)$$

This equation and the matrix equation is combined into another matrix equation, and after some algebraic manipulation, we have,

$$\begin{bmatrix} R_{11} & R_{12} & \cdots & R_{1N} & -1 \\ R_{21} & R_{22} & \cdots & R_{2N} & -1 \\ \vdots & \vdots & \ddots & \vdots & \vdots \\ R_{N1} & R_{N2} & \cdots & R_{NN} & -1 \\ 1 & 1 & \cdots & 1 & 0 \end{bmatrix} \begin{bmatrix} I_1 \\ I_2 \\ \vdots \\ I_N \\ \phi \end{bmatrix} = \begin{bmatrix} 0 \\ 0 \\ \vdots \\ 0 \\ I_{total} \end{bmatrix} \quad (2.6)$$

By solving this equation, the leakage current on each conductor segment and the potential of the conductor can be determined. Once the leakage current distribution has been determined, we can calculate the earth potential induced by this current distribution at any point in the soil by using the Green's function, which will be presented in the following sections.

2.2.2 The Green's function in a Two Layer Soil Model

The Green's function allows us to find the potential induced by a unit point source.

In a two-layer soil model, the literature [12] presents the necessary Green's function.

In order to implement the equations more conveniently, a new convention is used to label the regions and the parameters of the two-layer soil model, and is shown in Fig

2.3.

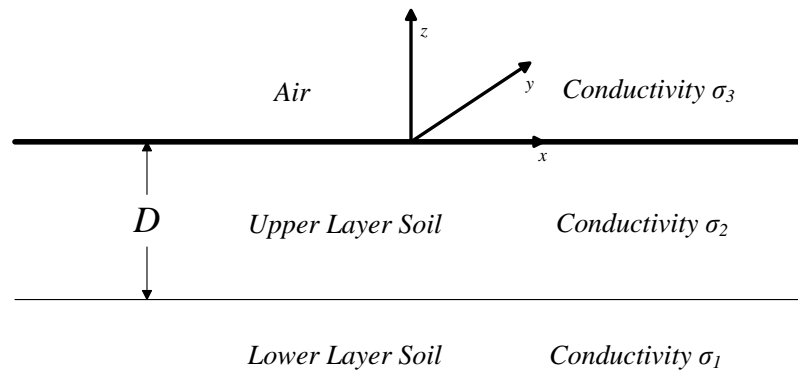


Fig 2.3 Two Layer Soil Model with 3 Regions

In Fig 2.3, D is the depth of the surface between the upper layer and the lower layer, and σ_1 is the conductivity of the soil of in the lower layer, σ_2 is the conductivity of the soil of in the upper layer, and σ_3 is the conductivity of the air and it is assumed to be zero.

Given the Bessel function of the first kind, $J_0(x)$, if a point source of unit intensity is located on the z -axis is in the upper layer of soil, as shown in Fig 2.4,

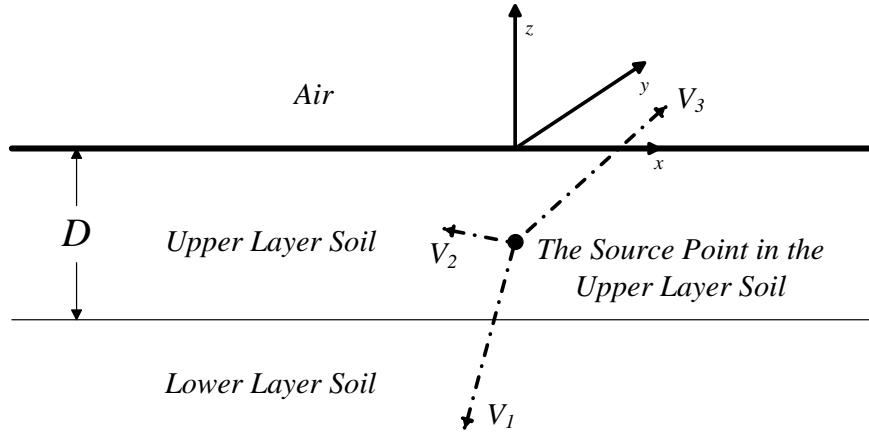


Fig 2.4 The Source Point in the Upper Layer Soil

$$V_2(r, z) = \frac{1}{4\pi\sigma_2} \left[\int_0^\infty J_0(kr) e^{-k|z-Z_1|} dk + \int_0^\infty \psi(k) J_0(kr) e^{-kz} dk + \int_0^\infty \theta(k) J_0(kr) e^{kz} dk \right] \quad (2.7)$$

for the field point (r, z) in the upper layer of soil, and

$$V_1(r, z) = \frac{1}{4\pi\sigma_2} \int_0^\infty \varphi(k) J_0(kr) e^{kz} dk \quad (2.8)$$

for the field point (r, z) in the lower layer of soil, and

$$V_3(r, z) = \frac{1}{4\pi\sigma_2} \int_0^\infty \Omega(k) J_0(kr) e^{-kz} dk \quad (2.9)$$

for the field point (r, z) in the air, where the unknown functions $\varphi(k)$, $\theta(k)$, $\Omega(k)$, and $\psi(k)$ must be found using the boundary conditions at the two boundaries $z=0$ and $z=D$, namely, the potential at the boundary and the current density normal to the boundary on each side of the boundary must be continuous.

After the four unknown functions are found using the boundary conditions and are substituted into the expressions of the Green's function, and after the terms with exponential functions are expanded into a series in order to facilitate calculation, then, by the identity

$$\int_0^{\infty} J_0(kr) e^{-k|z|} dk = \frac{1}{\sqrt{r^2 + z^2}} \quad (2.10)$$

(2.7) and (2.8)¹ can be rewritten as,

$$\begin{aligned} V_2(r, z) = & \frac{1}{4\pi\sigma_2} \left[\frac{1}{[r^2 + (z - Z_1)^2]^{1/2}} \right. \\ & - K_{12} \sum_{i=0}^{\infty} \frac{(K_{12}K_{32})^i}{[r^2 + (z + Z_1 - 2(i+1)D)^2]^{1/2}} \\ & + \sum_{i=1}^{\infty} \frac{(K_{12}K_{32})^i}{[r^2 + (z - Z_1 + 2iD)^2]^{1/2}} \\ & - K_{32} \sum_{i=0}^{\infty} \frac{(K_{12}K_{32})^i}{[r^2 + (z + Z_1 + 2iD)^2]^{1/2}} \\ & \left. + \sum_{i=1}^{\infty} \frac{(K_{12}K_{32})^i}{[r^2 + (z - Z_1 - 2iD)^2]^{1/2}} \right] \end{aligned} \quad (2.11)$$

$$\begin{aligned} V_1(r, z) = & \frac{1}{2\pi(\sigma_1 + \sigma_2)} \left[K_{12} \sum_{i=0}^{\infty} \frac{(K_{12}K_{32})^i}{[r^2 + (z - Z_1 + 2iD)^2]^{1/2}} \right. \\ & \left. - K_{32} \sum_{i=0}^{\infty} \frac{(K_{12}K_{32})^i}{[r^2 + (z + Z_1 + 2iD)^2]^{1/2}} \right] \end{aligned} \quad (2.12)$$

where the K_{ij} values in (2.11) and (2.12) are obtained from solution of the Green's functions

¹ There are typos in the equation, which is labeled as A-28, in page A-7 of the literature [12], including the misplacement of a square bracket, which makes the dimension of the equation incorrect; the sign between z and Z_1 in the denominator of the second last series should be plus, instead of minus; the sign between Z_1 and $2iD$ in the denominator of the last series should be minus instead of plus. If these were not typos, the equation wouldn't match the equation A-51b in the literature [12], which is derived from equation A-7. The typo is corrected in the presentation here.

We are not interested in rewriting (2.9), because that is the equation for a field point above the earth's surface.

By a similar process, the expressions of the Green's function for a point source of unit intensity in the lower soil layer, as shown in Fig 2.5, are

$$V_2(r, z) = \frac{1}{2\pi(\sigma_1 + \sigma_2)} \left[\sum_{i=0}^{\infty} \frac{(K_{12}K_{32})^i}{[r^2 + (z - Z_1 - 2iD)^2]^{1/2}} - K_{32} \sum_{i=0}^{\infty} \frac{(K_{12}K_{32})^i}{[r^2 + (z + Z_1 + 2iD)^2]^{1/2}} \right] \quad (2.13)$$

$$V_1(r, z) = \frac{1}{4\pi\sigma_1} \left[\frac{1}{[r^2 + (z - Z_1)^2]^{1/2}} + K_{12} \sum_{i=0}^{\infty} \frac{(K_{12}K_{32})^i}{[r^2 + (z + Z_1 + 2(i-1)D)^2]^{1/2}} - K_{32} \sum_{i=0}^{\infty} \frac{(K_{12}K_{32})^i}{[r^2 + (z + Z_1 + 2iD)^2]^{1/2}} \right] \quad (2.14)$$

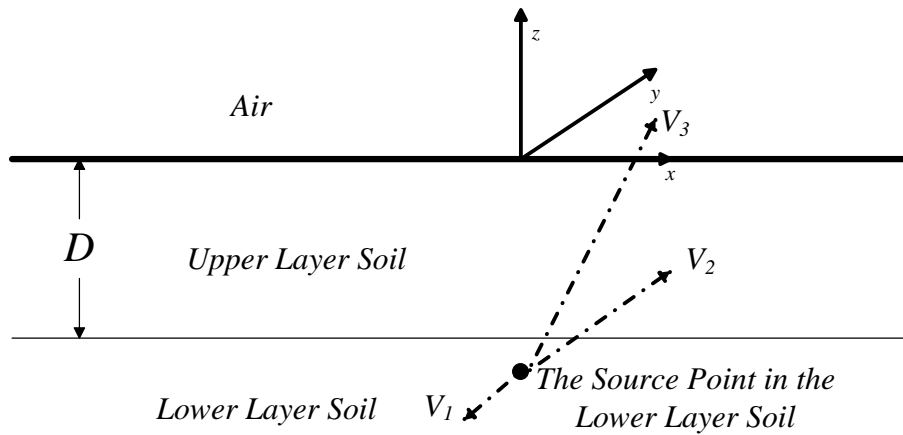


Fig 2.5 The Source Point in the Lower Layer Soil

Equations (2.11), (2.12), (2.13) and (2.14) are the expressions for the voltages a point (r, z) obtained by using Green's functions in a two layer soil model. They are used to derive the equations for the earth potential, the mutual resistance, and the self-

resistance. The series in these equations represents the effect of the images of the point source due to the stratification of the soil.

2.3 The Mutual Resistance Matrix Line-Line Model

In order to solve the matrix equation (2.6) for the leakage current on each conductor segment, the elements in the mutual resistance matrix, R_{ij} , need to be calculated first. The result of the mutual-resistance calculation should be accurate and the execution time should be acceptable, hence two ways of modeling the mutual resistance are used. They are the line-line model and the point-point model.

The criterion that is used to choose which model is used is based on the distance between the centers of the two conductor segments. If the distance between centers of the two conductor segments is less than the arithmetic average of the lengths of the two conductors, the line-line model is used; otherwise, the point-point model is used. In other words, if the two conductor segments are “close,” we use the line-line model. The line-line is always used to calculate the self-resistance of each conductor segment. In this section, the line-line model is presented.

To make the concept clearer, we may write the Green's function in a more general form

$$G(x_B, y_B, z_B; x_A, y_A, z_A) \quad (2.15)$$

where (x_A, y_A, z_A) is the coordinate of the source point, and (x_B, y_B, z_B) is the coordinate of the field point, as shown in Fig 2.6. So according to the definition of the

Green's function, (2.15) is the potential at point B induced by a point source of unit intensity at point A.

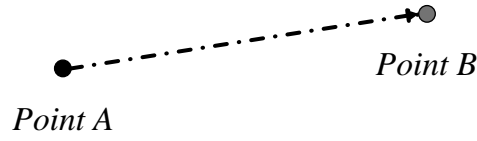


Fig 2.6 The Source Point and the Field Point

Assume that the leakage current I_A is uniform on the conductor segment A, the leakage current density on the conductor segment A is I_A/L_A , where L_A is the length of the conductor segment A. As shown in Fig 2.7, according to the definition of the Green's function, the line integration of the product of the leakage current density and the Green's function gives the earth potential induced by the leakage current on the conductor segment A at the field point (x_B, y_B, z_B)

$$V(x_B, y_B, z_B) = \frac{I_A}{L_A} \int_{L_A} G(x_B, y_B, z_B; x_A, y_A, z_A) dL_A \quad (2.16)$$

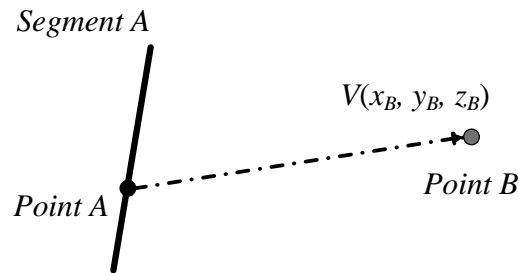


Fig 2.7 The Segment and the Field Point

The line integration of (2.16), along the conductor segment B divided by the length of the conductor segment B, L_B , gives the average potential of the conductor segment B induced by the leakage current on the conductor segment A, as shown in Fig 2.8.

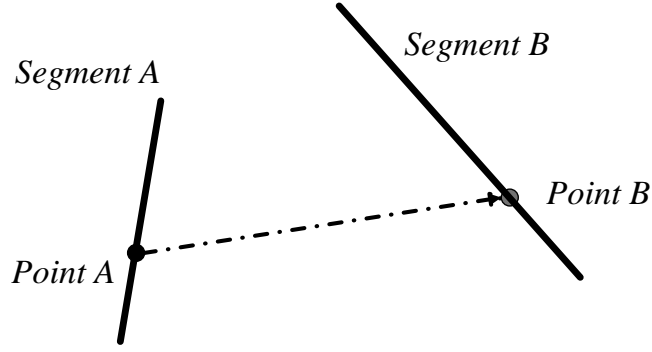


Fig 2.8 Two Segments

Divide the average potential on the conductor segment B by the leakage current on conductor segment A, we have the mutual resistance R_{BA} , which is expressed in terms of the Green's function as

$$R_{BA} = \frac{1}{L_A L_B} \int_{L_B} dL_B \int_{L_A} G(x_B, y_B, z_B; x_A, y_A, z_A) dL_A \quad (2.17)$$

As shown in (2.17), the general formula of the mutual resistance looks concise, but if we substitute the exact expressions of the Green's function (2.11), (2.12), (2.13), (2.14), and consider the different orientations of the two conductor segments placed in different regions of the two-layer soil, the expression of the mutual resistance turns out to be quite long.

Literature [13] shows the equations that are used to calculate the mutual resistance between any two conductor segments that are parallel to the x-, y-, or z-axis. There are many possible configurations of the two conductors, because the two conductor segments may be in different layers of the soil and may be parallel to different axes. The mutual resistance, however, does not depend on what coordinate-system we choose. In another words, if we have a conductor segment A along the y-axis, and a

conductor segment B along the z-axis, we can rotate the coordinate system about the z-axis so that after the rotation conductor segment A is along x-axis, but the mutual resistance between the two segments does not change after the rotation of the coordinate system. By virtue of the coordinate independence of the mutual resistance, we do not have to write down the equation for the mutual resistance of a conductor segment along the y-axis and a conductor segment along the z-axis, if we already have the equation for the mutual resistance between a conductor segment along the x-axis and a conductor segment along the z-axis. Note that we cannot rotate our coordinate systems about the y or x axes as the orientation with respect to being parallel or orthogonal to the layer interfaces must be preserved².

Based on the coordinate independence of the mutual resistance introduced (and as limited) in the previous paragraph, the required equations for the mutual resistance that need to be written down are greatly reduced.

Assume that the coordinate of the center of segment A or the image of segment A is (X_A, Y_A, Z_{Ai}) , where the index i is used to indicate that Z_{Ai} is the z coordinate of the i^{th} image of the segment A, and the coordinate of segment B is (X_B, Y_B, Z_B) . Assume that L_A is the length of segment A and L_B is the length of segment B. Because there are an infinite number of images of segment A, the expression of the mutual re-

² According to literature [13], rotation about the x and y axis is used for ground rod and does not introduce significant errors.

sistance includes a series with an infinite number of terms. When the conductor segment A is parallel to the conductor segment B, the process to calculate the mutual resistance R_{BA} is shown below.

If segment A and segment B are both parallel to the x-axis, according to literature [13], the difference between the coordinate of the centers of the two segments are

$$X = X_B - X_A \quad (2.18)$$

$$Y = Y_B - Y_A \quad (2.19)$$

$$Z = Z_B - Z_{Ai} \quad (2.20)$$

If segment A and segment B are both parallel to the y-axis, the difference between the coordinates of the centers of the two segments is written as [13]

$$X = Y_B - Y_A \quad (2.21)$$

$$Y = X_B - X_A \quad (2.22)$$

$$Z = Z_B - Z_{Ai} \quad (2.23)$$

If segment A and segment B are both parallel to the z-axis, the difference of between the coordinate of the centers of the two segments is written as [13]

$$X = Z_B - Z_{Ai} \quad (2.24)$$

$$Y = Y_B - Y_A \quad (2.25)$$

$$Z = X_B - X_A \quad (2.26)$$

In order to simplify the equations, some intermediate variables are defined in the following equations [13],

$$X_1 = X + HLB - HLA \quad (2.27)$$

$$X_2 = X + HLB + HLA \quad (2.28)$$

$$X_3 = X - HLB - HLA \quad (2.29)$$

$$X_4 = X - HLB + HLA \quad (2.30)$$

where HLA is half of the length of segment A, L_A , and HLB is half of the length of segment B, L_B .

Because the two segments are parallel, according to the variables defined in (2.19), (2.20), (2.22), (2.23), (2.25) and (2.26) the square of the distance between the two segments is:

$$YZSQR = Y^2 + Z^2 \quad (2.31)$$

When $YZSQR$ is less than 10^{-6} m^2 , the individual term, denoted by $PARL$, in the series in the expression of the mutual resistance between two parallel segments, such as (2.34), is calculated by the use of the following equation, omitting the dependence on HLA and HLB [13],

$$\begin{aligned} PARL(X_A, Y_A, Z_{Ai}; X_B, Y_B, Z_B) = & \sqrt{X_1^2 + Y^2 + Z^2} \\ & - \sqrt{X_2^2 + Y^2 + Z^2} - \sqrt{X_3^2 + Y^2 + Z^2} + \sqrt{X_4^2 + Y^2 + Z^2} \\ & - X_1 \ln(|X_1|) + X_2 \ln(|X_2|) \\ & + X_3 \ln(|X_3|) - X_4 \ln(|X_4|) \end{aligned} \quad (2.32)$$

When any of the X_i ($i=1, 2, 3, 4$) is less than 10^{-6} , the corresponding $X_i \ln(|X_i|)$ term should be removed from equation (2.32), because when the terms $X_i \ln(|X_i|)$ are small compared to other terms, they can be neglected.

When $YZSQR$ is greater than 10^{-6} , the individual term $PARL$ should be calculated according to the following equation, omitting the dependence on HLA and HLB [13],

$$\begin{aligned}
 PARL(X_A, Y_A, Z_{Ai}; X_B, Y_B, Z_B) = & \sqrt{X_1^2 + Y^2 + Z^2} \\
 & - \sqrt{X_2^2 + Y^2 + Z^2} - \sqrt{X_3^2 + Y^2 + Z^2} + \sqrt{X_4^2 + Y^2 + Z^2} \\
 & - X_1 \ln(X_1 + \sqrt{X_1^2 + Y^2 + Z^2}) + X_2 \ln(X_2 + \sqrt{X_2^2 + Y^2 + Z^2}) \\
 & + X_3 \ln(X_3 + \sqrt{X_3^2 + Y^2 + Z^2}) - X_4 \ln(X_4 + \sqrt{X_4^2 + Y^2 + Z^2})
 \end{aligned} \tag{2.33}$$

Now, we have the equations to calculate the terms in the series of the expression of the mutual resistance for two conductors segments that are parallel to each other and are parallel to the x-, y-, or z-axis. The expression of the mutual resistance is written as the followings, in terms of $PARL$.

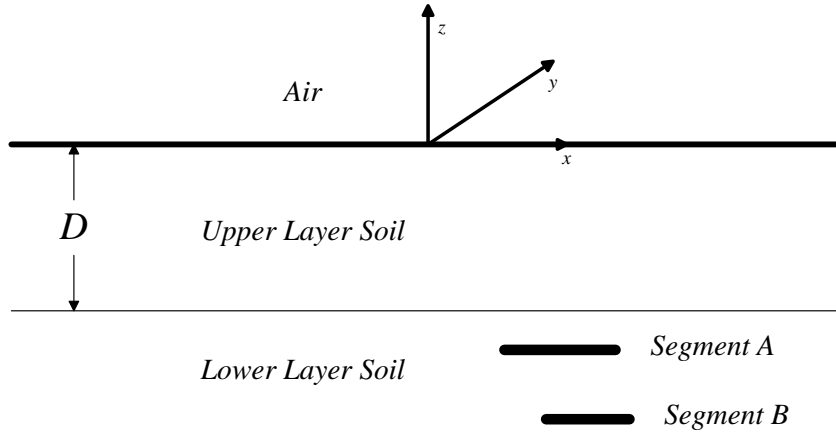


Fig 2.9 Two Parallel Segments in the Lower Layer

When the two segments are both in the lower layer of soil, as shown in Fig 2.9, the mutual resistance term is given by [13],

$$\begin{aligned}
 R_{BA} = & \frac{1}{4\pi\sigma_1 L_A L_B} \left(\sum_{i=0}^{\infty} K_{12} (K_{12} K_{32})^i PARL(X_A, Y_A, Z_{Ai}^{(1)}; X_B, Y_B, Z_B) \right. \\
 & \left. - \sum_{i=0}^{\infty} K_{32} (K_{12} K_{32})^i PARL(X_A, Y_A, Z_{Ai}^{(2)}; X_B, Y_B, Z_B) \right)
 \end{aligned} \tag{2.34}$$

where

$$Z_{Ai}^{(1)} = -Z_A - 2(i-1)D \quad (2.35)$$

$$Z_{Ai}^{(2)} = -Z_A - 2iD \quad (2.36)$$

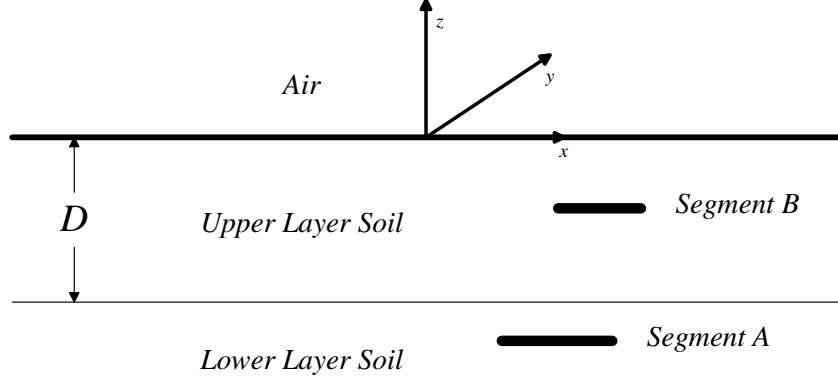


Fig 2.10 Segment A in the Lower Layer and Segment B in the Upper Layer

When segment A is in the lower layer of soil and segment B is in the upper layer of soil, as shown in Fig 2.10, the mutual resistance term is given by[13],

$$R_{BA} = \frac{1}{2\pi(\sigma_1 + \sigma_2)L_A L_B} \left(\sum_{i=0}^{\infty} (K_{12}K_{32})^i \text{PARL}(X_A, Y_A, Z_{Ai}^{(1)}; X_B, Y_B, Z_B) - \sum_{i=0}^{\infty} K_{32}(K_{12}K_{32})^i \text{PARL}(X_A, Y_A, Z_{Ai}^{(2)}; X_B, Y_B, Z_B) \right) \quad (2.37)$$

where

$$Z_{Ai}^{(1)} = Z_A + 2iD \quad (2.38)$$

$$Z_{Ai}^{(2)} = -Z_A - 2iD \quad (2.39)$$

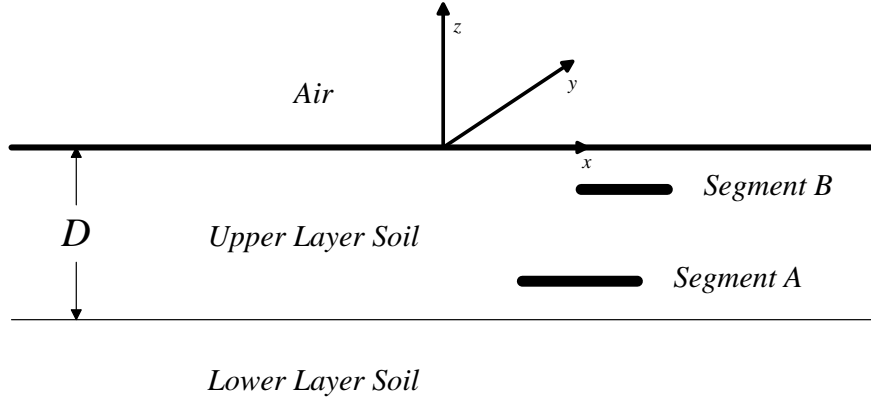


Fig 2.11 Two Parallel Segments in the Upper Layer

When both segment A and segment B are in the upper layer of soil, as shown in

Fig 2.11, the mutual resistance term is given by [13],

$$\begin{aligned}
 R_{BA} = \frac{1}{4\pi\sigma_2 L_A L_B} & \left(\sum_{i=0}^{\infty} (K_{12} K_{32})^i \text{PARL}(X_A, Y_A, Z_{Ai}^{(1)}; X_B, Y_B, Z_B) \right. \\
 & - \sum_{i=0}^{\infty} K_{12} (K_{12} K_{32})^i \text{PARL}(X_A, Y_A, Z_{Ai}^{(2)}; X_B, Y_B, Z_B) \\
 & + \sum_{i=0}^{\infty} (K_{12} K_{32})^i \text{PARL}(X_A, Y_A, Z_{Ai}^{(3)}; X_B, Y_B, Z_B) \\
 & \left. - \sum_{i=0}^{\infty} K_{32} (K_{12} K_{32})^i \text{PARL}(X_A, Y_A, Z_{Ai}^{(4)}; X_B, Y_B, Z_B) \right) \quad (2.40)
 \end{aligned}$$

where

$$Z_{Ai}^{(1)} = Z_A - 2iD \quad (2.41)$$

$$Z_{Ai}^{(2)} = -Z_A + 2(i+1)D \quad (2.42)$$

$$Z_{Ai}^{(3)} = Z_A + 2iD \quad (2.43)$$

$$Z_{Ai}^{(4)} = -Z_A - 2iD \quad (2.44)$$

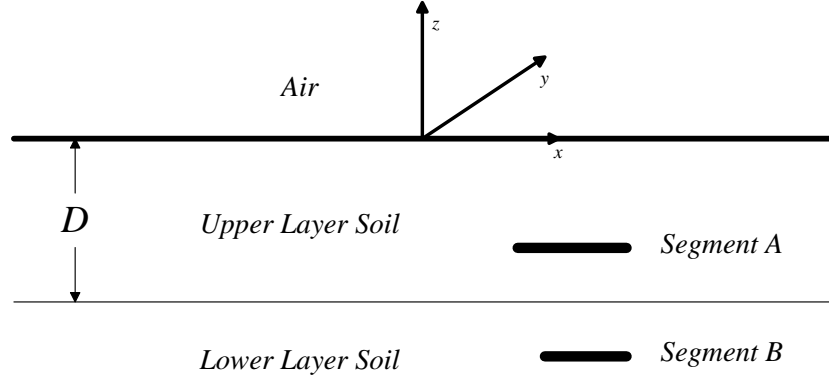


Fig 2.12 Segment A in the Upper Layer and Segment B in the Lower Layer

When segment A is in the upper layer of soil and segment B is in the lower layer of soil, as shown in Fig 2.12, the mutual resistance term is given by [13],

$$R_{BA} = \frac{1}{2\pi(\sigma_1 + \sigma_2)L_A L_B} \left(\sum_{i=0}^{\infty} (K_{12}K_{32})^i \text{PARL}(X_A, Y_A, Z_{Ai}^{(1)}; X_B, Y_B, Z_B) - \sum_{i=0}^{\infty} K_{32}(K_{12}K_{32})^i \text{PARL}(X_A, Y_A, Z_{Ai}^{(2)}; X_B, Y_B, Z_B) \right) \quad (2.45)$$

where

$$Z_{Ai}^{(1)} = Z_A - 2iD \quad (2.46)$$

$$Z_{Ai}^{(2)} = -Z_A - 2iD \quad (2.47)$$

Now we have the equations to calculate the mutual resistance when the two segments are parallel to each other and are parallel to any coordinate axis. The process of calculating the mutual resistance when the two conductors segments are perpendicular to each other is presented below.

First, some intermediate variables are defined to simplify the equations. When segment A is parallel to the x-axis and segment B is parallel to the y-axis [13],

$$X_1 = |X_B - X_A| + HLA \quad (2.48)$$

$$X_2 = |X_B - X_A| - HLA \quad (2.49)$$

$$Y_1 = |Y_B - Y_A| + HLB \quad (2.50)$$

$$Y_2 = |Y_B - Y_A| - HLB \quad (2.51)$$

$$Z = |Z_B - Z_{Ai}| \quad (2.52)$$

When segment A is parallel to the y-axis and segment B is parallel to the x-axis

$$X_1 = |X_B - X_A| + HLB \quad (2.53)$$

$$X_2 = |X_B - X_A| - HLB \quad (2.54)$$

$$Y_1 = |Y_B - Y_A| + HLA \quad (2.55)$$

$$Y_2 = |Y_B - Y_A| - HLA \quad (2.56)$$

$$Z = |Z_B - Z_{Ai}| \quad (2.57)$$

When segment A is parallel to the x-axis and segment B is parallel to the z-axis

$$X_1 = |X_B - X_A| + HLA \quad (2.58)$$

$$X_2 = |X_B - X_A| - HLA \quad (2.59)$$

$$Y_1 = |Z_B - Z_{Ai}| + HLB \quad (2.60)$$

$$Y_2 = |Z_B - Z_{Ai}| - HLB \quad (2.61)$$

$$Z = |Y_B - Y_A| \quad (2.62)$$

When segment A is parallel to the z-axis and segment B is parallel to the x-axis

$$X_1 = |X_B - X_A| + HLB \quad (2.63)$$

$$X_2 = |X_B - X_A| - HLB \quad (2.64)$$

$$Y_1 = |Z_B - Z_{Ai}| + HLA \quad (2.65)$$

$$Y_2 = |Z_B - Z_{Ai}| - HLA \quad (2.66)$$

$$Z = |Y_B - Y_A| \quad (2.67)$$

When segment A is parallel to the y-axis and segment B is parallel to the z-axis

$$Y_1 = |Y_B - Y_A| + HLA \quad (2.68)$$

$$Y_2 = |Y_B - Y_A| - HLA \quad (2.69)$$

$$X_1 = |Z_B - Z_{Ai}| + HLB \quad (2.70)$$

$$X_2 = |Z_B - Z_{Ai}| - HLB \quad (2.71)$$

$$Z = |X_B - X_A| \quad (2.72)$$

When segment A is parallel to the z-axis and segment B is parallel to the y-axis

$$Y_1 = |Y_B - Y_A| + HLB \quad (2.73)$$

$$Y_2 = |Y_B - Y_A| - HLB \quad (2.74)$$

$$X_1 = |Z_B - Z_{Ai}| + HLA \quad (2.75)$$

$$X_2 = |Z_B - Z_{Ai}| - HLA \quad (2.76)$$

$$Z = |X_B - X_A| \quad (2.77)$$

The following intermediate variables are also defined [13],

$$P_{Y1} = \begin{cases} Y_1 \ln \left(\frac{X_1 + \sqrt{X_1^2 + Y_1^2 + Z^2}}{X_2 + \sqrt{X_2^2 + Y_1^2 + Z^2}} \right) & , |Y_1| > 10^{-4} \\ 0 & , |Y_1| \leq 10^{-4} \end{cases} \quad (2.78)$$

$$P_{X1} = \begin{cases} X_1 \ln \left(\frac{Y_1 + \sqrt{X_1^2 + Y_1^2 + Z^2}}{X_2 + \sqrt{X_1^2 + Y_2^2 + Z^2}} \right) & , |X_1| > 10^{-4} \\ 0 & , |X_1| \leq 10^{-4} \end{cases} \quad (2.79)$$

$$P_{Y_2} = \begin{cases} Y_2 \ln \left(\frac{X_2 + \sqrt{X_2^2 + Y_2^2 + Z^2}}{X_1 + \sqrt{X_1^2 + Y_2^2 + Z^2}} \right) & , |Y_2| > 10^{-4} \\ 0 & , |Y_2| \leq 10^{-4} \end{cases} \quad (2.80)$$

$$P_{X_2} = \begin{cases} X_2 \ln \left(\frac{Y_2 + \sqrt{X_2^2 + Y_2^2 + Z^2}}{X_2 + \sqrt{X_2^2 + Y_1^2 + Z^2}} \right) & , |X_2| > 10^{-4} \\ 0 & , |X_2| \leq 10^{-4} \end{cases} \quad (2.81)$$

where the different values for the $|X|$ ranges mean that when the coefficients of the terms with the log functions are sufficiently small comparing to other terms, they can be neglected.

When $|Z|$ is greater than 0, the following intermediate variables are defined [13],

$$X_{\sin 1} = \frac{X_1 Y_1^2 + Z^2 \sqrt{X_1^2 + Y_1^2 + Z^2}}{(Y_1^2 + Z^2) \sqrt{X_1^2 + Z^2}} \quad (2.82)$$

$$X_{\sin 2} = \frac{X_1 Y_2^2 + Z^2 \sqrt{X_1^2 + Y_2^2 + Z^2}}{(Y_2^2 + Z^2) \sqrt{X_1^2 + Z^2}} \quad (2.83)$$

$$X_{\sin 3} = \frac{X_2 Y_1^2 + Z^2 \sqrt{X_2^2 + Y_1^2 + Z^2}}{(Y_1^2 + Z^2) \sqrt{X_2^2 + Z^2}} \quad (2.84)$$

$$X_{\sin 4} = \frac{X_1 Y_2^2 + Z^2 \sqrt{X_1^2 + Y_2^2 + Z^2}}{(Y_2^2 + Z^2) \sqrt{X_1^2 + Z^2}} \quad (2.85)$$

and

$$P_{\sin 1} = \begin{cases} -\sin^{-1}(\text{sign}(X_{\sin 1})) & , |X_{\sin 1}| > 1 \\ -\sin^{-1}(X_{\sin 1}) & , |X_{\sin 1}| \leq 1 \end{cases} \quad (2.86)$$

$$P_{\sin 2} = \begin{cases} \sin^{-1}(\text{sign}(X_{\sin 2})) & , |X_{\sin 2}| > 1 \\ \sin^{-1}(X_{\sin 2}) & , |X_{\sin 2}| \leq 1 \end{cases} \quad (2.87)$$

$$P_{\sin 3} = \begin{cases} \sin^{-1}(\text{sign}(X_{\sin 3})) & , |X_{\sin 3}| > 1 \\ \sin^{-1}(X_{\sin 3}) & , |X_{\sin 3}| \leq 1 \end{cases} \quad (2.88)$$

$$P_{\sin 4} = \begin{cases} -\sin^{-1}(\text{sign}(X_{\sin 4})) & , |X_{\sin 4}| > 1 \\ -\sin^{-1}(X_{\sin 4}) & , |X_{\sin 4}| \leq 1 \end{cases} \quad (2.89)$$

where the sign function is defined as,

$$\text{sign}(x) = \begin{cases} 1 & , x > 0 \\ 0 & , x = 0 \\ -1 & , x < 0 \end{cases} \quad (2.90)$$

Then the individual terms of the series in the expression of the mutual resistance can be calculated by the use of the following equation [13], omitting the dependence on HLA and HLB ,

$$\begin{aligned} PERP(X_A, Y_A, Z_A; X_B, Y_B, Z_B) = & P_{X1} + P_{X2} + P_{Y1} + P_{Y2} \\ & + P_{\sin 1} + P_{\sin 2} + P_{\sin 3} + P_{\sin 4} \end{aligned} \quad (2.91)$$

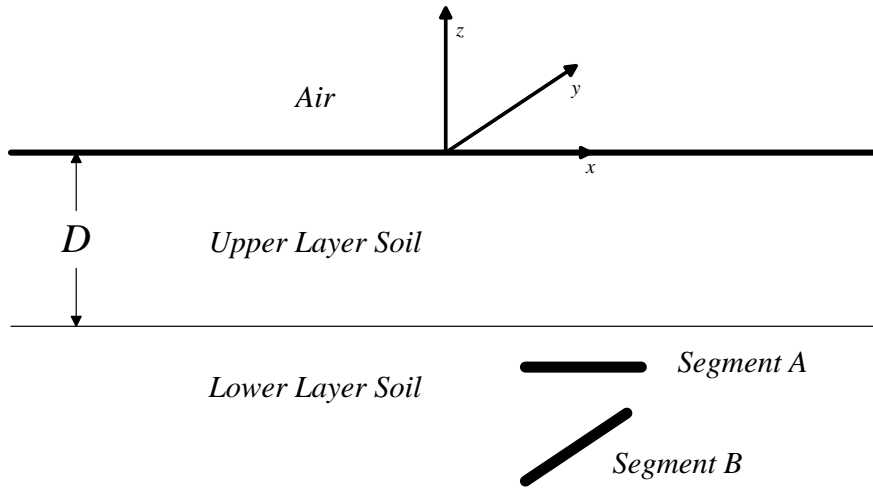


Fig 2.13 Two Perpendicular Segments in the Lower Layer

Now we can calculate the mutual resistance when the two conductor segments are perpendicular to each other. When the two segments are both in the lower layer of soil, as shown in Fig 2.13, the mutual resistance term is given by [13],

$$R_{BA} = \frac{1}{4\pi\sigma_1 L_A L_B} \left(\sum_{i=0}^{\infty} K_{12} (K_{12} K_{32})^i \text{PERP}(X_A, Y_A, Z_{Ai}^{(1)}; X_B, Y_B, Z_B) - \sum_{i=0}^{\infty} K_{32} (K_{12} K_{32})^i \text{PERP}(X_A, Y_A, Z_{Ai}^{(2)}; X_B, Y_B, Z_B) \right) \quad (2.92)$$

where

$$Z_{Ai}^{(1)} = -Z_A - 2(i-1)D \quad (2.93)$$

$$Z_{Ai}^{(2)} = -Z_A - 2iD \quad (2.94)$$

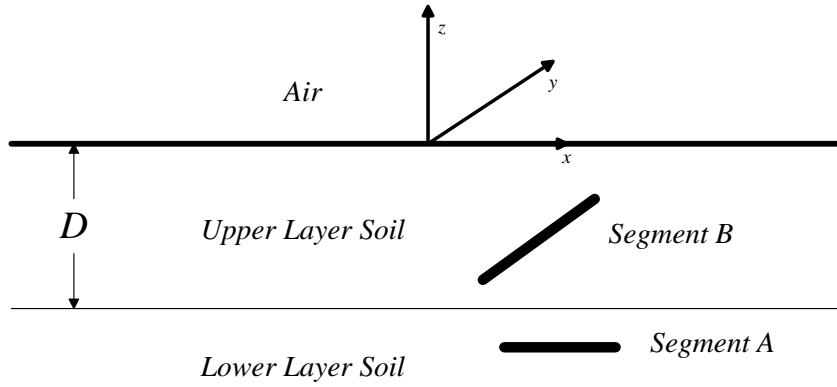


Fig 2.14 Segment A in the Lower Layer and Segment B in the Upper Layer

When segment A is in the lower layer of soil and segment B is in the upper layer of soil, as shown in Fig 2.14, the mutual resistance term is given by [13],

$$R_{BA} = \frac{1}{2\pi(\sigma_1 + \sigma_2) L_A L_B} \left(\sum_{i=0}^{\infty} (K_{12} K_{32})^i \text{PERP}(X_A, Y_A, Z_{Ai}^{(1)}; X_B, Y_B, Z_B) - \sum_{i=0}^{\infty} K_{32} (K_{12} K_{32})^i \text{PERP}(X_A, Y_A, Z_{Ai}^{(2)}; X_B, Y_B, Z_B) \right) \quad (2.95)$$

where

$$Z_{Ai}^{(1)} = Z_A + 2iD \quad (2.96)$$

$$Z_{Ai}^{(2)} = -Z_A - 2iD \quad (2.97)$$

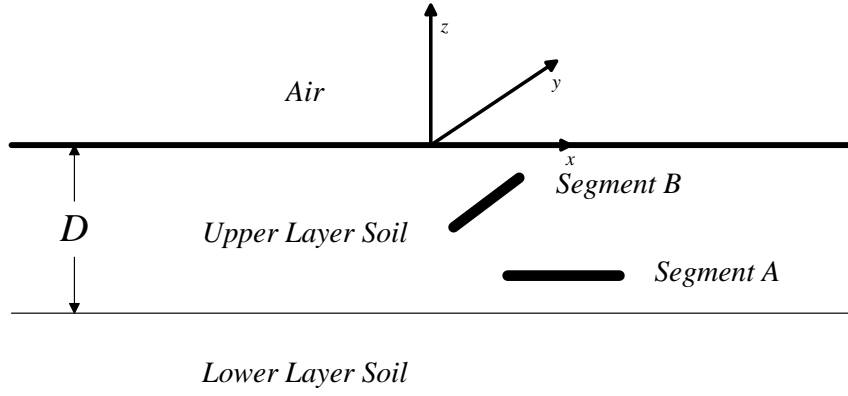


Fig 2.15 Two Perpendicular Segments in the Upper Layer

When both segment A and segment B are in the upper layer of soil, as shown in

Fig 2.15, the mutual resistance term is given by [13],

$$\begin{aligned}
 R_{BA} = & \frac{1}{4\pi\sigma_2 L_A L_B} \left(\sum_{i=0}^{\infty} (K_{12} K_{32})^i \text{PERP}(X_A, Y_A, Z_{Ai}^{(1)}; X_B, Y_B, Z_B) \right. \\
 & - \sum_{i=0}^{\infty} K_{12} (K_{12} K_{32})^i \text{PERP}(X_A, Y_A, Z_{Ai}^{(2)}; X_B, Y_B, Z_B) \\
 & + \sum_{i=0}^{\infty} (K_{12} K_{32})^i \text{PERP}(X_A, Y_A, Z_{Ai}^{(3)}; X_B, Y_B, Z_B) \\
 & \left. - \sum_{i=0}^{\infty} K_{32} (K_{12} K_{32})^i \text{PERP}(X_A, Y_A, Z_{Ai}^{(4)}; X_B, Y_B, Z_B) \right) \quad (2.98)
 \end{aligned}$$

where

$$Z_{Ai}^{(1)} = Z_A - 2iD \quad (2.99)$$

$$Z_{Ai}^{(2)} = -Z_A + 2(i+1)D \quad (2.100)$$

$$Z_{Ai}^{(3)} = Z_A + 2iD \quad (2.101)$$

$$Z_{Ai}^{(4)} = -Z_A - 2iD \quad (2.102)$$

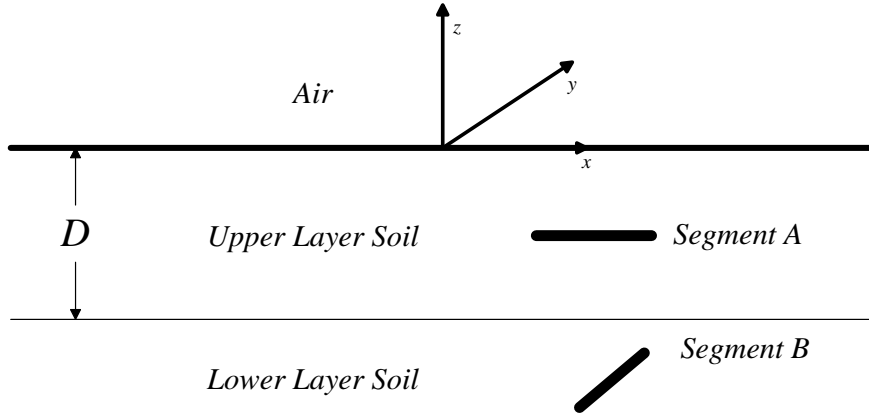


Fig 2.16 Segment A in the Upper Layer and Segment B in the Lower Layer

When segment A is in the upper layer of soil and segment B is in the lower layer of soil, as shown in Fig 2.16, the mutual resistance term is given by [13],

$$R_{BA} = \frac{1}{2\pi(\sigma_1 + \sigma_2)L_A L_B} \left(\sum_{i=0}^{\infty} (K_{12}K_{32})^i \text{PERP}(X_A, Y_A, Z_{Ai}^{(1)}; X_B, Y_B, Z_B) - \sum_{i=0}^{\infty} K_{32}(K_{12}K_{32})^i \text{PERP}(X_A, Y_A, Z_{Ai}^{(2)}; X_B, Y_B, Z_B) \right) \quad (2.103)$$

where

$$Z_{Ai}^{(1)} = Z_A - 2iD \quad (2.104)$$

$$Z_{Ai}^{(2)} = -Z_A - 2iD \quad (2.105)$$

The mutual resistance of each segment with each other segment is given by the off-diagonal elements of the mutual resistance matrix. The diagonal elements of the mutual resistance matrix give the self-resistance. According to [13], the process of calculating the self-resistance is presented below.

When a segment A is parallel to the x-axis or the y-axis, the following substitution of coordinates is performed

$$X_B = X_A \quad (2.106)$$

$$Y_B = Y_A \quad (2.107)$$

$$Z_B = Z_A + a \quad (2.108)$$

where a is the diameter of the conductor segment A.

When segment A is parallel to the z-axis, the following substitution of coordinates is used

$$X_B = X_A \quad (2.109)$$

$$Y_B = Y_A + a \quad (2.110)$$

$$Z_B = Z_A \quad (2.111)$$

Then when segment A is in the lower soil layer, the new coordinate is substituted into (2.34). The result of (2.34) is the self-resistance of conductor segment A and is put into the corresponding diagonal position of the mutual resistance matrix.

When segment A is in the upper soil layer, the new coordinate is substituted into (2.40). The result of (2.40) is the self-resistance of conductor segment A and is put into the corresponding diagonal position of the mutual resistance matrix.

We conclude that when the two conductor segments are parallel with the coordinate axes, the mutual resistance and self-resistance can be calculated using the line-line model, using the equations given above. They are used to calculate the self-resistance and the mutual resistance when the distance between two conductor segments is less than the arithmetic average of the lengths of the two segments.

2.4 The Mutual Resistance Matrix Point-Point Model

When the distance between the centers of the two conductor segments is greater than the arithmetic average of the lengths of the two segments, the point-point model is used to calculate the mutual resistance. Using the point-point model, the mutual resistance between segment A and segment B is simply the Green's function with the source point at the center of segment A and the field point at the center of segment B, which can be found in the literature [12].

The following intermediate function is defined to simplify the expression of the mutual resistance,

$$F(X_A, Y_A, Z_A; X_B, Y_B, Z_B) = \frac{1}{\sqrt{(X_B - X_A)^2 + (Y_B - Y_A)^2 + (Z_B - Z_A)^2}} \quad (2.112)$$

When both segment A and segment B are in the lower layer of soil,

$$\begin{aligned} R_{BA} = & \frac{1}{4\pi\sigma_1} [F(X_A, Y_A, Z_A; X_B, Y_B, Z_B) \\ & + K_{12} \sum_{i=0}^{\infty} (K_{12} K_{32})^i F(X_A, Y_A, Z_{Ai}^{(1)}; X_B, Y_B, Z_B) \\ & - K_{32} \sum_{i=0}^{\infty} (K_{12} K_{32})^i F(X_A, Y_A, Z_{Ai}^{(2)}; X_B, Y_B, Z_B)] \end{aligned} \quad (2.113)$$

where

$$Z_{Ai}^{(1)} = -Z_A - 2(i-1)D \quad (2.114)$$

$$Z_{Ai}^{(2)} = -Z_A - 2iD \quad (2.115)$$

When segment A is in the lower layer and segment B is in the upper layer,

$$R_{BA} = \frac{1}{2\pi(\sigma_1 + \sigma_2)} \left[\sum_{i=0}^{\infty} (K_{12}K_{32})^i F(X_A, Y_A, Z_{Ai}^{(1)}; X_B, Y_B, Z_B) \right. \\ \left. - K_{32} \sum_{i=0}^{\infty} (K_{12}K_{32})^i F(X_A, Y_A, Z_{Ai}^{(2)}; X_B, Y_B, Z_B) \right] \quad (2.116)$$

where

$$Z_{Ai}^{(1)} = Z_A + 2iD \quad (2.117)$$

$$Z_{Ai}^{(2)} = -Z_A - 2iD \quad (2.118)$$

When both segment A and segment B are in the upper layer,

$$R_{BA} = \frac{1}{4\pi\sigma_2} \left[F(X_A, Y_A, Z_A; X_B, Y_B, Z_B) \right. \\ - K_{12} \sum_{i=0}^{\infty} (K_{12}K_{32})^i F(X_A, Y_A, Z_{Ai}^{(1)}; X_B, Y_B, Z_B) \\ + \sum_{i=1}^{\infty} (K_{12}K_{32})^i F(X_A, Y_A, Z_{Ai}^{(2)}; X_B, Y_B, Z_B) \\ - K_{32} \sum_{i=0}^{\infty} (K_{12}K_{32})^i F(X_A, Y_A, Z_{Ai}^{(3)}; X_B, Y_B, Z_B) \\ \left. + \sum_{i=1}^{\infty} (K_{12}K_{32})^i F(X_A, Y_A, Z_{Ai}^{(4)}; X_B, Y_B, Z_B) \right] \quad (2.119)$$

where

$$Z_{Ai}^{(1)} = -Z_A + 2(i+1)D \quad (2.120)$$

$$Z_{Ai}^{(2)} = Z_A - 2iD \quad (2.121)$$

$$Z_{Ai}^{(3)} = -Z_A - 2iD \quad (2.122)$$

$$Z_{Ai}^{(4)} = Z_A + 2iD \quad (2.123)$$

When segment A is in the upper layer and segment B is in the lower layer,

$$R_{BA} = \frac{1}{2\pi(\sigma_1 + \sigma_2)} \left[\sum_{i=0}^{\infty} (K_{12}K_{32})^i F(X_A, Y_A, Z_{Ai}^{(1)}; X_B, Y_B, Z_B) \right. \\ \left. - K_{32} \sum_{i=0}^{\infty} (K_{12}K_{32})^i F(X_A, Y_A, Z_{Ai}^{(2)}; X_B, Y_B, Z_B) \right] \quad (2.124)$$

where

$$Z_{Ai}^{(1)} = Z_A - 2iD \quad (2.125)$$

$$Z_{Ai}^{(2)} = -Z_A - 2iD \quad (2.126)$$

These equations are used to calculate the mutual resistance when the point-point model is used.

2.5 Modeling the Non-Orthogonal Ground Grid

A trapezoid is defined as a convex quadrilateral with at least one pair of parallel sides. The two sides of a trapezoid that are not necessarily parallel to each other are called legs.

When dealing with a non-orthogonal ground grid, such as the trapezoidal ground grid, if we put the x-axis parallel with the base of the trapezoid, then the ground conductors along the sides of the trapezoid are not necessarily parallel or perpendicular to the x-axis or the y-axis. Additionally, the conductor segment on the leg is not necessarily orthogonal to the conductor segment on the base. So the equations of the line-line model that are used to calculate the mutual resistance of any two segments described in the previous section cannot be used when dealing with the non-orthogonal ground grid.

Alternatively, one may suggest the use of the point-point model instead of using the line-line model, because in the point-point model the direction of the conductor segment is not considered. But a comparison of this approach with a WinIGS simulation has shown that if only the point-point model is used when calculating the mutual resistance, the relative difference between the result of the touch potential of our application and that of WinIGS will be as large as 25%, which is not acceptable. The line-line model must be used.

In this section, the equations that are used to calculate the touch potential, the step potential, and a numerical integration method that is used to calculate the mutual resistance of a trapezoidal ground grid are presented.

2.5.1 The Earth Potential Equation for the Trapezoidal Ground Grid

In the literature [12], the equations that are used to calculate the earth potential induced by a conductor segment that is parallel with the x-, y-, or z-axis are given. The equations are derived by the integration of the corresponding Green's function, listed in section 2.2.2, along the conductor segment. What is done in this section is similar to the process presented in the literature [12]; the difference is that in this section, the conductor segment can have any orientation in a horizontal (x-y) plane.

Noting that in the Green's functions in section 2.2.2 the source point is put on the z-axis, and each term in the expressions can be written in a more general form,

$$G_{term}(x_1, y_1; x_2, y_2; U(z_1; z_2; E_i)) = \frac{1}{\sqrt{(x_2 - x_1)^2 + (y_2 - y_1)^2 + U^2}} \quad (2.127)$$

where (x_1, y_1, z_1) is the source point, (x_2, y_2, z_2) is the field point, E_i is an intermediate parameter that associates the z coordinate of the i^{th} image of the source point, and U is an intermediate function of z_1 , z_2 and E_i . The specific forms of E_i and U and how they are used can be found in the (2.128) and the (2.131), but the specific forms of them do not affect the derivation of the (2.128) and the (2.131).

By a process similar to that given in the literature [12], the integration of the Green's function along the conductor segment in a horizontal plane includes the integration of (2.127). Assume that the angle between this conductor segment and a line that is parallel with x -axis in the same horizontal plane is α , then the integration of (2.127) can be written as

$$\begin{aligned} IG_{term}(x_1, y_1, Lh1, \alpha; x_2, y_2; U(z_1; z_2; E_i)) \\ = \ln \frac{\sqrt{(X + Lh1)^2 + Y^2 + U^2} + X + Lh1}{\sqrt{(X - Lh1)^2 + Y^2 + U^2} + X - Lh1} \end{aligned} \quad (2.128)$$

where (x_1, y_1, z_1) is the coordinate of the center of the conductor segment, $Lh1$ is half of the length of the conductor segment, and the intermediate functions X and Y are defined as

$$X = (x_2 - x_1) \cos \alpha + (y_2 - y_1) \sin \alpha \quad (2.129)$$

$$Y = (x_2 - x_1) \sin \alpha - (y_2 - y_1) \cos \alpha \quad (2.130)$$

By comparing the equation (2.128) with the equations in literature [12], it is easy to verify that by setting α to zero, equation (2.128) will reduce to the corresponding

equation for a conductor segment parallel to the x-axis, and by setting α to $\pi/2$, equation (2.128) will reduce to the corresponding equation for a conductor segment parallel to the y-axis in the literature [12].

Equation (2.128) is substituted into the integration of the Green's function to derive the equation that is used to calculate the earth potential induced by the leakage current of a conductor segment that is along any direction in a horizontal plane,

$$\begin{aligned}
& E_{earth}(x_1, y_1, z_1, Lh1, \alpha; x_2, y_2, z_2) \\
&= \frac{I_A}{8\pi\sigma_2 Lh1} [IG_{term}(x_1, y_1, Lh1, \alpha; x_2, y_2; z_2 - z_1) \\
&- K_{12} \sum_{i=0}^{\infty} (K_{12} K_{32})^i IG_{term}(x_1, y_1, Lh1, \alpha; x_2, y_2; z_2 + z_1 - 2(i+1)D) \\
&+ \sum_{i=1}^{\infty} (K_{12} K_{32})^i IG_{term}(x_1, y_1, Lh1, \alpha; x_2, y_2; z_2 - z_1 + 2iD) \\
&- K_{32} \sum_{i=0}^{\infty} (K_{12} K_{32})^i IG_{term}(x_1, y_1, Lh1, \alpha; x_2, y_2; z_2 + z_1 + 2iD) \\
&+ \sum_{i=1}^{\infty} (K_{12} K_{32})^i IG_{term}(x_1, y_1, Lh1, \alpha; x_2, y_2; z_2 - z_1 - 2iD)] \tag{2.131}
\end{aligned}$$

Equation (2.131) is used when calculating the touch potential contributed by the leakage current on a conductor segment on the leg of a trapezoidal grid.

Suppose there is a second horizontal conductor segment and we want to calculate the mutual resistance between the first horizontal conductor segment and the second horizontal conductor segment. Assume that $Lh2$ is half the length of the second conductor segment, and the angle between the second conductor segment and a line parallel with the x-axis in the same plane is β , and the coordinate of the center of the second segment is (x_2, y_2, z_2) . The mutual resistance between the first segment and the

second segment is just the line integration of the equation (2.131) along the second segment from the endpoint

$$(x_2 - Lh2\cos\beta, y_2 - Lh2\sin\beta, z_2) \quad (2.132)$$

to the other endpoint

$$(x_2 + Lh2\cos\beta, y_2 + Lh2\sin\beta, z_2) \quad (2.133)$$

divided by the total length of the second segment and the leakage current on the first segment.

A closed form equation of the mutual resistance is desirable, but using MATLAB and Mathematica, the closed form expression cannot be found. Mathematica does give a result of the indefinite integral of a simplified version of the equation (2.128), with t as the parameter of the second segment

$$\int \ln(c_1 t + c_2 + \sqrt{t^2 + c_3^2}) dt \quad (2.134)$$

where c_1 , c_2 , and c_3 are constants related with the positions and the orientations and the lengths of the two segments; however, if one takes the derivative of the result, it will not give the integrand of (2.134). Additionally, the implementation of the closed form result of the integration given by Mathematica yields complex mutual resistance, which is not acceptable. MATLAB says that (2.134) is not integrable.

One remaining method to solve the definite integration of (2.131) along the second conductor is to use the numerical integration method. In this work, the rectangle rule and Simpson's rule (both discussed below) are used to calculate the integration of (2.131).

The definite integration of (2.128) is rewritten, and after some arithmetic and trigonometric manipulations, we have the expression of the integration, which is a single term of the series of the integration of (2.131),

$$RM_{nterm}(x_1, y_1, Lh1, \alpha; x_2, y_2, Lh2, \beta; U(z_1, z_2, E_i)) \quad (2.135)$$

$$= \frac{1}{2Lh2} \int_{-Lh2}^{Lh2} \frac{\sqrt{NX^2 + NY^2 + U^2} + NX2}{\sqrt{DX^2 + DY^2 + U^2} + DX2} dt$$

where the new intermediate functions are defined as,

$$NX = t + (x_2 - x_1) \cos \beta + (y_2 - y_1) \sin \beta + Lh1 \cos(\beta - \alpha) \quad (2.136)$$

$$NY = (x_2 - x_1) \sin \beta - (y_2 - y_1) \cos \beta + Lh1 \sin(\beta - \alpha) \quad (2.137)$$

$$NX2 = t \cos(\beta - \alpha) + (x_2 - x_1) \cos \alpha + (y_2 - y_1) \sin \alpha + Lh1 \quad (2.138)$$

$$DX = t + (x_2 - x_1) \cos \beta + (y_2 - y_1) \sin \beta - Lh1 \cos(\beta - \alpha) \quad (2.139)$$

$$DY = (x_2 - x_1) \sin \beta - (y_2 - y_1) \cos \beta - Lh1 \sin(\beta - \alpha) \quad (2.140)$$

$$DX2 = t \cos(\beta - \alpha) + (x_2 - x_1) \cos \alpha + (y_2 - y_1) \sin \alpha - Lh1 \quad (2.141)$$

The mutual resistance matrix must be a symmetric matrix, which means if we calculate the earth potential induced by the leakage current on the second segment, and integrate along the first conductor then divide the result by the length of the first segment and the leakage current on the first segment, we should get the same result as if we calculate according to (2.135); but this is not so manifest that one can see it directly from the equation (2.135) and the corresponding definitions of the intermediate functions, though this must be true for any bilateral system, of which our problem is one.

Given the equation (2.135), we write the expression of mutual resistance between any two segments in the same horizontal plane in any directions as

$$\begin{aligned}
& RM(x_1, y_1, z_1, Lh1, \alpha; x_2, y_2, z_2) \\
&= \frac{1}{8\pi\sigma_2 Lh1} [RM_{nterm}(x_1, y_1, Lh1, \alpha; x_2, y_2, Lh2, \beta; z_2 - z_1) \\
&- K_{12} \sum_{i=0}^{\infty} (K_{12} K_{32})^i RM_{nterm}(x_1, y_1, Lh1, \alpha; x_2, y_2, Lh2, \beta; z_2 + z_1 - 2(i+1)D) \\
&+ \sum_{i=1}^{\infty} (K_{12} K_{32})^i RM_{nterm}(x_1, y_1, Lh1, \alpha; x_2, y_2, Lh2, \beta; z_2 - z_1 + 2iD) \\
&- K_{32} \sum_{i=0}^{\infty} (K_{12} K_{32})^i RM_{nterm}(x_1, y_1, Lh1, \alpha; x_2, y_2, Lh2, \beta; z_2 + z_1 + 2iD) \\
&+ \sum_{i=1}^{\infty} (K_{12} K_{32})^i RM_{nterm}(x_1, y_1, Lh1, \alpha; x_2, y_2, Lh2, \beta; z_2 - z_1 - 2iD)] \tag{2.142}
\end{aligned}$$

This equation (2.142) and the numerical integration methods are all that we need to calculate the mutual resistance between a segment on the leg of the trapezoidal ground grid and other segments.

2.5.2 The Rectangle Rule

The Rectangle Rule is one of the numerical integration methods that is used when calculating (2.142). When the intermediate function U has the value zero, the Rectangle Rule is used to calculate the single term in the series of (2.142).

The interval $[-Lh2, Lh2]$ is divided into N uniform sections in order to implement the Rectangle Rule.

$$[-Lh2, Lh2] = [x_0, x_1) \cup [x_1, x_2) \cup \dots \cup [x_{N-1}, x_N] \tag{2.143}$$

where

$$-Lh2 = x_0 < x_1 < x_2 < \dots < x_{N-1} < x_N = Lh2 \tag{2.144}$$

and

$$x_i - x_{i-1} = \frac{2Lh2}{N}, \quad i = 1, 2, \dots, N \quad (2.145)$$

The Rectangle Rule says that a definite integral over the interval $[-Lh2, Lh2]$ can be approximated by the summation

$$\int_{-Lh2}^{Lh2} f(t) dt \approx \frac{2 \times Lh2}{N} \sum_{i=1}^N f(c_i) \quad (2.146)$$

where

$$c_i = \frac{x_i - x_{i-1}}{2}, \quad i = 1, 2, \dots, N \quad (2.147)$$

2.5.3 Simpson's Rule

Simpson's Rule is the other numerical integration method that is used when calculating (2.142). When the intermediate function U has a non-zero value, Simpson's Rule is used to calculate the single term in the series of (2.142).

The interval $[-Lh2, Lh2]$ is divided into N number of uniform sections in order to implement Simpson's Rule.

$$[-Lh2, Lh2] = [x_0, x_1) \cup [x_1, x_2) \cup \dots \cup [x_{N-1}, x_N] \quad (2.148)$$

where

$$-Lh2 = x_0 < x_1 < x_2 < \dots < x_{N-1} < x_N = Lh2 \quad (2.149)$$

and

$$x_i - x_{i-1} = \frac{2Lh2}{N}, \quad i = 1, 2, \dots, N \quad (2.150)$$

The middle point of each interval is defined as

$$c_i = \frac{x_i - x_{i-1}}{2}, \quad i = 1, 2, \dots, N \quad (2.151)$$

The Simpson's Rule says that a definite integral over the interval $[-Lh/2, Lh/2]$ can be approximated by the summation

$$\int_{-Lh/2}^{Lh/2} f(t)dt \approx \frac{Lh}{3N} \sum_{i=1}^N [f(x_{i-1}) + 4f(c_i) + f(x_i)] \quad (2.152)$$

For a given integration step h , the truncation error of Simpson's Rule is $O(h^4)$ while the truncation error of the Rectangle Rule is $O(h^2)$. This is the reason why Simpson's Rule is used when the value of the intermediate function U is not zero: for a smooth integrand, Simpson's Rule converges much faster than the Rectangle Rule and fewer terms are needed in the summation.

Using the Rectangle Rule and Simpson's Rule and equation (2.142), the mutual resistance between a conductor segment on the leg of the trapezoidal ground grid and other horizontal conductor segments can be calculated.

2.5.4 Coordinate Transformation

Do we need a new equation to calculate the mutual resistance between a segment on the leg of a trapezoidal ground grid and a segment on a vertical ground rod? A new equation is not needed for this purpose, but a coordinate transformation is needed so that we can use the equations that we already have.

Even if the angle between the leg and the base, or the x-axis, is not ninety degrees, the segment on a horizontal conductor is still perpendicular to every segment on a vertical rod. This means if we rotate the coordinate system about the z-axis, so that the

horizontal segment is perpendicular or parallel to the new x-axis, we can use the equations presented in section 2.3 and section 2.4 to calculate the mutual resistance between a segment on the leg of the trapezoidal ground grid and a segment on a vertical rod.

The essence is that the value of the mutual resistance between any two specified conductor segments should not depend on the choice of the coordinate system. The relationships between the coordinates in the new coordinate system and the coordinates in the old coordinate system are

$$x_{n1} = 0 \quad (2.153)$$

$$y_{n1} = (x_{o2} - x_{o1}) \cos \alpha + (y_{o2} - y_{o1}) \sin \alpha \quad (2.154)$$

$$z_{n1} = z_{o1} \quad (2.155)$$

$$x_{n2} = (x_{o2} - x_{o1}) \sin \alpha - (y_{o2} - y_{o1}) \cos \alpha \quad (2.156)$$

$$y_{n2} = 0 \quad (2.157)$$

$$z_{n2} = z_{o2} \quad (2.158)$$

where (x_{o1}, y_{o1}, z_{o1}) is the coordinate of the center of the horizontal (ground conductor) segment before the coordinate transformation, and (x_{o2}, y_{o2}, z_{o2}) is the coordinate of the center of the segment on a ground rod before the coordinate transformation, and (x_{n1}, y_{n1}, z_{n1}) is the coordinate of the center of the same horizontal segment after the coordinate transformation, and (x_{n2}, y_{n2}, z_{n2}) is the coordinate of the center of the segment on a ground rod after the coordinate transformation, and α is the angle between the horizontal segment and the x-axis before the coordinate transformation.

Because in the new coordinate system, the horizontal segment is perpendicular to the x-axis, and the segment on the rod is still parallel to the z-axis, the equations in section 2.3 and section 2.4 can be used to calculate the mutual resistance between the two segments

2.5.5 The Centroid of a Polygon

For a trapezoidal ground grid, the touch potential is calculated at the centroid of each corner mesh and the meshes that are adjacent to each corner mesh. In general these meshes are polygons and are not necessarily rectangular. In order to tell the computer program where the centroid is, we need the coordinate of the centroid of a polygon. The equations from Wikipedia [22] are presented below.

c

Fig 2.17 A Polygon

The centroid of a non-self-intersecting closed polygon defined by n vertices $(x_0, y_0), (x_1, y_1), \dots, (x_{n-1}, y_{n-1})$, as shown in Fig 2.17, is the point (C_x, C_y) , where

$$C_x = \frac{1}{6A} \sum_{i=0}^{n-1} (x_i + x_{i+1})(x_i y_{i+1} - x_{i+1} y_i) \quad (2.159)$$

$$C_y = \frac{1}{6A} \sum_{i=0}^{n-1} (y_i + y_{i+1})(x_i y_{i+1} - x_{i+1} y_i) \quad (2.160)$$

and where A is the polygon's area,

$$A = \frac{1}{2} \sum_{i=0}^{n-1} (x_i y_{i+1} - x_{i+1} y_i) \quad (2.161)$$

In these formulas, the vertices are assumed to be numbered in order of their occurrence along the polygon's perimeter [22]. Furthermore, the vertex (x_n, y_n) is assumed to be the same as (x_0, y_0) , meaning $n + 1$ is equivalent to $i = 0$ [22].

2.6 The Current Distribution Factor and the Ground Potential Rise

For convenience, (2.6), which is used to define the leakage current and ground potential rise, is given again here.

$$\begin{bmatrix} R_{11} & R_{12} & \cdots & R_{1N} & -1 \\ R_{21} & R_{22} & \cdots & R_{2N} & -1 \\ \vdots & \vdots & \ddots & \vdots & \vdots \\ R_{N1} & R_{N2} & \cdots & R_{NN} & -1 \\ 1 & 1 & \cdots & 1 & 0 \end{bmatrix} \begin{bmatrix} I_1 \\ I_2 \\ \vdots \\ I_N \\ \phi \end{bmatrix} = \begin{bmatrix} 0 \\ 0 \\ \vdots \\ 0 \\ I_{total} \end{bmatrix} \quad (2.162)$$

The equations presented in section 2.2 and section 2.5 may be used to calculate the mutual resistance between any two segments of the ground grid. So the entries in the N by N matrix on the left side of (2.162) can be calculated. The column vector on the right side of the equation is known because the fault current I_{total} is calculated from the electric power system model and is a design problem input. MATLAB can solve the matrix equation for the $(N+1)$ by 1 column vector

$$\begin{bmatrix} I_1 \\ I_2 \\ \vdots \\ I_N \\ \phi \end{bmatrix} \quad (2.163)$$

The first N elements of (2.163) are the leakage currents on the corresponding segments. They are also called current distribution factors. The last element of (2.163) is the ground potential rise (GPR). Using the ground potential rise, the ground resistance to the remote earth, R_g , can be calculated as (2.164) where I_{total} is the fault current.

$$R_g = \frac{\phi}{I_{total}} \quad (2.164)$$

2.7 Calculating the Earth Potential, the Touch Potential, and the Step Potential

After the current distribution factors and the GPR are solved from the equation (2.162), we need to calculate the earth potential induced by such a distribution of the leakage current. For a given conductor segment whose length is $L_A = 2L_1$ with leakage current I , where L_1 is half the length of the conductor segment, the earth potential induced by the leakage current on this segment is just the line integration of the Green's function times the leakage current density on the segment.

Using the exact formula of the Green's function, i.e. Equations (2.11), (2.12), (2.13) and (2.14), the exact formula of the earth potential can be derived. The literature [12] gives the derived equations to calculate the earth potential of a conductor segment that is parallel to the x-, y-, or z-axis. The equations are presented below.

The intermediate function G is defined according to [12] in order to simplify the equation of the earth potential

$$G(t, u, v) = F(t, u, v, L) \quad (2.165)$$

$$= \ln \frac{\sqrt{(t+L)^2 + u^2 + v^2} + t + L}{\sqrt{(t-L)^2 + u^2 + v^2} + t - L}$$

Let (x_1, y_1, z_1) be the coordinate of the center of segment And (x, y, z) be the point where the earth potential is calculated.

When the segment is parallel to the x-axis, and located in the upper layer of soil, and the point where the earth potential is calculated is also at the upper layer of soil, the earth potential induced by the leakage current is

$$VX_{22}(x, y, z) = S_{22}\{G(x, y, z)\} \quad (2.166)$$

where

$$S_{22}\{G(x, y, z)\} = \frac{I}{8\pi L_1 \sigma_2} [G(x - x_1, y - y_1, z - z_1) \quad (2.167)$$

$$- K_{12} \sum_{i=0}^{\infty} (K_{12} K_{32})^i G(x - x_1, y - y_1, z + z_1 - 2iD + 2D)$$

$$+ \sum_{i=1}^{\infty} (K_{12} K_{32})^i G(x - x_1, y - y_1, z - z_1 + 2iD)$$

$$- K_{32} \sum_{i=0}^{\infty} (K_{12} K_{32})^i G(x - x_1, y - y_1, z + z_1 + 2iD)]$$

When the segment is parallel to the x-axis, and located in the lower layer of soil, and the point where the earth potential is calculated is at the upper layer of soil, the earth potential induced by the leakage current is

$$VX_{21}(x, y, z) = S_{21}\{G(x, y, z)\} \quad (2.168)$$

where

$$\begin{aligned}
& S_{21}\{G(x, y, z)\} \\
&= \frac{I}{4\pi L_1(\sigma_1 + \sigma_2)} \left[\sum_{i=0}^{\infty} (K_{12}K_{32})^i G(x - x_1, y - y_1, z - z_1 - 2iD) \right. \\
&\quad \left. - K_{32} \sum_{i=0}^{\infty} (K_{12}K_{32})^i G(x - x_1, y - y_1, z + z_1 + 2iD) \right]
\end{aligned} \tag{2.169}$$

When the segment is parallel to the y-axis, one just needs to exchange the first two entries of the G function. Because the manipulation is simple, the resultant equations for a segment parallel to the y-axis are not presented.

When the horizontal segment is not parallel to either the x- or y-axis, equation (2.131) should be used to calculate the earth potential.

For any segment comprising associate with a vertical ground rod, that is, when the segment is parallel to the z-axis, located in the upper layer of soil, and the point where the earth potential is calculated is located in the upper soil layer, the earth potential induced by the leakage current is

$$VZ_{22}(x, y, z) = S_{22}\{G(z, x, y)\}^3 \tag{2.170}$$

where

$$\begin{aligned}
& S_{22}\{G(z, x, y)\} \\
&= \frac{I}{8\pi L_1\sigma_2} \left[G(z - z_1, x - x_1, y - y_1) \right. \\
&\quad - K_{12} \sum_{i=0}^{\infty} (K_{12}K_{32})^i G(z + z_1 - 2iD + 2D, x - x_1, y - y_1) \\
&\quad + \sum_{i=1}^{\infty} (K_{12}K_{32})^i G(z - z_1 + 2iD, x - x_1, y - y_1) \\
&\quad \left. - K_{32} \sum_{i=0}^{\infty} (K_{12}K_{32})^i G(z + z_1 + 2iD, x - x_1, y - y_1) \right]
\end{aligned} \tag{2.171}$$

³ In literature [12], there is a typo in this equation that cause the violation of self-consistency and symmetry, which will be introduced in Chapter 3.

When the segment is parallel to the z-axis, and located in the lower layer of soil, and the point where the earth potential is calculated is in the upper soil layer, the earth potential induced by the leakage current is

$$VZ_{21}(x, y, z) = S_{21}\{G(z, x, y)\} \quad (2.172)$$

where

$$\begin{aligned} & S_{21}\{G(z, x, y)\} \\ &= \frac{I}{4\pi L_1(\sigma_1 + \sigma_2)} \left[\sum_{i=0}^{\infty} (K_{12}K_{32})^i G(z - z_1 - 2iD, x - x_1, y - y_1) \right. \\ & \quad \left. - K_{32} \sum_{i=0}^{\infty} (K_{12}K_{32})^i G(z + z_1 + 2iD, x - x_1, y - y_1) \right] \end{aligned} \quad (2.173)$$

Since the equations above can be used to calculate the earth potential for any point in the top-soil layer, they can be used to calculate the touch potential and the step potential at the earth's surface. Let E_{earth} be the earth potential calculated at the surface of the soil at point $(x, y, 0)$, and let the ground potential rise (GPR) be ϕ , then the touch potential can be calculated by the following equation,

$$E_{touch}(x, y, 0) = \phi - E_{earth}(x, y, 0) \quad (2.174)$$

The touch potential constraints used in the application are based on touch potential calculated at the centroids of each corner mesh for square grids, rectangular grids, and L-shaped grids, and are also calculated at the centroid of the meshes that are adjacent to the corner meshes for trapezoidal grids.

The step potential constraints are the step potential values calculated for a one-meter step length more radially outward at each grid corner whose direction is taken as the bisector of angle at the outside corner of each corner mesh. More precisely, let

the earth potential at the corner $(x_1, y_1, 0)$ be denoted as $E_{earth}(x_1, y_1, 0)$. Let the earth potential at the point $(x_2, y_2, 0)$ on the extension of the bisector that is one meter away (radially outward) from the first point be denoted as $E_{earth}(x_1, y_1, 0)$. Then the step potential is calculated as

$$E_{step}(x, y, 0) = E_{earth}(x_1, y_1, 0) - E_{earth}(x_2, y_2, 0) \quad (2.175)$$

3 PROGRAM VALIDATION

In this chapter, the idea of self-consistency and a self consistency validation method are presented. Ground grid symmetry and coordinate independence are also discussed. First, the self-consistency of our application is checked using the symmetry of the ground grid. Then the program validation is performed by comparison of the touch potential and the step potential calculated by our application and the touch potential and the step potential calculated by WinIGS.

3.1 Self-Consistency, Symmetry and Coordinate Independence

A system or a theory is said to be self-consistent if the system or the theory itself does not contain any contradiction. If the system or the theory is not self-consistent, the system or the theory is easily identified to be problematic. The first aspect that one should check with our application is self-consistency.

The symmetry of a system is, by definition, the invariance under a given operation acting on the system. For our ground grid, symmetry means the invariance of the touch potential and the step potential under the rotation of the ground grid about the z-axis, or under the mirroring of the ground grid about the vertical plane whose equation is $y=x$.

The invariance under the rotation operation acting on the ground grid is easy to understand. If the ground grid is rotated by 90 degrees, about the vertical axis, for ex-

ample, the touch potential and the step potential shouldn't change, because the geometry of the ground grid has not changed after the rotation operation. It is the same ground grid after the rotation operation, and the only thing changed is the orientation of the ground grid. Therefore the touch potential and the step potential should not change. On the other hand, if the touch potential and the step potential calculated by our application change after the rotation operation of the ground grid, our application would be problematic, because there would be a contradiction of our program which means our program would not be self-consistent.

For our ground grid, any vertical plane can be considered as the mirror plane, and the mirrored ground grid and the original ground grid should have the same touch potential and the same step potential. If the touch potential and the step potential calculated by our application changed after the mirroring operation, there would be a contradiction, and our application would not be self-consistent.

The coordinate independence means that the physical objective does not depend on the subjective choice of a coordinate system. For example, a vector in a three dimensional space is an object that is independent of any choice of orthonormal basis vectors. For our ground grid, the mutual resistance between any two conductor segments is independent of the choice of the coordinate system. This fact was used in Chapter 2, when discussing the mutual resistance between a vertical segment on the ground rod and a horizontal segment on the leg of a trapezoid.

3.2 The Validation of Self-Consistency

In this section the validation of self-consistency is performed by means of the rotation operation acting on the rectangular ground grid, and the mirroring operation acting on both the L-shaped ground grid and the trapezoidal ground grid.

3.2.1 The Self-Consistency of the Rectangular Ground Grid

To calculate the touch potential and the step potential of the ground grid, a soil model has to be given first. The earth resistivity of the upper layer soil is taken as $100 \Omega \cdot \text{m}$. The earth resistivity of the lower layer soil is taken as $30 \Omega \cdot \text{m}$. The thickness of the upper layer soil is taken as 10 ft. The reader may assume that this soil model is used throughout this section and subsequent sections unless stated otherwise.

Suppose that there is a rectangular ground grid buried 1.5 ft below the earth surface. The dimensions of the ground grid are 600 ft by 400 ft. The number of meshes along the x axis is 12, and the number of meshes along the y-axis is 8. There are 12 rods placed along the perimeter of the grid. Four rods are on the corners, and there are 2 rods on each side so that the distance between each two rods on a given side is uniform. The length of each rod is 30 ft. The fault current is 3780 A. The geometry of the ground grid is shown in the figure. This is called Case A.

To show that the MATLAB program yields self-consistent results, the rotation operation is performed on the ground grid, so that the ground grid in Case A now becomes a rectangular grid that has the dimension 400 ft by 600 ft, with 8 meshes along

the x-axis, and 12 meshes along the y-axis. The number of rods and the length of each rod are unchanged. There are still 2 rods on each side of the rectangular grid and there is one rod on each corner. The fault current is unchanged. This is called Case B. If the self-consistency condition is satisfied, the touch/step potentials calculated for Case A must be equal to the touch/step potentials calculated for Case B.

The result of the touch potential and the result of the step potential calculated by the MATLAB program are shown in Table 3.1

Table 3.1 Validation of Symmetry for the Rectangular Ground Grid

	Etouch (V)	Estep (V)
Case A	170.78	64.53
Case B	170.78	64.53

Therefore, the self-consistency of the rectangular ground grid calculation is validated.

3.2.2 The Self-Consistency of the L-Shaped Ground Grid

Assume the following soil model. The earth resistivity of the upper layer soil is $100 \Omega \cdot \text{m}$. The earth resistivity of the lower layer soil is $30 \Omega \cdot \text{m}$. The thickness of the upper layer soil is 10 ft. The geometry of the L-shaped ground grid is shown in Fig 3.1.

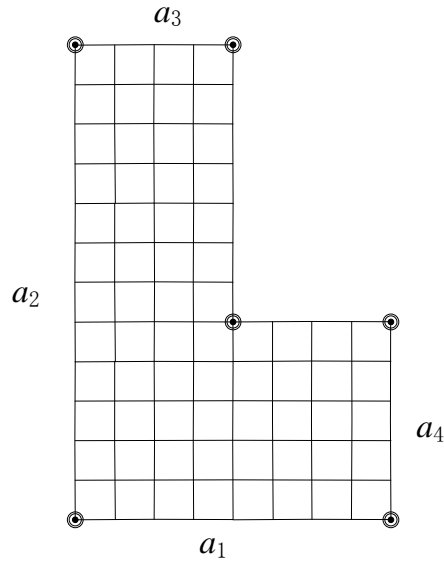


Fig 3.1 The L-Shaped Ground Grid in Case C

The length a_1 is 400 ft, the length a_2 is 600 ft, the length a_3 is 200 ft, and the length a_4 is 250 ft as shown in Fig 3.1. The number of meshes along the x-axis is 8 and the number of meshes along the y axis is 12. The rods are placed on the corners of the L-shaped grid. The length of each rod is 30 ft. The fault current is 3.3 kA. This is called Case C.

Using the same soil model of Case C, and after mirroring the ground grid in Case C about the $y=x$ plane while keeping the fault current unchanged, a new case, called Case D, is obtained, as shown in Fig 3.2.

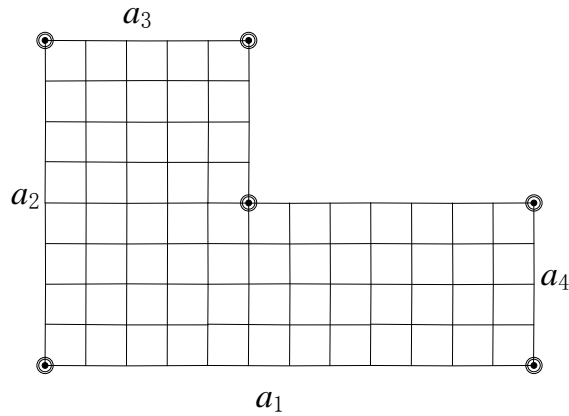


Fig 3.2 The L-Shaped Ground Grid in Case D.

If the MATLAB program yields self-consistent results for L-shaped ground grids, both the touch potential and the step potential calculated for Case C should be equal to the touch potential and the step potential calculated for Case D respectively. The results of the potentials calculated for these two cases is shown in Table 3.2.

Table 3.2 Validation of Symmetry for the L-Shaped Ground Grid

	Etouch (V)	Estep (V)
Case C	183.01	62.56
Case D	183.01	62.56

Therefore, the self-consistency of the L-shaped ground grid calculation is validated.

3.2.3 The Self-Consistency of the Trapezoidal Ground Grid

Assume the following soil model. The earth resistivity of the upper layer soil is $100 \Omega \cdot \text{m}$. The earth resistivity of the lower layer soil is $20 \Omega \cdot \text{m}$. The thickness of the upper layer soil is 10 ft. The geometry of the trapezoidal ground grid is described as the following, as shown in Fig 3.3.

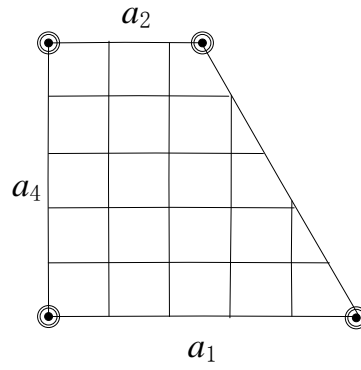


Fig 3.3 The Trapezoidal Ground Grid in Case E

The length a_1 is 170 ft, the length a_2 is 85 ft, the length a_4 is 150 ft. The left leg of the trapezoid is perpendicular to the bottom side. The number of meshes along the x-axis is 5 and the number of meshes along the y-axis is 5. The rods are placed on the corners of the trapezoidal ground grid. The length of each rod is 30 ft. The fault current is 2.1 kA. This is called Case E.

Using the same soil model of Case E, if the ground grid is mirrored about the $x = 85$ (ft) plane, the geometry of the new ground grid is as described by Fig 3.4.

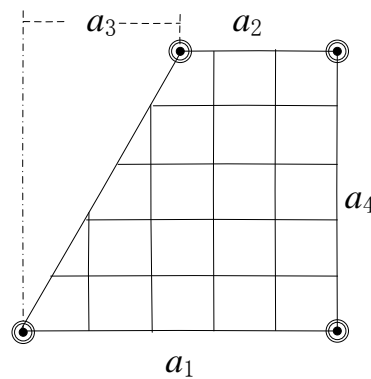


Fig 3.4 The Trapezoidal Ground Grid in Case F

The length a_1 is 170 ft, the length a_2 is 85 ft, the length a_3 is 85 ft and the length a_4 is 150 ft. The number of meshes along the x-axis is 5 and the number of meshes along

the y axis is 5. The rods are placed on the corners of the trapezoidal grid. The length of each rod is 30 ft. The fault current is 2.1 kA. This Case is called Case F.

The results of the potentials calculated for these two cases is shown in Table 3.3.

Table 3.3 Validation of Symmetry for the Trapezoidal Ground Grid

	Etouch (V)	Estep (V)
Case E	175.74	88.22
Case F	175.80	88.27
Difference	0.034%	0.057%

As seen in the table, the values of the touch and step potentials are not exactly the same for both cases. The reason is that for the two cases, the segmentation process yields a different number of segments for the two ground grids. The segmentation process tries to assign the number of segments of each ground conductor and rod such that every segment has the same length or at least so the lengths are close to each other. But because the number of segments must be an integer, the length of each segments cannot be exactly the same. The MATLAB functions that is used to do rounding is used to get the integer number of segments. Because there one leg of the trapezoid that is not perpendicular to the x-axis, the floating point rounding error and the functions that are used to do rounding (in order to make the number of segments an integer number) yield a different number of segments on the conductors that have intersections with this leg.

Since the difference between the results are less than 0.1% and are caused purely by the use of a different numbers of segments, the self-consistency test applied to the trapezoidal ground grid is considered to be passed.

3.3 The Accuracy Requirement

After the self-consistency is validated, to validate the MATLAB program, OL-GGA, it is necessary to compare the results calculated by the MATLAB program with the results calculated by the commercial grounding system design software, WinIGS. The relative difference of the touch potential is calculated as (3.1) and the relative difference of the step potential is calculated as (3.2),

$$\textit{Touch Potential Difference} = \frac{E_{touch_OLGGA} - E_{touch_WinIGS}}{E_{touch_WinIGS}} \times 100\% \quad (3.1)$$

$$\textit{Step Potential Difference} = \frac{E_{step_OLGGA} - E_{step_WinIGS}}{E_{step_WinIGS}} \times 100\% \quad (3.2)$$

where E_{touch_OLGGA} and E_{step_OLGGA} are the touch potential and the step potential calculated by OLGGA, respectively, and E_{touch_WinIGS} and E_{step_WinIGS} are the touch potential and the step potential calculated by WinIGS, respectively.

The accuracy requirement of the MATLAB program established by agreement with Tom LaRose of SRP, is that the relative difference between the touch potential and the step potential calculated by the MATLAB program must be less than 2.5% when compared to those calculated by WinIGS; however, when the touch potential or the step potential calculated by the MATLAB program is greater than those calculated by WinIGS, i.e., conservative, the difference is allowed to be greater than 2.5%.

3.4 The Parameter Limitations and the Segmentation Method

Experiments have shown that when the earth resistivity ratio ρ_1/ρ_2 is too large or too small, or when the aspect ratio of the mesh is too large or too small, the difference between the result calculated by the MATLAB program and the result calculated by the WinIGS is out of the bound of the 2.5% accuracy requirement. The limitations on the soil resistivity ratio ρ_1/ρ_2 and mesh aspect ratio have been set within the MATLAB program, OLGGA, in order to mark the range within which the results calculated by the MATLAB program match the results calculated by WinIGS.

Given the upper layer soil earth resistivity ρ_1 and the lower layer earth resistivity ρ_2 , and the length of the side of the mesh along the x- axis L_{mesh_x} , and the length of the side of the mesh along the y- axis L_{mesh_y} , the limitation on the earth resistivity ratio and the limitation on the aspect ratio of the mesh are:

- 1) When the length of any side of the ground grid is shorter than 100 ft,

$$0.2 \leq \frac{\rho_1}{\rho_2} \leq 40 \quad (3.3)$$

$$\frac{1}{3} \leq \frac{L_{mesh_x}}{L_{mesh_y}} \leq 3 \quad (3.4)$$

- 2) When the length of any side of the ground grid is shorter than 500 ft, but every side is longer than 100 ft,

$$0.2 \leq \frac{\rho_1}{\rho_2} \leq 20 \quad (3.5)$$

$$\frac{1}{3} \leq \frac{L_{mesh_x}}{L_{mesh_y}} \leq 3 \quad (3.6)$$

3) When all sides are longer than 500 ft,

$$0.1 \leq \frac{\rho_1}{\rho_2} \leq 40 \quad (3.7)$$

Other than the aspect ratio limit, no limit on $\frac{L_{mesh_x}}{L_{mesh_y}}$

The segmentation method is dependent of the shape of the ground grid. For rectangular ground grids, the length of each segment along the x-axis is equal to the length of each mesh side along the x-axis, and the length of each segment along the y-axis is equal to the length of each mesh side along the y axis.

For L-shaped ground grids, a reference length is calculated by dividing the length of the longest conductor in each direction by the number of meshes along that direction and then divided by 3; the length of the segment on each conductor along each side is calculated using the Ceil function of MATLAB, so that the length of each segment is approximately equal to the reference length, while the number of segments on each conductor is an integer.

For trapezoidal ground grids, the length of each conductor is generally different, because in a trapezoidal ground grid there are two sides that are not perpendicular or parallel to the other two sides. The reference length is calculated by dividing the length of the longest conductor by 20 and the length of each segment is calculated us-

ing the Ceil function of MATLAB, so that the length of each segment is approximately equal to the reference length, while the number of segments on each conductor is an integer.

The segmentation method has been so chosen that the touch potential and the step potential calculated by the MATLAB program best match those calculated by WinIGS.

3.5 The Validation with WinIGS

In this section the validation of the MATLAB program, OLGGA, is presented by comparing the touch potential and the step potential calculated by the MATLAB program and those calculated by WinIGS. It will be shown that the accuracy is satisfied within the parameter limitations presented in 3.4.

3.5.1 The Validation for Square Ground Grids and Rectangular Ground Grids

Case I: The following soil model is assumed. The upper layer soil earth resistivity ρ_1 is $100 \Omega \cdot \text{m}$, the lower layer soil earth resistivity ρ_2 is $10 \Omega \cdot \text{m}$, and the thickness of the upper layer soil is 10 ft.

The ground grid is a square ground grid as shown in Fig 3.5. The length of the side of the ground grid is 50 ft. The number of meshes along the x-axis is 5 and the number of meshes along the y-axis is 5. There are 4 ground rods placed on 4 corners,

and another 4 ground rods placed on the centers of the 4 sides. The length of each rod is 20 ft.

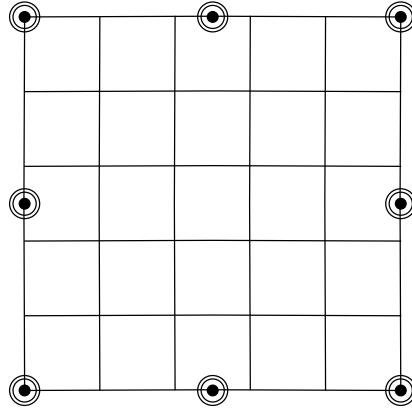


Fig 3.5 The Square Ground Grid

The fault current is assumed to be 1.9 kA. The touch potential and the step potential calculated by OLGGA as compared with those calculated by WinIGS are shown in Table 3.4.

Table 3.4 The Touch Potential and the Step Potential of Case I

Case I	Etouch (V)	Estep (V)
MATLAB	177.38	159.46
WinIGS	179.77	158.06
Difference	-1.33%	0.89%

Case II: The following soil model is assumed. The upper layer soil earth resistivity ρ_1 is 100 $\Omega \cdot m$, and the lower layer soil earth resistivity ρ_2 is 10 $\Omega \cdot m$, and the thickness of the upper layer soil is 10 ft.

The ground grid is a rectangular ground grid. The length of one side of the ground grid is 200 ft, and the length of another side of the ground grid is 50ft. The number of meshes along the x-axis is 16 and the number of meshes along the y-axis is 2. There

are 4 rods placed on the 4 corners, and another 20 ground rods placed on the perimeter of the ground grid as shown in Fig 3.6, so that the distance between any two adjacent rods on a side is uniform. The length of each rod is 20 ft.

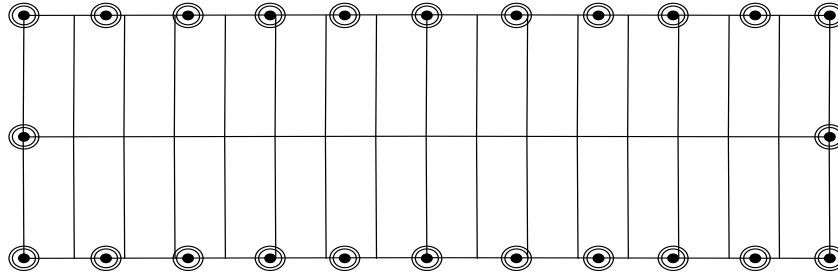


Fig 3.6 The Rectangular Ground Grid in Case II

The fault current is assumed to be 3.78 kA. The touch potential and the step potential calculated by OLGGA as compared with those calculated by WinIGS are shown in Table 3.5.

Table 3.5 The Touch Potential and the Step Potential of Case II

Case II	Etouch (V)	Estep (V)
MATLAB	179.36	120.02
WinIGS	179.11	116.76
Difference	0.14%	2.79%

Case III: The following soil model is assumed. The upper layer soil earth resistivity ρ_1 is $20 \Omega \cdot \text{m}$, the lower layer soil earth resistivity ρ_2 is $100 \Omega \cdot \text{m}$, and the thickness of the upper layer soil is 10 ft.

The ground grid is a rectangular ground grid. The length of one side of the ground grid is 200 ft, and the length of another side of the ground grid is 50ft. The number of meshes along the x-axis is 8 and the number of meshes along the y-axis is 4. There are 4 rods placed on the 4 corners, as shown in Fig 3.7. The length of each rod is 10 ft.

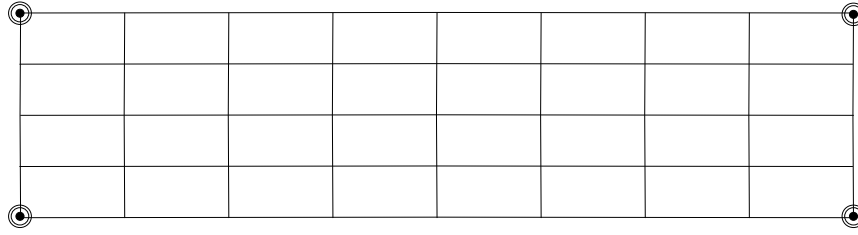


Fig 3.7 The Rectangular Ground Grid in Case III

The fault current is assumed to be 3.78 kA. The touch potential and the step potential calculated by OLGGA as compared with those calculated by WinIGS are shown in Table 3.6.

Table 3.6 The Touch Potential and the Step Potential of Case III

Case III	Etouch (V)	Estep (V)
MATLAB	194.30	247.81
WinIGS	195.51	244.65
Difference	-0.62%	1.29%

3.5.2 The Validation for L-Shaped Ground Grids

Case IV: The following soil model is assumed. The upper layer soil earth resistivity ρ_1 is $100 \Omega \cdot \text{m}$, the lower layer soil earth resistivity ρ_2 is $20 \Omega \cdot \text{m}$, and the thickness of the upper layer soil is 10 ft.

The ground grid is L-shaped, as shown in Fig 3.8. The length of the side a_1 is 400 ft, the length of the side a_2 is 400 ft, the length of the side a_3 is 200 ft, and the length of the side a_4 is 200 ft. The number of meshes along the x-axis is 8 and the number of meshes along the y-axis is 24. There are 6 rods on the corners, and there are 10 other rods placed as shown in the Fig 3.8, so that the distance between any two adjacent rods on a side is uniform. The length of any each is 30 ft.

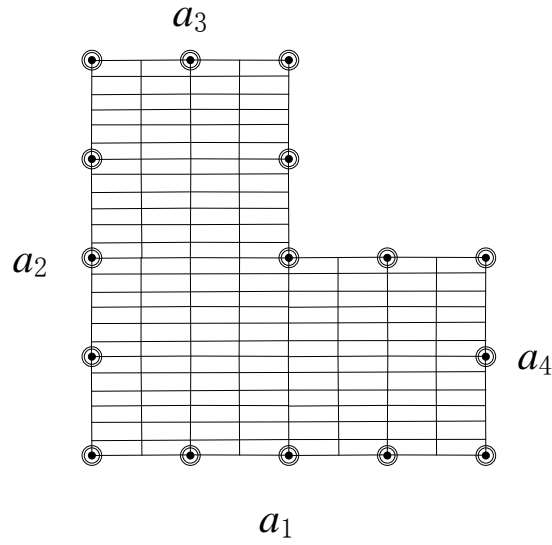


Fig 3.8 The L-Shaped Ground Grid in Case IV

The fault current is assumed to be 3.78 kA. The touch potential and the step potential calculated by OLGGA as compared with those calculated by WinIGS are shown in Table 3.7.

Table 3.7 The Touch Potential and the Step Potential of Case IV

Case IV	Etouch (V)	Estep (V)
MATLAB	122.65	60.61
WinIGS	123.52	61.01
Difference	-0.71%	-0.65%

Case V: The following soil model is given. The upper layer soil earth resistivity ρ_1 is $20 \Omega \cdot \text{m}$, the lower layer soil earth resistivity ρ_2 is $100 \Omega \cdot \text{m}$, and the thickness of the upper layer soil is 10 ft.

The ground grid is L-shaped as shown in Fig 3.9. The length of the side a_1 is 400 ft, the length of the side a_2 is 400 ft, the length of the side a_3 is 200 ft, and the length of the side a_4 is 200 ft. The number of meshes along the x-axis is 8 and the number of

meshes along the y-axis is 8 as shown in Fig 3.9. There are 6 rods on the corners. The length of each rod is 10 ft.

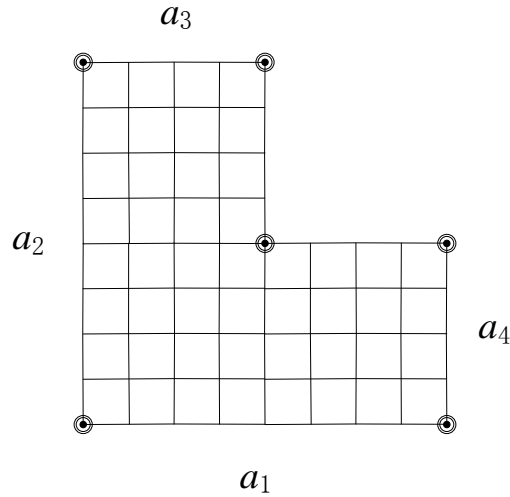


Fig 3.9 The L-Shaped Ground Grid in Case V

The fault current is assumed to be 3.78 kA. The touch potential and the step potential calculated by OLGGA are compared with those calculated by WinIGS are shown in Table 3.8.

Table 3.8 The Touch Potential and the Step Potential of Case V

Case V	Etouch (V)	Estep (V)
MATLAB	87.35	76.75
WinIGS	88.07	75.00
Difference	-0.82%	1.00%

Case VI: The following soil model is assumed. The upper layer soil earth resistivity ρ_1 is $100 \Omega \cdot \text{m}$, the lower layer soil earth resistivity ρ_2 is $20 \Omega \cdot \text{m}$, and the thickness of the upper layer soil is 10 ft.

The ground grid is L-shaped. The length of the side a_1 is 400 ft, the length of the side a_2 is 600 ft, the length of the side a_3 is 200 ft, and the length of the side a_4 is 250 ft. The number of meshes along the x-axis is 8 and the number of meshes along the y-

axis is 24. There are 6 rods placed on the corners, and there are another 4 rods placed as shown in Fig 3.10, so that the distance between any two adjacent rods on a side is uniform. The length of each rod is 30 ft.

The fault current is assumed to be 3.78 kA. The touch potential and the step potential calculated by OLGGA as compared with those calculated by WinIGS are shown in Table 3.9.

Table 3.9 The Touch Potential and the Step Potential of Case VI

Case VI	Etouch (V)	Estep (V)
MATLAB	141.03	57.94
WinIGS	142.03	56.53
Difference	-0.71%	2.49%

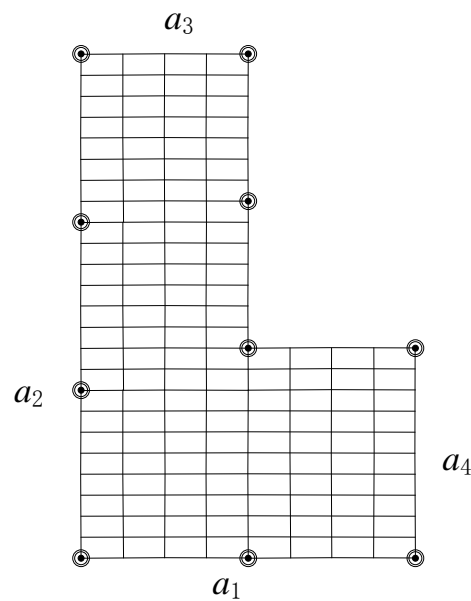


Fig 3.10 The L-Shaped Ground Grid in Case VI

3.5.3 The Validation for Trapezoidal Ground Grids

Case VII: The following soil model is assumed. The upper layer soil earth resistivity ρ_1 is $100 \Omega \cdot \text{m}$, and the lower layer soil earth resistivity ρ_2 is $20 \Omega \cdot \text{m}$, and the thickness of the upper layer soil is 10 ft.

The ground grid is a trapezoid. The length of the side a_1 is 120 ft, the length of the side a_2 is 100 ft, the length of the offset a_3 is 10 ft, and the height a_4 is 100 ft, as shown in Fig 3.11. The number of meshes along the x-axis is 4 and the number of meshes along the y-axis is 10. There are 4 rods placed on the corners, and there are another 8 rods placed as shown in the figure Fig 3.11 so that the distance between any two adjacent rods on each side is uniform. The length of each rod is 30 ft.

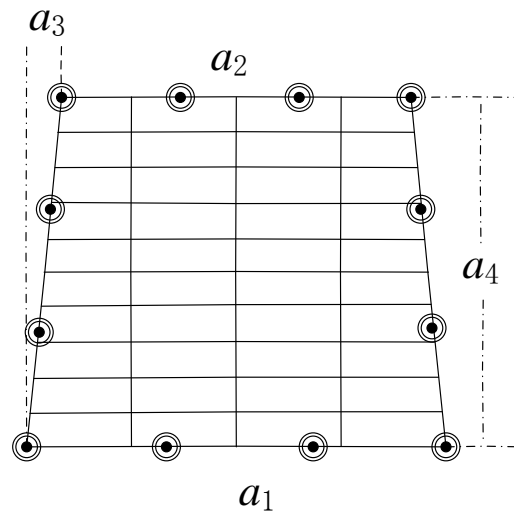


Fig 3.11 The Trapezoidal Ground Grid in Case VII

The fault current is assumed to be 3.78 kA. The touch potential and the step potential calculated by OLGGA as compared with those calculated by WinIGS are shown in Table 3.10.

Table 3.10 The Touch Potential and the Step Potential of Case VII

Case VII	Etouch (V)	Estep (V)
MATLAB	264.45	200.42
WinIGS	267.12	199.00
Difference	-1.00%	0.71%

Case VIII: The following soil model is assumed. The upper layer soil earth resistivity ρ_1 is $10 \Omega \cdot \text{m}$, and the lower layer soil earth resistivity ρ_2 is $100 \Omega \cdot \text{m}$, and the thickness of the upper layer soil is 5 ft.

The ground grid is a trapezoid as shown in Fig 3.12. The length of the side a_1 is 150 ft, the length of the side a_2 is 100 ft, the length of the offset a_3 is 10 ft, and the length of the side a_4 is 100 ft. The number of meshes along the x-axis is 4 and the number of meshes along the y-axis is 4. There are 4 rods placed on the corners. The length of each rod is 10 ft.

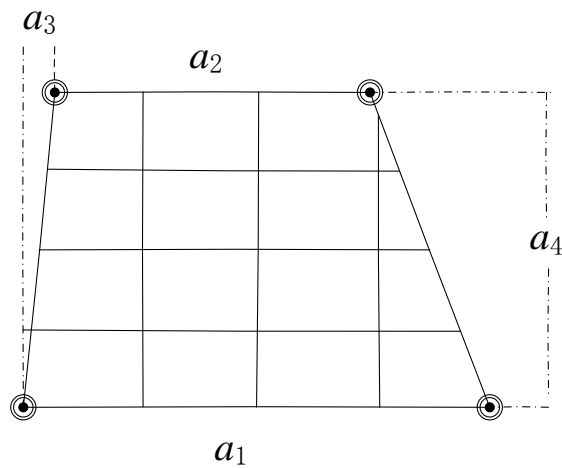


Fig 3.12 The Trapezoidal Ground Grid in Case VIII

The fault current is assumed to be 3.78 kA. The maximum touch and step potentials calculated OLGGA as compared with those calculated by WinIGS is shown in Table 3.11.

Table 3.11 The Touch Potential and the Step Potential of Case VIII

Case VIII	Etouch (V)	Estep (V)
MATLAB	130.70	220.08
WinIGS	130.73	219.78
Difference	-0.02%	0.14%

Case IX: The following soil model is assumed. The upper layer soil earth resistivity ρ_1 is $100 \Omega \cdot \text{m}$, and the lower layer soil earth resistivity ρ_2 is $20 \Omega \cdot \text{m}$, and the thickness of the upper layer soil is 10 ft.

The ground grid is a trapezoid. The length of the side a_1 is 150 ft, the length of the side a_2 is 100 ft, the length of the offset a_3 is -20 ft, and the length of the side a_4 is 100 ft. The number of meshes along the x-axis is 4 and the number of meshes along the y-axis is 10. There are 4 rods placed on the corners, and there are another 5 rods placed as shown in Fig 3.13 so that the distance between any two adjacent rods on a given side is uniform. The length of each rod is 30 ft.

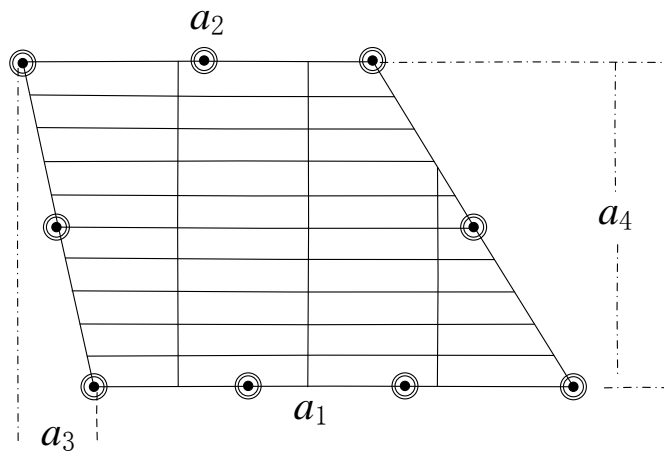


Fig 3.13 The Trapezoidal Ground Grid in Case IX

The fault current is assumed to be 3.78 kA. The touch potential and the step potential calculated by the MATLAB program as compared with those calculated by WinIGS are shown in Table 3.12.

Table 3.12 The Touch Potential and the Step Potential of Case IX

Case IX	Etouch (V)	Estep (V)
MATLAB	320.04	232.11
WinIGS	321.20	221.45
Difference	-0.36%	4.81%

As shown in the previous cases, for Case II and Case IX, the difference of the step potential is greater than 2.5%. But the step potentials calculated by the MATLAB program are greater than those calculated by WinIGS, hence the MATLAB program gives conservative step potential results.

3.5.4 Plots of Errors

More cases were tested and the difference in the touch potential and the step potential between the results of the proposed program and the results of WinIGS is plotted against the touch potential and the step potential respectively as shown in Fig 3.14 and Fig 3.15.

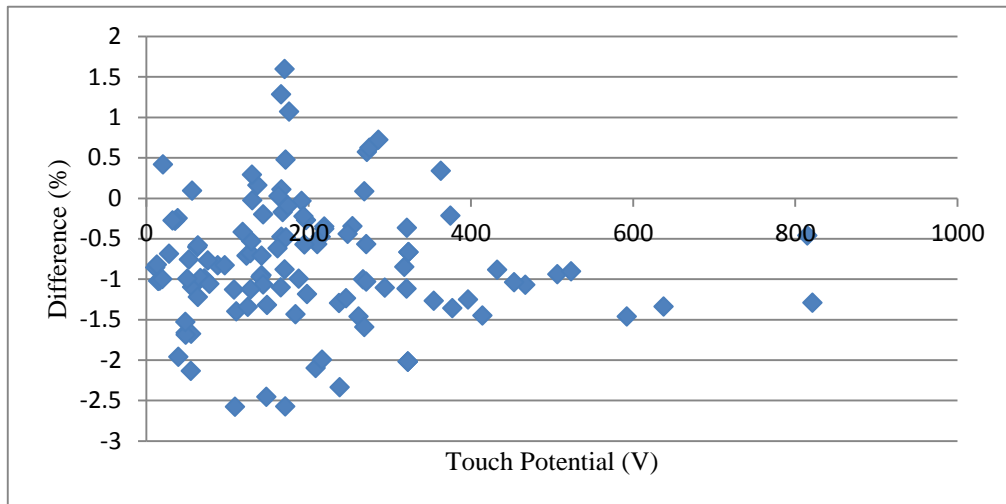


Fig 3.14 The Difference in Percent for the Touch Potential

In Fig 3.15, the difference of the step potential calculated by the MATLAB program and that calculated by WinIGS is plotted. In Fig 3.15, a positive difference means the step potential calculated by the MATLAB program is greater than that calculated by WinIGS. Positive error means the step potentials calculated by the MATLAB program is conservative.

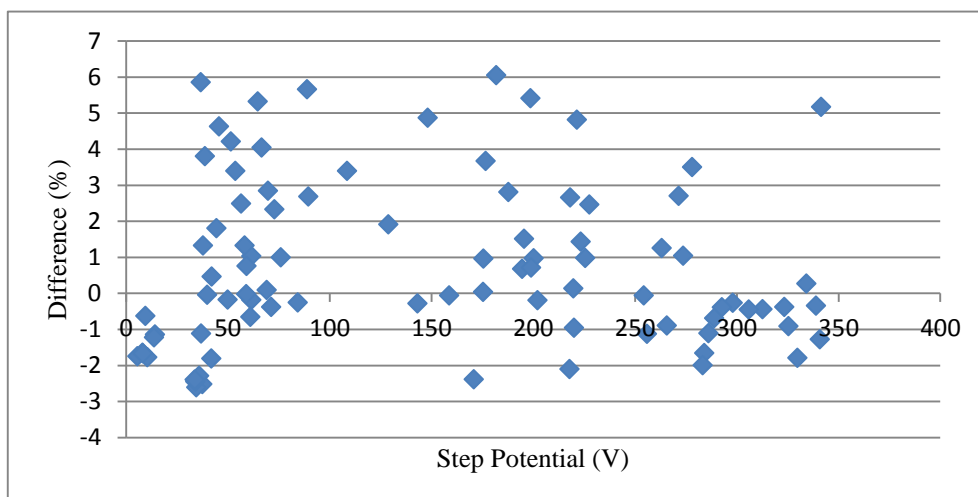


Fig 3.15 The Difference in Percent for the Step Potential

4 GROUND GRID OPTIMIZATION

The Optimal Ground Grid Application (OLGGA) was developed to optimize the design of the substation ground grid. The optimal design of the ground grid should satisfy the safety requirement, and the cost of material and labor should be minimized. In this chapter, the optimization model and the optimization algorithms used by OLGGA are presented. The case studies are also presented at the end of the chapter.

4.1 The Safety Requirement

As it is shown in Chapter 1, the safety requirement is that the maximum touch and step potentials of a ground grid must be less than the respective maximum allowable values. The maximum allowable touch and step potentials are obtained from the equations in the IEEE standard [1]:

1. The maximum allowable touch potential calculated may be calculated from IEEE Std 80-2000 [1]

$$E_{touch_allowable} = (1000 + 1.5\rho) \frac{0.116}{\sqrt{t_f}} \quad (4.1)$$

where ρ is the upper soil earth resistivity and t_f is the time duration of the fault.

2. The maximum allowable is also calculated from IEEE Std 80-2000 [1] is:

$$E_{step_allowable} = (1000 + 6\rho) \frac{0.116}{\sqrt{t_f}} \quad (4.2)$$

In addition to the restrictions on the touch and step potentials, the SRP rules require that the ground resistance to the remote earth must be lower than 0.5 Ω .

The safety requirements are used as a set of nonlinear constraints in the optimization problem formulation. The content of Chapter 2 presents the method of calculating the touch potential, the step potential and the ground resistance to the remote earth.

4.2 The Objective Function and Constraints

For the ground grid optimization, the objective function is the total cost of building a ground grid. It includes the cost of labor and the cost of materials. The objective function should be minimized while the design should satisfy the constraints. In this section, the objective function and the constraints are presented.

4.2.1 The Parameters and the Ground Grid Design Rules

The construction parameters include the cost of materials and the cost of labor, and physical specifications for the horizontal conductors and ground rods.

- The cost of the horizontal ground conductor copper is \$ 3.77 /ft (C_{cond}).
- The cost of labor to trench, install cable, and backfill is \$ 4 /ft (C_{trench}).
- The cost of labor to drive rods up to 10 ft is \$ 10 /ft , and the cost of labor to drive rods 11 to 40 ft is \$ 32 /ft (C_{drive}).
- The cost of labor to make exothermic connections from cable to cable or from cable to ground rod is \$ 40 each ($C_{connect}$)
- The cost of the exothermic connector material and mold is \$ 19.25 each (C_{exo})

The ground grid design rules include the followings.

- The bury depth of the horizontal ground mat is 1.5 ft (h).
- The coarsest allowable mesh dimension is 50 ft (L_{mesh_max}).
- The smallest allowable mesh dimension is 8.5 ft (L_{mesh_min}).
- The type of the horizontal conductors is 4/0 copper conductor.
- The type of the ground rods is 5/8 copper conductor.
- The distance between any two adjacent ground rods should be greater than the length of the ground rod.
- The maximum touch potential of the ground grid must not be greater than the maximum allowable touch potential.
- The maximum step potential of the ground grid must not be greater than the maximum allowable step potential.
- The ground resistance must not be greater than 0.5 Ω .

4.2.2 The Objective Function

The objective function to be minimized is the total cost of building a ground grid. It includes the cost of materials and the cost of labor. Using the construction parameters and the design rules, the objective function and the constraints can be summarized as given by (4.3) to (4.9).

$$\begin{aligned} \min. \text{ Cost} = & L_{h_total}(C_{cond} + C_{trench}) \\ & + L_{v_total}(C_{cond} + C_{drive}) + N_{joints}(C_{connect} + C_{exo}) \end{aligned} \quad (4.3)$$

s.t.

$$E_{touch} \leq E_{touch_allowable} \quad (4.4)$$

$$E_{step} \leq E_{step_allowable} \quad (4.5)$$

$$R_g \leq 0.5 \Omega \quad (4.6)$$

$$8.5 \text{ ft} \leq L_{mesh_x} \leq 50 \text{ ft} \quad (4.7)$$

$$8.5 \text{ ft} \leq L_{mesh_y} \leq 50 \text{ ft} \quad (4.8)$$

$$N_{min} \leq N_{rod} \leq N_{rod_max} \quad (4.9)$$

In the objective function and the constraints, L_{h_total} is the total length of the horizontal conductors; L_{v_total} is the total length of the ground rods; N_{min} is the number of corners of the ground grid; N_{rod_max} is the maximum allowable total number of rods that does not violate the design rule for ground rods; N_{joints} is the total number of points where two conductors overlay each other or where a grid conductor overlays a ground rod; E_{touch} is the calculated touch potential; E_{step} is the calculated step potential; L_{mesh_x} is the length of the mesh side that is parallel to the x-axis; L_{mesh_y} is the length of the mesh side that is parallel to the y-axis; R_g is the ground resistance to the remote earth; N_{rod} is the total number of rods; $E_{touch_allowable}$ and $E_{step_allowable}$ are the maximum allowable touch potential and the maximum allowable step potential respectively.

For rectangular ground grids, N_{joints} is equal to $[(N_x+1) (N_y+1)) + N_{rod}]$, where N_x is the number of meshes along the x-axis and N_y is the number of meshes along the y-

axis. For L-shaped ground grids and trapezoidal ground grids, the expression is complicated and requires an algorithmic approach, which is not reproduced here.

According to the SRP design rules [23] for ground rods, the length of the ground rod depends on the soil model. When the upper layer earth resistivity is less than or equal to the lower layer earth resistivity, or the thickness of the upper layer soil is greater than 30 ft, the length of the ground rod is 10 ft. When the upper layer earth resistivity is greater than the lower layer earth resistivity, and the thickness of the upper layer soil is less than 10 ft, the length of the ground rod is 20ft. When the upper layer earth resistivity is greater than the lower layer earth resistivity, and the thickness of the upper layer soil is greater than 10 ft but less than 30ft, the length of the ground rod is 30 ft.

4.3 Genetic Algorithm and Pattern Search

Compared to traditional optimization algorithms, the capability of dealing with complex optimization problems is the motivation for selecting the genetic algorithm for ground grid optimization. In ground grid optimization, the objective function involves integer design parameters and the constraints, whose number can change with each iteration, include nonlinear constraints on the touch and step potentials and the ground resistance to the remote earth.

In the genetic algorithm, the parameters and the fitness function related to the objective function are encoded into binary strings. The initial population is created, and

in each generation, the fitness of all the individuals in the population is evaluated. A new population is created by performing crossover and mutation, and the old population is replaced, and the new population is used in the new iteration. When the convergence criterion is met or the maximum number of iterations is reached, the result is decoded to obtain the solution to the optimization problem. The most fit individual in each generation is not being modified by crossover and mutation, so that the best solution is achieved more quickly [17].

The pseudo code of the genetic algorithm can be found in page 42 of [17], however, the implementation of the genetic algorithm is done by using the GA function of MATLAB. References [20] and [21] have defined the convergence criterion for the genetic algorithm as applied to the ground grid optimization, and introduced a pattern search algorithm together with the genetic algorithm to speed up the overall optimization process. An introduction of the pattern search algorithm is presented in [20] and [21].

4.4 Case Studies

In this section, the OptimaL Ground Grid Application (OLGGA) is used to solve ground grid optimization problems and find the optimal designs for the rectangular ground grid, the L-shaped ground grid and the trapezoidal ground grid. For the following cases, the fault current I_f is assumed to be 3780 A, and the duration of the fault is assumed to be 0.53 s.

Case 1. The goal is to find the optimal design of a rectangular ground grid. The length of the side of the horizontal ground mat is 200 ft and the width of it is 100 ft. In the two layer soil model, the earth resistivity of the upper layer soil is $150 \Omega \cdot \text{m}$, and the earth resistivity of the lower layer soil is $30 \Omega \cdot \text{m}$, and the thickness of the upper layer soil is 10 ft.

OLGGA gives the optimal design after taking approximately 20 minutes. The performance of the proposed design is shown in Table 4.1.

As shown Table 4.1, the number of meshes along the x-axis is 18 and the number of meshes along the y-axis is 11. The length of the mesh along the x-axis is 11.11 ft and the length of the mesh along the y-axis is 9.09 ft. The number of rods placed on the side of the grid that is parallel to the x-axis is 5, and the number of rods placed on the side that is parallel to the y-axis is 2. The total number of rods is 18, which includes the 4 rods on 4 corners. The touch potential of the optimal design is 194.75 V while the maximum allowable touch potential is 195.19 V. The calculated step potential is 188.8 V while the maximum allowable step potential is 302.74 V. The ground resistance to the remote earth is 0.35Ω while the maximum allowable ground resistance is 0.5Ω . The total cost of ground grid installation, labor and materials, is \$ 67302.

Table 4.1 The Optimal Design for the Rectangular Ground Grid

Number of Meshes		Mesh Size		Number of Rods	
Nx	Ny	x-side	y-side	x-side	y-side
18	11	11.11 ft	9.09 ft	5	2
Touch Potential				(Plus rods on corners)	
Proposed	Maximum Allowable			Total Number of Rods	
194.75 V	195.19 V			18	
Step Potential					
Proposed	Maximum Allowable				
188.8 V	302.74 V				
Ground Resistance					
Proposed	Maximum Allowable			Total Cost: \$ 67302	
0.35 Ω	0.50 Ω				

The geometry of the proposed design is shown in Fig 4.1.

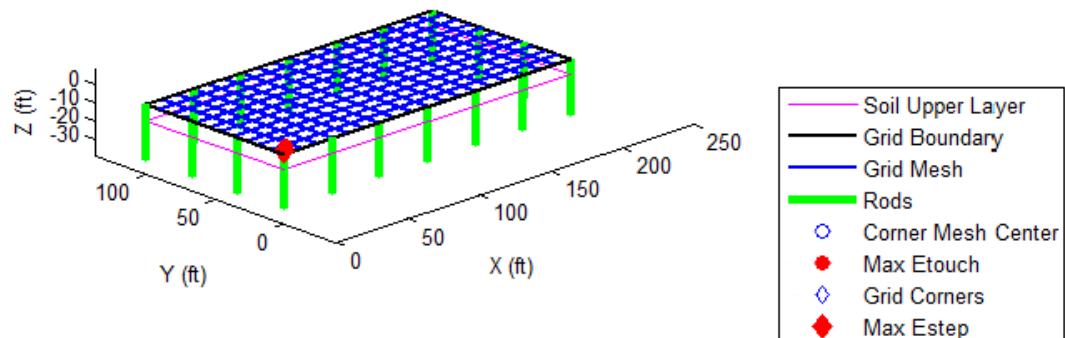


Fig 4.1 The Geometry of the Optimal Design

OLGGA is capable of showing a 2D plot and a 3D plot of the touch potential of the optimal design of the rectangular ground grid, as shown in Fig 4.2. In the 2D plot, the horizontal axis is along the diagonal line of the rectangular ground grid. The unit of the horizontal axis is ft. The vertical axis is the touch potential in Volts.

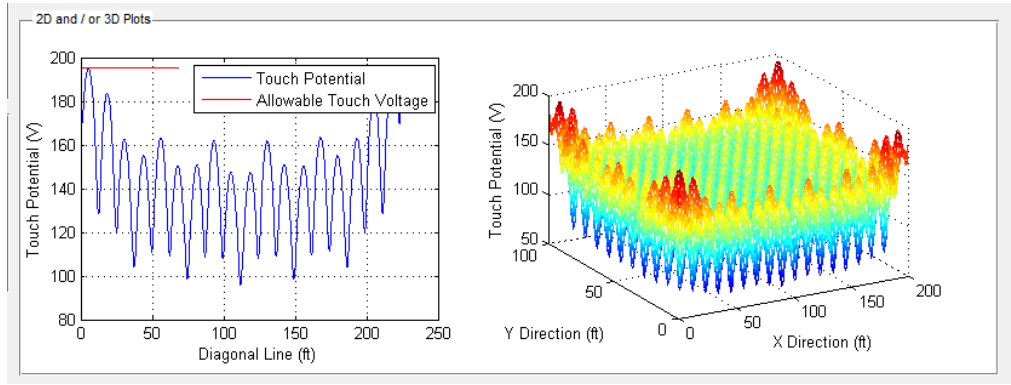


Fig 4.2 2D Plot and 3D Plot of the Touch Potential

Case 2. In this case, the goal is to find the optimal design of a L-shaped ground grid. The length of the side a_1 is 500 ft, and the length of the side a_2 is 400 ft, and the length of the side a_3 is 200 ft, and the length of the side a_4 is 200 ft. The perimeter of the ground grid is shown in Fig 4.3, which also defines the length parameters a_1 to a_6 .

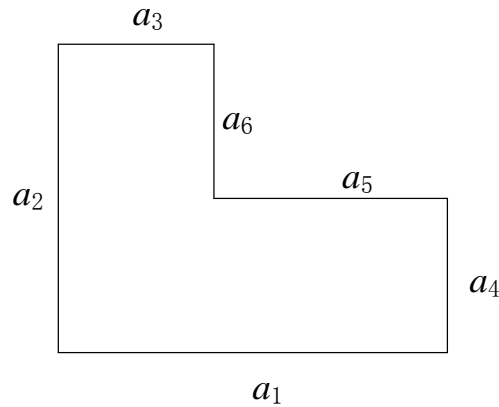


Fig 4.3 The Perimeter of the L-Shaped Ground Grid

In the two layer soil model, the earth resistivity of the upper layer soil is $100 \Omega \cdot \text{m}$, and the earth resistivity of the lower layer soil is $20 \Omega \cdot \text{m}$, and the thickness of the upper layer soil is 10 ft.

OLGGA gives the optimal design in Table 4.2 after taking approximately 30 minutes. The performance of the proposed design is shown in Table 4.2.

Table 4.2 The Optimal Design for the L-Shaped Ground Grid

Number of Meshes		Mesh Size		Number of Rods	
Nx	Ny	x-side	y-side	a ₁ -side	a ₂ -side
11	9	45.45 ft	44.44 ft	4	3
Touch Potential				a ₃ -side	a ₄ -side
Proposed	Maximum Allowable			1	1
182.72	183.24			a ₅ -side	a ₆ -side
Step Potential				2	1
Proposed	Maximum Allowable			(Plus rods on corners)	
73.02	254.94 V			Total Number of Rods	
Ground Resistance				18	
Proposed	Maximum Allowable				
0.11 Ω	0.50 Ω			Total Cost: \$ 82931	

The geometry of the proposed design is shown in Fig 4.4.

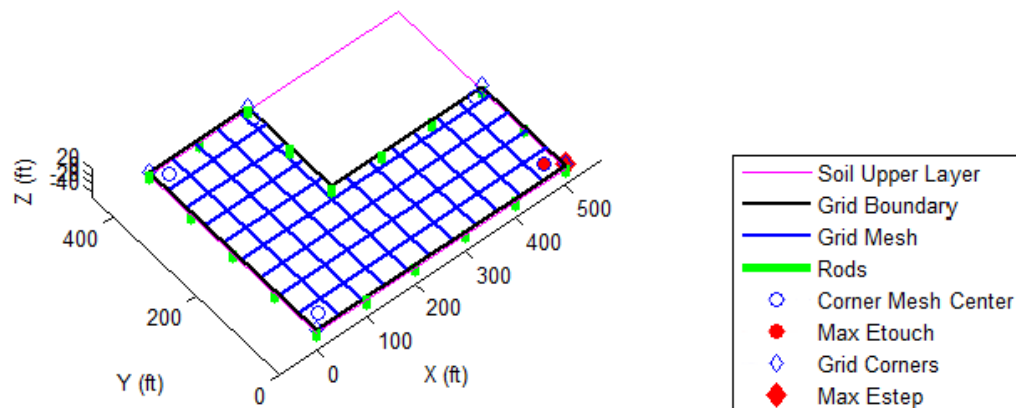


Fig 4.4 The Geometry of the Optimal Design

OLGGA is also capable of showing a 3D plot of the touch potential of the optimal design of the L-shaped ground grid, as shown in Fig 4.5.

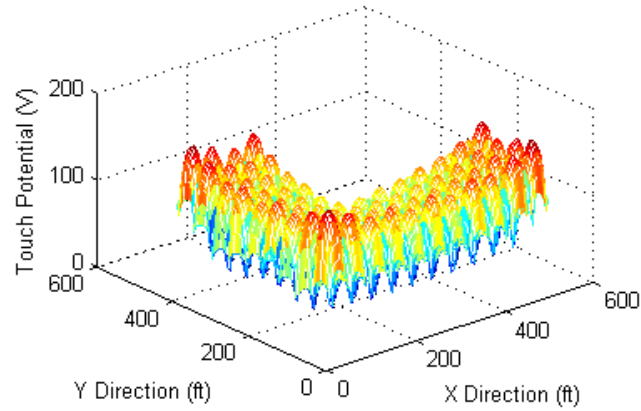


Fig 4.5 3D Plot of the Touch Potential

Case 3. In this case, the goal is to find the optimal design of a trapezoidal ground grid. The length of the bottom side a_1 is 200 ft, and the length of the top side a_2 is 150 ft, and the length of the offset of the left leg a_3 is 0 ft, and the length of the height of the trapezoid a_4 is 200 ft. In the two layer soil model, the earth resistivity of the upper layer soil is $100 \Omega \cdot \text{m}$, and the earth resistivity of the lower layer soil is $20 \Omega \cdot \text{m}$, and the thickness of the upper layer soil is 10 ft.

OLGGA gives the optimal design after approximately 20 minutes of execution time. The geometry of the proposed design is shown in Fig 4.6.

The performance of the proposed design is shown in Table 4.3.

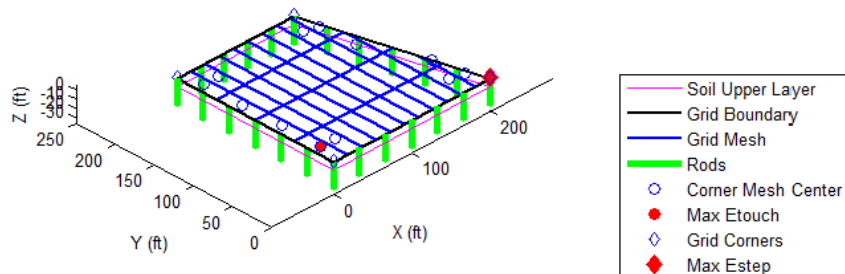


Fig 4.6 The Geometry of the Optimal Design

Table 4.3 The Optimal Design for the Trapezoidal Ground Grid

Number of Meshes		Mesh Size		Number of Rods	
Nx	Ny	x-side	y-side	Bottom	Top
11	4	18.18	50	5	4
Touch Potential				Left	Right
Proposed	Maximum Allowable			5	5
177.07	183.24			(Plus rods on corners)	
Step Potential				Total Number of Rods	
Proposed	Maximum Allowable			23	
108.88	254.94 V				
Ground Resistance					
Proposed	Maximum Allowable				
0.19 Ω	0.50 Ω			Total Cost: \$ 59385	

The 3D plot of the touch potential of the optimal design of the trapezoidal ground grid is shown in Fig 4.7.

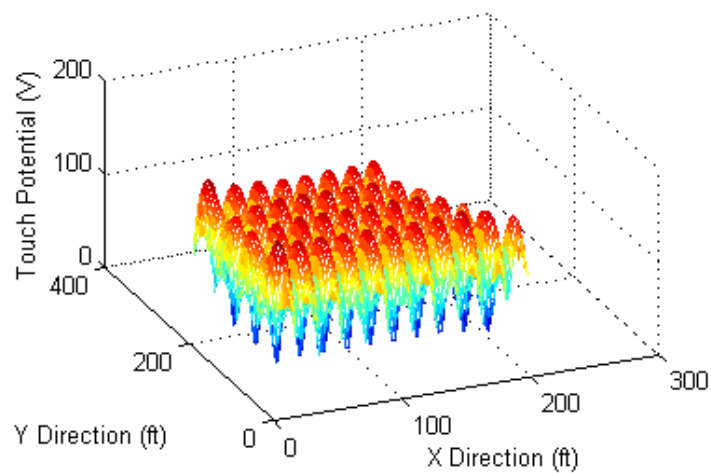


Fig 4.7 The 3D Plot of the Touch Potential for the Trapezoidal Ground Grid

5 CONCLUSIONS

5.1 Conclusions

This work is based on a project sponsored by Salt River Project (SRP). In this work, the OptimaL Ground Grid Application (OLGGA) is presented. OLGGA is designed to solve the ground grid optimization problem. The proposed application (OLGGA) is capable of handling square, rectangular, L-shaped, and trapezoidal ground grids.

The equations that are used to calculate the touch potential, the step potential and the ground resistance to the remote earth in a two layer soil model are presented, and they are used as nonlinear constraints in the optimization.

The line-line model and the point-point model are introduced in Chapter 2. They are used to derive the equations for the mutual resistance between two conductor segments. The equations used to deal with the sides of a trapezoidal ground grid are derived from the line-line model.

In Chapter 3 the concept of self-consistency and the ways to test the self-consistency of the application are introduced. The validation of the application is also presented.

The optimization model is presented in Chapter 4. The optimization algorithms are also introduced. The optimal design of the ground grid satisfies the safety requirements, which are presented both in Chapter 1 and in Chapter 4.

The graphical user interface is further developed to accommodate the trapezoidal ground grid and the L-shaped ground grid and the user's manual of OLGGA is presented in Appendix A.

This work is built upon the work of two predecessors. The author started the work reported here on May 2014. At that time, a version of the graphic interface of OLGGA and the graphical user interface of the Soil Model Builder were available from predecessors of this project, and for the rectangular ground grids without any ground rod, the program was able to yield relatively accurate results. In the graphical user interface, the number of ground rods could only be an integer times the number of sides, and the maximum number of ground rods was 12. The optimization algorithms were already chosen.

The author's contribution is shown below.

- 1) Made the application self-consistent.
- 2) Improved the accuracy so that the accuracy requirement was satisfied.
- 3) Updated the ground rod placement method so that the placement of ground rods satisfied the SRP rules for ground rods.
- 4) Reduced the execution time by changing parts of the MATLAB code into MATLAB executable C code.
- 5) Derived new equations so that the application could be capable of handling trapezoidal ground grids.
- 6) Added new functionality to the graphical user interface.

7) Wrote the user's manual of OLGGA.

8) Completed code documentation.

REFERENCES

- [1] IEEE Guide for Safety in AC Substation Grounding, IEEE Std 80-2000 (Revision of IEEE Std 80-1986). New York, USA. 2000
- [2] E. D. Sunde, *Earth Conduction Effects in Transmission Systems*. New York: Dover, 1968
- [3] A.P. Meliopoulos, R. P. Webb, E. B. Joy, Analysis of Grounding Systems, IEEE Transactions Power Apparatus and Systems, vol. PAS-100, no. 3, Mar, 1981
- [4] F. Dawalibi, D. Mukhedkar, Parametric Analysis of Grounding Grids, IEEE Transactions Power Apparatus and Systems, vol. PAS-98, no. 5, Sept/Oct, 1979
- [5] R. J. Heppe, "Computation of potential at surface above an energized grid or other electrode, allowing for non-uniform current distribution," IEEE Transactions Power Apparatus and Systems, vol. PAS-98, no.6, Nov./Dec, 1979
- [6] F. Dawalibi, "Optimum design of substation ground in a two layer earth structure Part II: Comparison between theoretical and experimental results," IEEE Trans. Power App., vol. PAS-94, no.2, Mar, 1975
- [7] Y. L. Chow, J. J. Yang, K. D. Srivastava, "Complex Images of a Ground Electrode in Layered Soils," Journal of Applied Physics, vol. 71, issue 2, 1992, pp. 560-574.
- [8] Bo Zhang, Research on the Numerical Methods for Electromagnetic Fields of Substations' Grounding Systems in Frequency Domain and Application, Ph.D. Dissertation, North China Electric Power University, 2003
- [9] Zhi-Bin Zhao, Analysis of Characteristics of Grounding Grids in Complex Soil and Calculation of Electromagnetic Field in Substations, Ph.D. Dissertation, North China Electric Power University, 2004
- [10] Zhong-Xin Li, Weijiang Chen, Jian-Bin Fan, and Jiayu Lu, A Novel Mathematical Modeling of Grounding System Buried in Multilayer Earth, IEEE Transactions on Power Delivery, vol. 21, no. 3, Jul, 2006
- [11] Zhong-Xin Li, Jian-Bin Fan, "Numerical calculation of grounding system in low-frequency domain based on the boundary element method", Int. J. Numer. Meth. Engng 2008, vol. 73, pp. 685-705
- [12] E. B. Joy, A.P. Meliopoulos, R. P. Webb, Graphical and Tabular Results of Computer Simulation of Faulted URD Cables, Georgia Institute of Technology, 1981.

- [13]SOMIP: Fortran code taken from the industry standard open source program
SOMIP
- [14]Windows Based Integrated Grounding System Design Program, WinIGS Applications & Training Guides, January 2012, http://www.ap-concepts.com/_downloads/IGS_SDA_AppGuide.pdf
- [15]B. Thapar, V. Gerez, A. Balakrishnan, D. A. Blank, "Evaluation of ground resistance of a grounding grid of any shape", IEEE Transactions on Power Delivery, vol. 6, No.2, April 1991
- [16]J. H. Holland, Adaptation in Natural and Artificial Systems: An Introductory Analysis with Applications to Biology, Control, and Artificial Intelligence, Ann Arbor, University of Michigan Press, 1975, Reprinted by MIT press, 1992
- [17]Xin-She Yang, Nature-Inspired Metaheuristic Algorithms, UK, University of Cambridge, Luniver Press, 2010
- [18]A. F. Otero, J. Cidras, C. Garrido, Genetic Algorithm Based Method for Grounding Grid Design, 1998 IEEE International Conference on Evolutionary Computation Proceedings. IEEE World Congress on Computational Intelligence, 1998, pp. 120-123.
- [19]A. Covitti, G. Delvecchio, A. Fusco, F. Lerario, and F. Neri, Two Cascade Genetic Algorithms to Optimize Unequally Spaced Grounding Grids with Rods, EUROCON 2005 - The International Conference on "Computer as a Tool", 2005, pp. 1533-1536
- [20]Xuan Wu, Ground System Analysis and Optimization, MS Thesis, Arizona State University, 2013
- [21]Qianzhi Zhang, Optimal Substation Ground Grid Design Based on Genetic Algorithm and Pattern Search, MS Thesis, Arizona State University, 2014
- [22]Centroid - Wikipedia, <https://en.wikipedia.org/wiki/Centroid>
- [23]SRP Design Standards BI03.05

APPENDIX A
THE USER'S MANUAL

ARIZONA STATE UNIVERSITY

OptimaL Ground Grid Application

User's Manual

A.1 Overview

The user manual provides general information on how to use the "OptimaL Ground Grid Application" (OLGGA). The objective of the manual is to assist the user in: (1) updating the grid construction parameters, (2) creating the soil model or reading the Wenner-method measured field data from a specific Excel file, (3) selecting the shape of the ground grid, (4) selecting the optimization options, (5) starting the the program, and (6) saving the results. This manual does not provide information about the structure of the program or the mathematical modeling techniques employed.

This manual contains three sections. This section, Section A.1 contains an overview of the User Manual. Section A.2 is a brief description of the program. Section A.3 contains detailed information about how to use the program.

A.2 Program Description

The program "OptimaL Ground Grid Application" optimize the placement of horizon ground conductor and ground rods for a ground grid with a fixed perimeter set by the user for a given two-layer soil model prescribed by the user. After the optimization is performed, the results are displayed on a user interface and the user may save the results to an independent pdf file.

A.3 How to Use the Program

A.3.1 What the interface looks like

The OptimaL Ground Grid Application (OLGGA) is designed using MATLAB's Graphical User Interface tools. The OLGGA main window is shown in Figure 3.1.

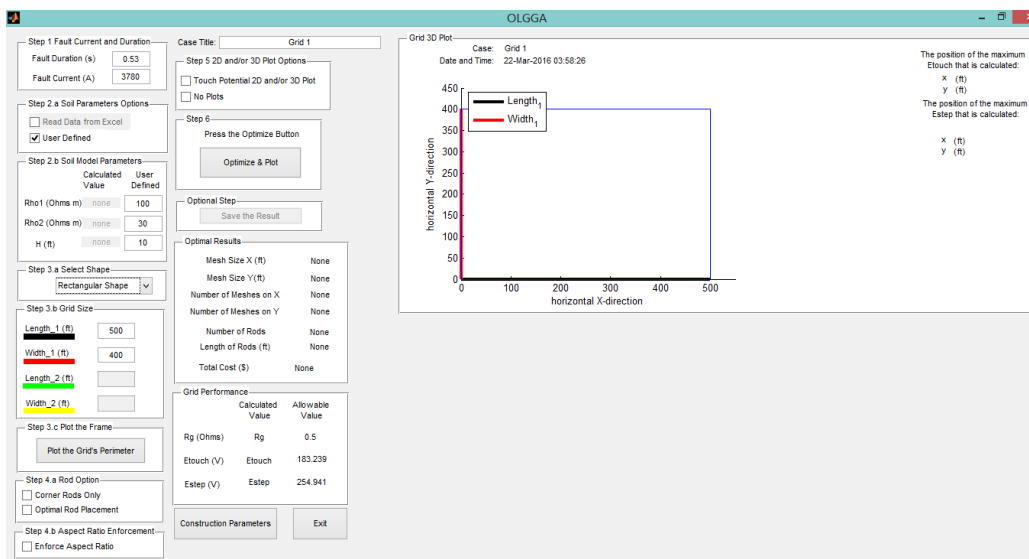
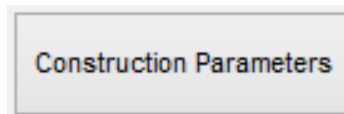


Figure 3.1.

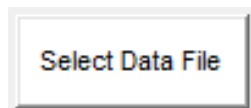
A brief description of these buttons and check boxes is given below.

A.3.2 Push Buttons

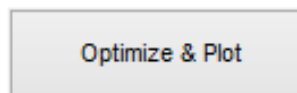
Opens a window in which the construction parameters (ground conductor size, etc.) may be updated.



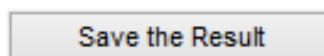
the construction



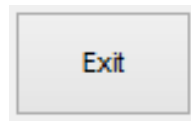
Selects the data file that is used to construct the soil model from the Wenner-method-measured field data.



Starts the ground-grid-design optimization.

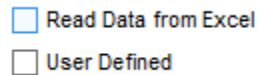


Saves OLGGA's results to a pdf or png file.

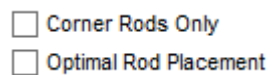


Exits OLGGA.

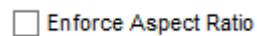
A.3.3 Check Boxes



These two boxes are used to input the soil model. By checking the first box, the user chooses to load an Excel file to construct the soil model using the Wenner-method-measured field data. The details of how to use the Soil Model Application are shown in its User's Manual. By checking the second box, the user will need to fill in the text boxes in Step 2.b.



These two boxes allow the user to choose how to control how OLGGA handles the ground rod placement.



This box is used to by the user to choose if the aspect ratio of the mesh constraint will be added for the optimization. The aspect ratio will be restrained between 1/3 and 3 if the box is checked. (Accuracy of results is only guaranteed if this box is checked. Otherwise, results will be approximate only.)

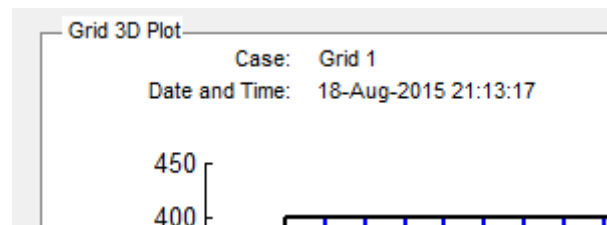
- ☐ Grid Touch Potential 2D and 3D
- ☐ No Plots

These two boxes allow the user to choose if the 2D and/or 3D plots of the touch potential will be drawn. Checking the first box typically increases the execution time significantly.

A.3.4 Case Title

Case Title:

The user may name the case by type its name in the text box. The name of the case and the date and the time of the optimization will be displayed with the results and in any pdf file saved.



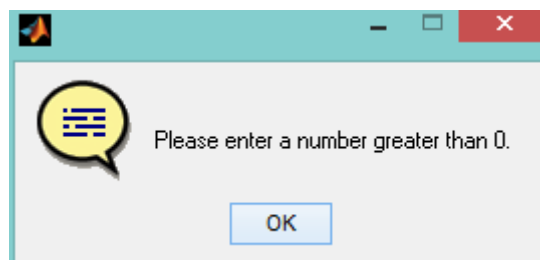
A.3.5 Setting the Fault Current and the Fault Duration

Step 1 Fault Current and Duration

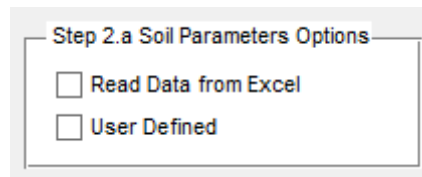
Fault Duration (s)

Fault Current (A)

This entry field allows the user to enter the fault duration and fault current. The unit of the fault duration is s, and the unit of the fault current is A. These must be positive values, or there will be a warning window to tell the user that only positive numbers can be entered, as shown in the following figure.



A.3.6 Setting the Soil Model



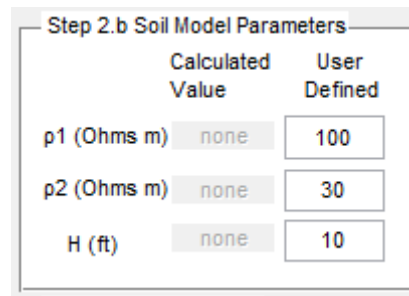
Step 2.a Soil Parameters Options

☐ Read Data from Excel

☐ User Defined

If checking the first box, the user will need to choose an Excel file. Then the soil model will be constructed automatically.

If checking the second box, the user will need to input the soil model parameters manually in the text boxes on the right side shown in the figure below:

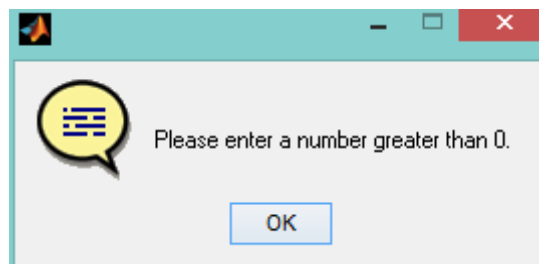


	Calculated Value	User Defined
p1 (Ohms m)	none	100
p2 (Ohms m)	none	30
H (ft)	none	10

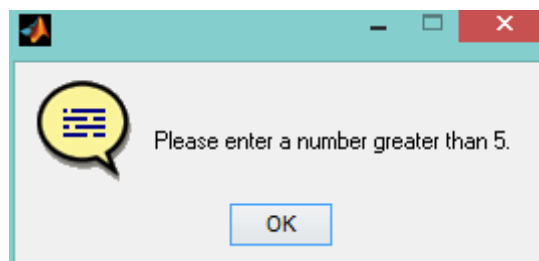
The notation used in this entry box is:

- ρ_1 : The earth resistivity of the top soil layer. The unit is $\Omega \cdot m$.
- ρ_2 : The earth resistivity of the bottom soil layer. The unit is $\Omega \cdot m$.
- H: The thickness of the top soil layer. The unit is ft.

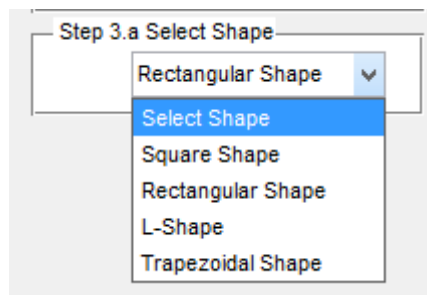
The data in these boxes must be positive, or there will be a warning window to tell the user that the numbers must be positive, as shown in the figure below:



The thickness of the top soil layer should not be less than 5 ft. So if the user types a number less than 5 in the third text box, there will be a warning window shown in the figure below to tell the user to re-enter the data:



A.3.7 Setting the Shape of the Grid

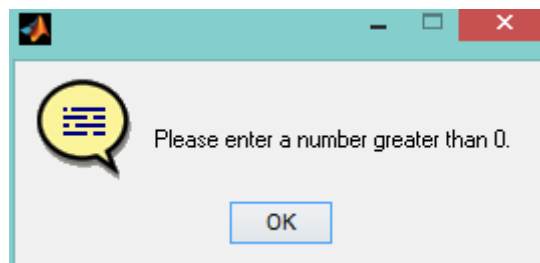


There are four grids shapes that may be chosen by the user in this application. They are square, rectangular, L-shape, and trapezoid.

•Square Grids:



The user needs to enter only the length of one side of the square grid in the first text box. Other dimension-entry boxes shown above are disabled. The number typed in the box must be larger than 0, or there will be a warning window appear is the entry is nonconforming:



For other shapes, if the user types non-positive numbers in the last three text boxes, the user will see this same warning window.

•Rectangular Grids:

Step 3.a Select Shape

Rectangular Shape

Step 3.b Grid Size

Length_1 (ft)

500

Width_1 (ft)

400

Length_2 (ft)

200

Width_2 (ft)

200

The number in the first text box is the length of the side that is along x-axis. The number in the second text box is the length of the side that is along y-axis. The units are all ft.

•L-Shape Grids:

Step 3.a Select Shape

L-Shape

Step 3.b Grid Size

Length_1 (ft)

500

Width_1 (ft)

400

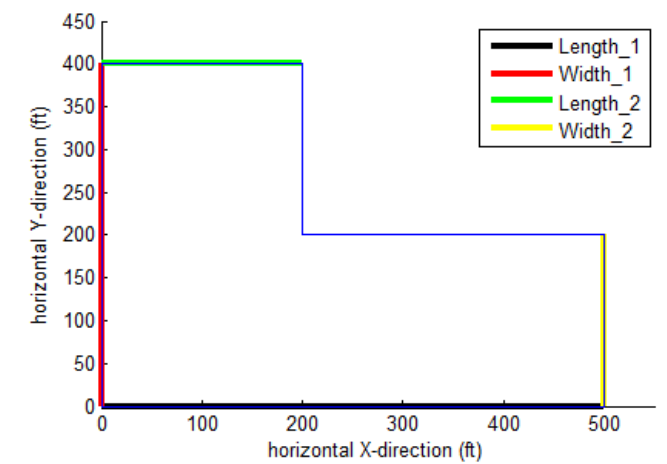
Length_2 (ft)

200

Width_2 (ft)

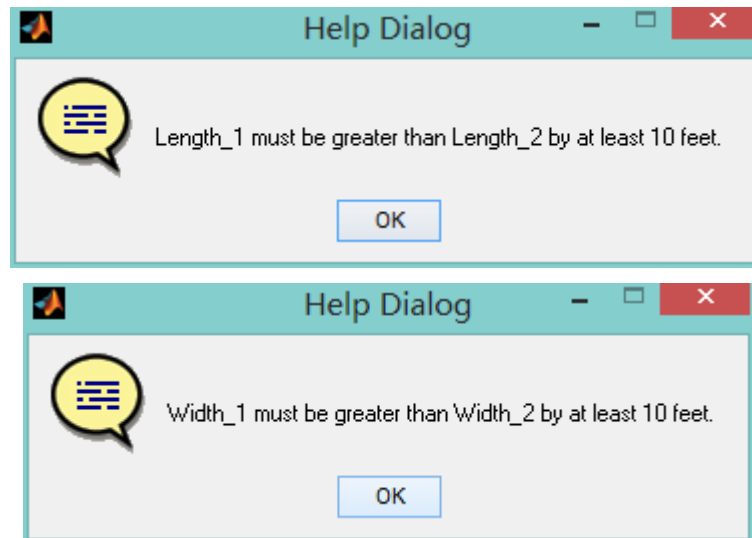
200

The definitions of Length_1, Width_1, Length_2, Width_2 are shown in the following figure:



Length_1 must be 10ft greater than Length_2, and Width_1 must be 10ft greater than Width_2. If the data the user enters violate these requirements, warning windows

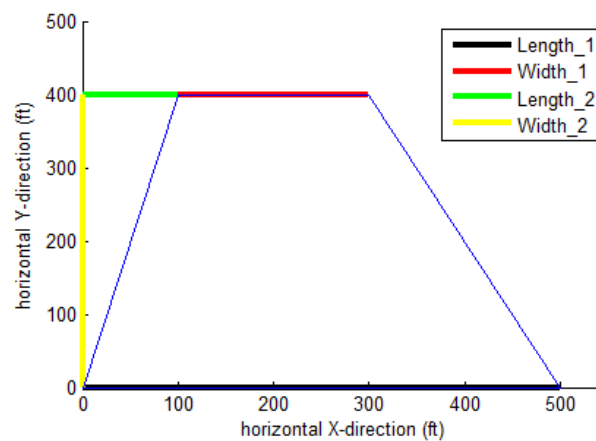
will be shown when the user pushes the "Plot the Grid's Perimeter " button in the next section.



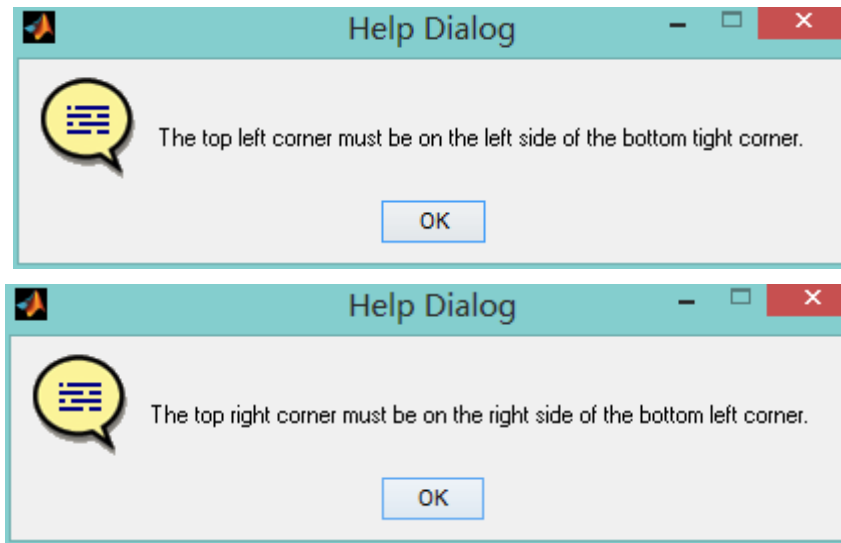
•Trapezoidal Grids:

The screenshot shows a software interface for defining a trapezoidal grid. It consists of two main sections: 'Step 3.a Select Shape' and 'Step 3.b Grid Size'. In 'Step 3.a', a dropdown menu is set to 'Trapezoidal Shape'. In 'Step 3.b', there are four input fields with corresponding colored bars: Length_1 (ft) is 500 (black bar), Width_1 (ft) is 200 (red bar), Length_2 (ft) is 200 (green bar), and Width_2 (ft) is 400 (yellow bar).

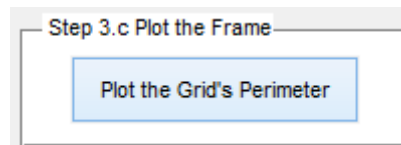
The definition of Length_1, Width_1, Length_2, Width_2 is shown in the following figure:



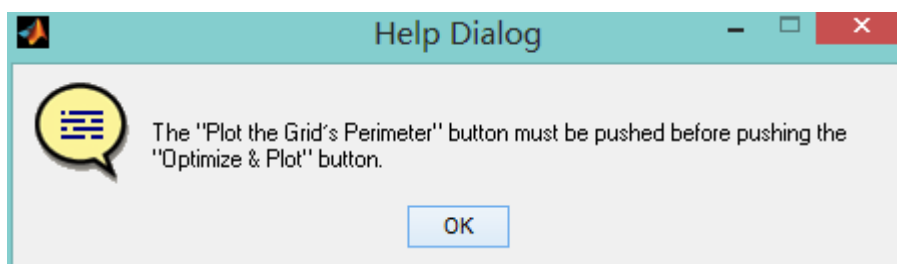
The top *left* corner of the grid cannot be to the *right* of the bottom *right* corner. The top *right* corner cannot be to the *left* of the bottom *left* corner. If these requirements are violated based on the user's entries, once the "Plot the Grid's Perimeter" button is pushed, there will be a warning windows to tell the user to re-enter corrected data.



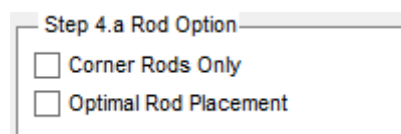
A.3.8 Plotting the Grid's Perimeter



Pushing this button causes the perimeter of the grid to be drawn on the interface at the top left of the main window. This button needs to be pushed to check if there are any typos in the text boxes in Step 3.b. If the grid perimeter is not plotted, and the user wants to start the optimization, a warning window will be shown:



A.3.9 Rod Options



If the user checks the first box, OLGGA will install ground rods only on the corners of the grid. If the user checks the second box, rods will be placed at the corners and optimally along the perimeter.

A.3.10 Aspect Ratio Enforcement

Step 4.b Aspect Ratio Enforcement
☐ Enforce Aspect Ratio

If this box is checked, the aspect ratio of the mesh will be restricted in the range between 1/3 and 3. (Accuracy of results is only guaranteed if this box is checked. Otherwise, results will be approximate only.)

A.3.11 2D and/or 3D Plot of the Touch Potential

Step 5 2D and/or 3D Plot Options
☐ Touch Potential 2D and/or 3D Plot
☐ No Plots

Checking the first box, the 2D and/or 3D plot(s) will be drawn.

A.3.12 Start the Optimization

Step 6

Press the Optimize Button

Optimize & Plot

Push this button to start the optimization.

A.3.13 Results of the Optimization

Optimal Results	
Mesh Size X (ft)	35.7143
Mesh Size Y(ft)	50
Number of Meshes on X	14
Number of Meshes on Y	8
Number of Rods	4
Total Cost (\$)	94113.1

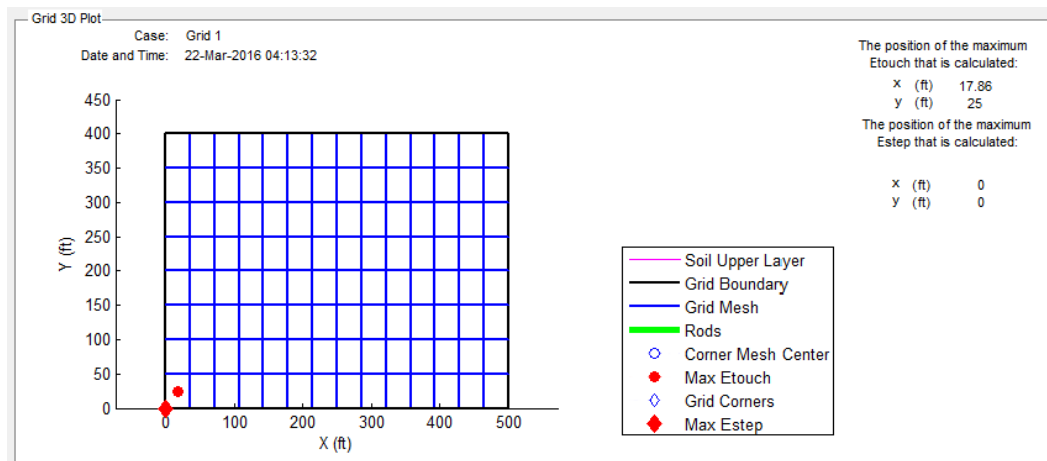
The result of the optimization is provided in the Optimal Results panel as shown in the figure above. The items in the list are:

- Mesh Size X(ft) : The width of the uniform mesh along x-axis.
- Mesh Size Y(ft) : The width of the uniform mesh along y-axis.
- Number of Meshes on X : The number of meshes along the x-axis.
- Number of Meshes on Y : The number of meshes along the y-axis.
- Number of Rods: The number of rods that are installed.
- Total Cost (\$): The total cost.

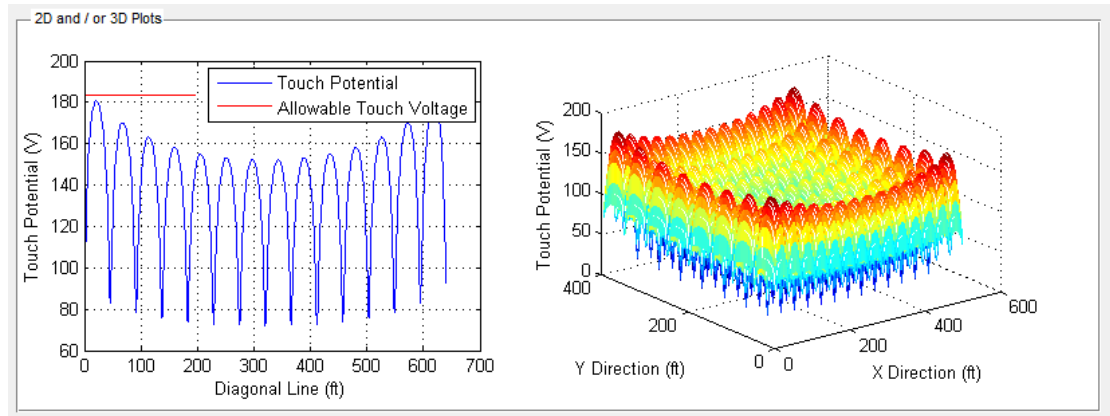
The grid performance is shown below. The calculated values and the allowable values of the ground grid resistance, touch potential and step potential are displayed in the Grid Performance panel, and shown in the figure below.

Grid Performance		
	Calculated Value	Allowable Value
Rg (Ohms)	0.134393	0.5
Etouch (V)	180.316	183.239
Estep (V)	71.9232	254.941

The grid will be drawn in the Grid 3D Plot panel. The position where the maximum touch potential is calculated is indicated by the solid red circle on the grid plot and its coordinates are displayed at the top right of this panel. The position where the maximum step potential is indicated by the solid red diamond on the grid plot and its coordinates are displayed at the bottom right of this panel.

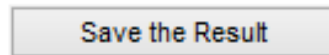


The 2D and/or 3D plot of the touch potential will also be drawn only if the user chooses the corresponding check box in Step 5. (For L-shaped ground grids and trapezoidal ground grids, only the 3D plot can be shown.)

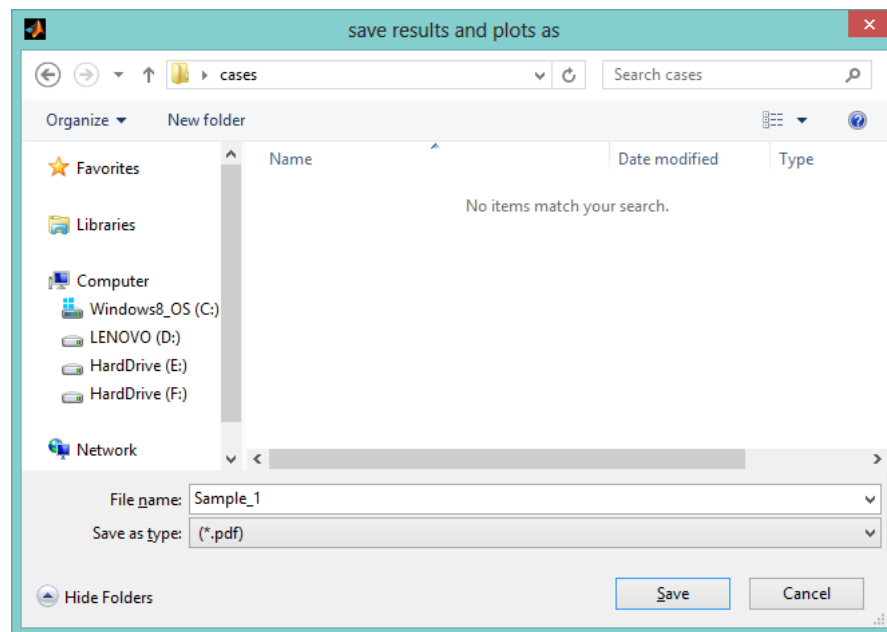


A.3.14 Save the Result

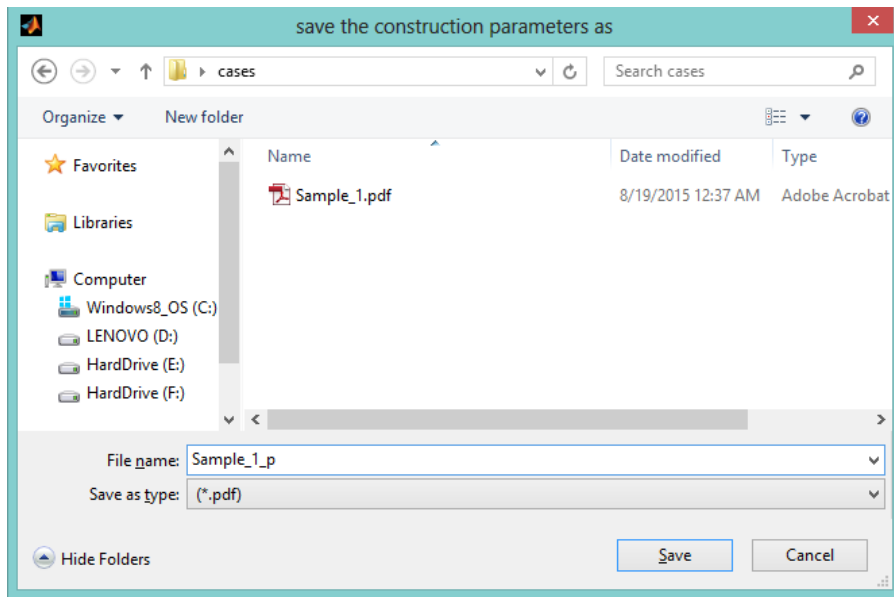
After the optimization, The user may save the result to a pdf file by pushing the button shown in the figure,



and then the user may name the file and save it to a folder, as shown in the next figure.



Similarly, after saving the results of the optimization, the window below will pop up automatically where the user can save a copy the construction parameters used in the optimization.



A.3.15 Changing Construction Parameters



The user can push this button to open the window to change the construction parameters for the ground-grid currently being optimized. The window opened is shown in the figure below.

Case: Grid 1
Date and Time: 22-Mar-2016 00:55:55

Horizontal ground conductor copper (\$/ft) 3.77
Labor to trench, install cable, and backfill (\$/ft) 4
Labor to drive rods up to 10 ft (\$/ft) 10
Labor to drill, insert, and backfill rods 11 ft to 40 ft (\$/ft) 32
Labor to make exothermic connection cable to cable or cable to rod (\$ each) 40
Exothermic connector material and mold (\$ each) 19.25
Ground conductor diameter (in) 0.528
Ground rod diameter (in) 0.628
Bury depth (ft) 1.5
Coarsest allowable mesh dimension (ft) 50
Smallest allowable mesh dimension (ft) 8.5
Sum of the number of meshes along the x and y axes parameter ¹ : 100

☒ Check this box below if you want a warning to pop up that this parameter has been changed from the default value.

Apply New Parameters Cancel Restore Default Parameters Change Default Parameters

1. The sum of the number of meshes along the x and y axes is by default limited to 100, which allows the program to execute with 1GB of free memory. If you increase this "number of meshes" parameter, that could cause OLGA to run more slowly or could cause OLGA to crash if it tries to use more than the available amount of free memory.

The name of the case and the time and date is shown on the top left corner of the window. The listed terms fall into the following categories (listed in order):

(1) The price:

- Horizontal ground conductor copper (\$/ft)
- Labor to trench, install cable, and backfill (\$/ft)
- Labor to drive rods up to 10 ft (\$/ft)
- Labor to drill, insert, and backfill rods 11 ft to 40 ft (\$/ft)
- Labor to make exothermic connection cable-to-cable or cable-to-rod (\$ each)
- Exothermic connector material and mold (\$ each)

(2) The Size:

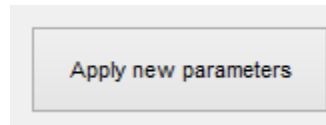
- Ground conductor diameter (in)
- Ground rod diameter (in)
- Bury depth (ft)

(3) The Constraints

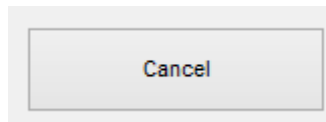
- Maximum mesh length size (ft)
- Minimum mesh length size (ft)

The numbers that appear in the Construction Parameters window text boxes when the user opens the window are the values that will be used for the present design optimization and for all future designs until they are changed. If the user makes any changes to

these numbers via the Construction Parameters window and wants to apply them, the user should push the button shown below.

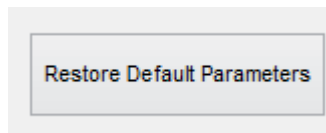


If the user changes these values and closes the program, the program remembers these changes, and the next time the program is opened, these applied parameters will be used. If the user does not want to apply the changes he made, he may push the cancel button.

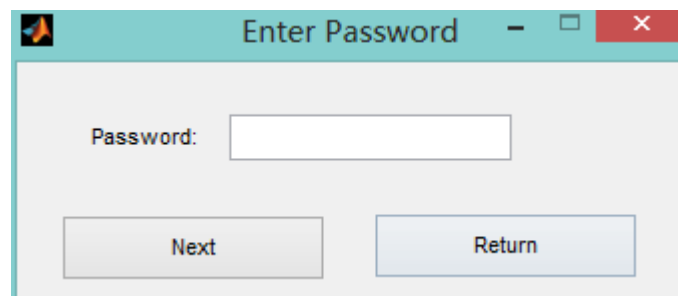
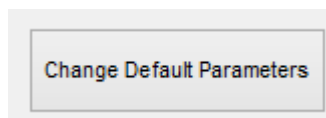


and then the changes that the user made will not be applied.

The button shown below restores the parameters to default parameters.



The Change Default Parameters button allows the user change the default parameters in a new window. The user needs to enter the correct password to open this window. The password is: SRP.



A.3.16 Changing Default Parameters

After pressing the ‘Change Default Parameters’ button, the user can change the default parameters in the window that will appear, which is similar to that shown below. After entering any changes, press the Apply New Default Parameters button below.

Apply New Default Parameters

Change Default Parameters

Horizontal ground conductor copper (\$/ft)

3.77

Labor to trench, install cable, and backfill (\$/ft)

4

Labor to drive rods up to 10 ft (\$/ft)

10

Labor to drill, insert, and backfill rods 11 ft to 40 ft (\$/ft)

32

Labor to make exothermic connection cable to cable or cable to rod (\$ each)

40

Exothermic connector material and mold (\$ each)

19.25

Ground conductor diameter (in)

0.528

Ground rod diameter (in)

0.628

Bury depth (ft)

1.5

Coarsest allowable mesh dimension (ft)

50

Smallest allowable mesh dimension (ft)

8.5

Sum of the number of meshes along the x and y axes parameter ¹ :

100

Apply New Default Parameters

Cancel

Factory Default Settings

1. The sum of the number of meshes along the x and y axes is by default limited to 100, which allows the program to execute with 1GB of free memory. If you increase this “number of meshes” parameter, that could cause OLGA to run more slowly or could cause OLGA to crash if it tries to use more than the available amount of free memory.

If the Cancel button is pressed, the change will not be applied. To restore the default parameters to factory default parameters, the Factory Default Settings button needs to be pressed and then the Apply New Default Parameters button must be pressed.

A.3.17 Parameters Limits on N_x+N_y

At the time that this MATLAB based program was developed, there was an additional limit that was used to prevent memory leakage and unacceptable execution time. Because of the solution of the dense matrix equation in the mutual resistance sub problem requires a large amount of RAM, where the amount of storage is a function of the parameters N_x and N_y (where N_x and N_y are the number of meshes on x side and y side, respectively), a limit was put on maximum value that N_x+N_y can attain. This

limit, which may be changed using the change parameters window, is in place to limit memory leakage and prevent exorbitant execution times. It has been found experimentally that if $x\%$ of RAM is used by the background-processes and active programs, then when the MATLAB program is doing optimization, the total amount of memory used (in %) should be less than the following to prevent memory leakage and exorbitant execution times,

$$y\%=(2.28/R*100+x)\%,$$

where R is the number of GB of the RAM that the user's computer has. Notice that the value of $Nx+Ny$ for a given design is dependent on many design parameters. The max value of $Nx+Ny$ has been set at 100 in the change parameters window to maintain program efficiency for the worst case scenario of 4 GB RAM memory as of this writing in 2016. The upper bound of the memory used by the MATLAB program may be estimated using the following equation.

$$\text{The upper bound of the memory used} = 8*10^{-9}*(Nx + Ny)^4 \text{ GB}$$

Three changes are expected in the future.

1. Computers are expected to have more RAM.
2. Computer architecture is expected to evolve.
3. MATLAB is expected to recruit SSD memory as additional RAM.

It is impossible to know whether the equation that sets a responsible limit on the percent of RAM used by the app to ensure efficient execution will be valid into the future; however, it is hoped that this equation along with the equation that defines the maximum amount of memory used by the app will provide some guidance, should the user want to increase the $Nx+Ny$ limit through the change parameters window in the future.

Once the equation that represents the memory the app can use becomes antiquated, the user can establish the $Nx+Ny$ limit through cut and try methods by using a ground grid parameter case that hits the $Nx+Ny$ value. The user can increase the values of a combination of the following parameters to cause $Nx+Ny$ to reach its limit: soil model resistivity, substation size and fault current.

APPENDIX B
LIST OF SOURCE CODE FILES OF OLGGA AND IMPLEMENTATION
DIAGRAM

The source code files, listed below in alphabetical order along with a summary of their function, can be found in the directory where OLGGA is installed.

List of Source Code Files

CDS_trapezoid_s1.m: This is the function that performs segmentation for trapezoidal ground grids when the bottom left corner is to the left of the top left corner and the bottom right corner is to the right of the top right corner.

CDS_trapezoid_2.m: This is the function that performs segmentation for trapezoidal ground grids when the top left corner is to the left side of the bottom left corner and the top right corner is to the left side of the bottom right corner.

CDS_trapezoid_3.m: This is the function that performs segmentation for trapezoidal ground grids when the top right corner is to the right side of the bottom right corner and the top left corner is to the right side of the bottom left corner.

CDS_worst_case.m: This is the function that performs segmentation for square and rectangular ground grids.

CDS_worst_case_LShape.m: This is the function that performs segmentation for L-shaped ground grids.

change_parameters.m: This is the code for the interface that lets the user change the construction parameters.

ConCImag.m: This is the function that calculates the nonlinear constraints for the square and rectangular ground grids when the mesh aspect ratio is not enforced.

ConCImag_ratio_enf.m: The function that calculates the nonlinear constraints for the square and rectangular ground grids when the mesh aspect ratio is enforced.

ConCImag_LshapeL.m: This is the function that calculates the nonlinear constraints for the L-shaped ground grids when the mesh aspect ratio is not enforced.

ConCImag_LshapeL_ratio_enf.m: This is the function that calculates the nonlinear constraints for the L-shaped ground grids when the mesh aspect ratio is enforced.

cond_num_test.m: This is the function that assigns design variables (e.g., the number of meshes along the x-axis, the number of meshes along the y-axis and the number of rods) before testing to see if there is a feasible solution within the mesh-aspect-ratio range, where OLGGA is accurate.

cond_num_test_ind.m: This is the function that tests if there is a feasible solution within the mesh-aspect-ratio range where OLGGA is accurate.

coordinate_tran.m: This is the function that does coordinate transformation.

determine_shape.m: This is the function that identifies the shapes of trapezoidal ground grids.

Ee_single_termcalculation.m: This is the function that calculates each single term in the series expansion of the earth potential due to the leakage current on the segments on the left leg or the right leg of the trapezoidal ground grid.

Estep_Point_1.m: This function calculates the earth potential at the first point for calculating the step potential, i.e., the corner point of the ground grid, for rectangular ground grids.

Estep_Point_2.m: This function calculates the earth potential at the second point for calculating the step potential, i.e., the point exterior to the ground grid 1 meter away from the corner on the bisector of the corner, for rectangular ground grids.

Estep_trapezoid.m: This function calculates the step potential at the corners for trapezoidal ground grids.

Etouch.m: This function calculates the maximum touch potential for square and rectangular ground grids.

Etouch_2D_L.m: This function calculates the touch potential along the diagonal line of the square and rectangular ground grids and is used in plotting the touch potential 2D plot.

Etouch_3D.m: This function calculates the touch potential in the square and rectangular ground grids. The output is used to plot the touch potential 3D plot.

Etouch_3D_L_Shape.m: This is the function that calculates the touch potential in the L-shaped ground grid, and the output is used to plot the touch potential 3D plot.

Etouch_3D_Trapezoid.m: This is the function that calculates the touch potential in the trapezoidal ground grid, and the output is used to plot the touch potential 3D plot.

Etouch_L_point_arb.m: This is the function that calculates the touch potential at an arbitrary point in the L-shaped ground grid.

Etouch_trapezoid.m: This is the function that calculates the touch potential for trapezoidal ground grids.

feasibility_test.m: This is the function that checks whether there is a feasible solution or not.

feasibility_test_M3.m: This is the function that checks the feasibility and returns the performance (i.e., touch and step potentials and their respective safety limits) of the design.

find_corner_center_points.m: This function calculates the coordinates of the centroids of the corner meshes of the L-shaped ground grid.

find_Estep_values.m.m: This function returns the step potential values at the corners of a L-shaped ground grid.

find_Etouch_values.m: This function returns the touch potential values at the centroids of the corner meshes of a L-shaped ground grid.

Find_Maximum_Et.m: This function returns the maximum touch potential and the coordinates of the point where the maximum touch potential occurs for a trapezoidal ground grid.

Find_Positions_Et_s1.m: This function returns the coordinates of the point where the touch potential is calculated in a trapezoidal ground grid when its bottom left corner is to the left side of its top left corner and its bottom right corner is to the right side of its top right corner.

Find_Positions_Et_s2.m: This function returns the coordinates of the point where the touch potential is calculated in a trapezoidal ground grid when its bottom left corner is to the right side of its top left corner and its bottom right corner is to the right side of its top right corner.

Find_Positions_Et_s3.m: This function returns the coordinates of the point where the touch potential is calculated in a trapezoidal ground grid when its bottom left corner is to the left side of its top left corner and its bottom right corner is to the left side of its top right corner.

memory_speed_test.m: This is the function that checks whether memory leakage is likely to occur and whether the optimization will finish within an acceptable time.

Non_Linear_Con_Trapezoid.m: This function calculates the nonlinear constraints for trapezoidal ground grids when the mesh aspect ratio is not enforced.

ConCImag_LshapeL_ratio_enf.m: This function calculates the nonlinear constraints for trapezoidal ground grids when the mesh aspect ratio is enforced.

NRODmax_standard_trapezoid.m: This function calculates the maximum allowable number of rods for the trapezoidal ground grids.

objfun.m: This is the objective function for square and rectangular ground grids.

objfun_Lshape_new.m: This is the objective function for L-shaped ground grids.

objfun_trapezoid.m: This is the objective function for trapezoidal ground grids.

OLGGA_v1: This is the code for the GUI main window.

Passworddlg.m: This file contains the code for window where the password is entered.

ResMatrix.m: This function calculates the mutual resistance matrix for square, rectangular and L-shaped ground grids.

ResMatrix_trapezoid.m: This function calculates the mutual resistance matrix for trapezoidal ground grids.

SBNUM.m: This function uses the Rectangle Rule defined in Chapter 2 to calculate each single term in the series expansion of the mutual resistance between a segment on the left or right leg and another segment for trapezoidal ground grids.

SBNUMSIMP.m: This function uses Simpson's Rule defined in Chapter 2 to calculate each single term in the series expansion of the mutual resistance between a segment on the left or right leg and another segment for trapezoidal ground grids.

SBPARL.m: This function calculates each single term in the series expansion of the mutual resistance between two parallel segments.

SBPERP.m: This function calculates each single term in the series expansion of the mutual resistance between two perpendicular segments.

SegmCond.m: This function returns the segment length for square and rectangular ground grids.

SegmCond_Lshape.m: This function returns the reference segment length on each side of a L-shaped ground grid.

segment_trapezoid.m: This function returns the reference segment length for trapezoidal ground grids when the bottom left corner is to the left side of the top left corner and the bottom right corner is to the right side of the top right corner.

segment_trapezoid_s2.m: This function returns the reference segment length for trapezoidal ground grids when the bottom left corner is to the right side of the top left corner and the bottom right corner is to the right side of the top right corner.

segment_trapezoid_s3.m: This function returns the reference segment length for trapezoidal ground grids when the bottom left corner is to the left side of the top left corner and the bottom right corner is to the left side of the top right corner.

setting_default_parameters.m: This is the source code of the GUI window where the user can set the default parameters.

show_the_rod_positons.m: This function returns the maximum allowable number of rods for square, rectangular and L-shaped ground grids.

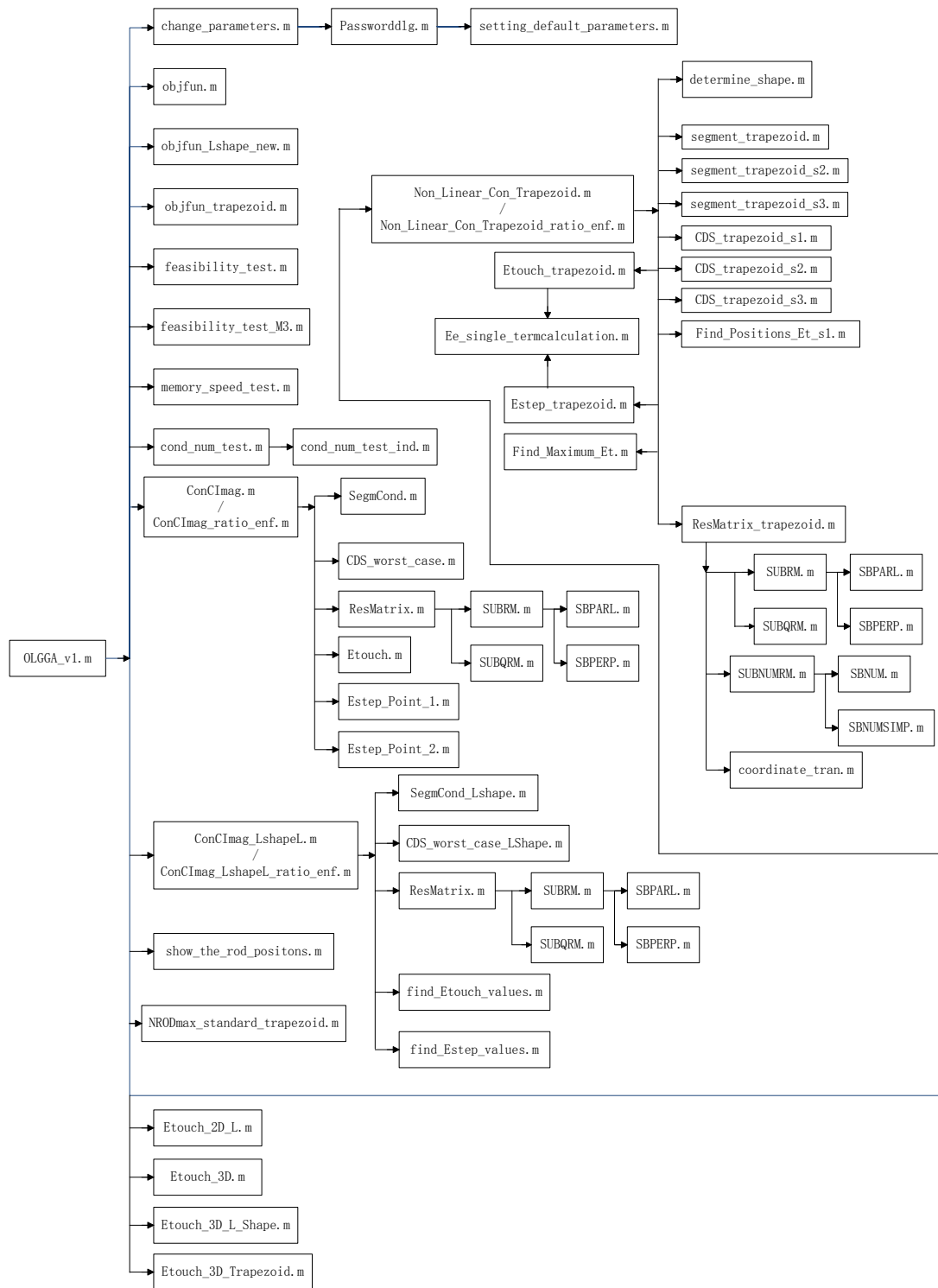
SUBNUMRM.m: This function calculates the mutual resistance between any two segments that are not parallel or perpendicular to each other.

SUBQRM.m: This function calculates the mutual resistance using the Point-Point model.

SUBRM.m: This function calculates the mutual resistance between two segment that are parallel or perpendicular to each other using the Line-Line model.

sum_calc_xy.m: This function calculates the coordinates of the centroid of each corner mesh.

Implementation Diagram



APPENDIX C
OLGGA INSTALLATION INSTRUCTION
CONTAINED IN THE README.TXT FILE

OLGGA INSTALLATION INSTRUCTION
CONTAINED IN THE README.TXT FILE

Step 1. Install MATLAB COMPILER RUNTIME (MCR) following the process of the installation wizard. MCR is available on the following website:

http://www.mathworks.com/supportfiles/MCR_Runtime/R2013a/MCR_R2013a_win64_installer.exe

Step 2. Copy the folder called OLGGA located in the directory where this readme.txt file is located to the directory chosen by the user.

Step 3. Open OLGGA.exe in the pasted folder to use OptimaL Ground Grid Application.